

AD-A242 768



WL-TR-91-3067

10
3-50
c



EVOLUTION AND DEVELOPMENT OF HYPERSONIC CONFIGURATIONS
1958-1990

ALFRED C. DRAPER AND THOMAS R. SIERON

HIGH SPEED AERO PERFORMANCE BRANCH
AEROMECHANICS DIVISION

SEPTEMBER 1991

FINAL REPORT FOR PERIOD JULY 1990 TO MARCH 1991

APPROVED FOR PUBLIC RELEASE; DISTRIBUTION UNLIMITED

FLIGHT DYNAMICS DIRECTORATE
WRIGHT LABORATORY
AIR FORCE SYSTEMS COMMAND
WRIGHT-PATTERSON AIR FORCE BASE, OHIO 45433-6553

91-16265



91 16265 001

NOTICE

When Government drawings, specifications, or other data are used for any purpose other than in connection with a definitely Government-related procurement, the United States Government incurs no responsibility nor any obligation whatsoever. The fact that the government may have formulated, or in any way supplied the said drawings, specifications, or other data, is not to be regarded by implication or otherwise in any manner construed, as licensing the holder or any other person or corporation, or as conveying any rights or permission to manufacture, use, or sell any patented invention that may in any way be related thereto.

This report is releasable to the National Technical Information Service (NTIS). At NTIS, it will be available to the general public, including foreign nations.

This technical report has been reviewed and is approved for publication.

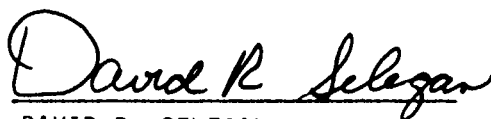


THOMAS R. SERION
Technical Manager
Flight Evaluation Group



VALENTINE DAHLEM III
Chief
High Speed Aero Performance Branch

FOR THE COMMANDER



DAVID R. SELEGAN
Acting Chief
Aeromechanics Division

If your address has changed, if you wish to be removed from our mailing list, or if the addressee is no longer employed by your organization, please notify WL/FIMG, Wright-Patterson AFB, OH 45433-6553 to help us maintain a current mailing list.

Copies of this report should not be returned unless return is required by security considerations, contractual obligations, or notice on a specific document.

REPORT DOCUMENTATION PAGE			Form Approved OMB No. 0704-0188	
Public reporting burden for this collection of information is estimated to average 1 hour per response, including the time for reviewing instructions, searching existing data sources, gathering and maintaining the data needed, and completing and reviewing the collection of information. Send comments regarding this burden estimate or any other aspect of this collection of information, including suggestions for reducing this burden, to Washington Headquarters Services, Directorate for Information Operations and Reports, 1215 Jefferson Davis Highway, Suite 1204, Arlington, VA 22202-4302, and to the Office of Management and Budget, Paperwork Reduction Project (0704-0188), Washington, DC 20503				
1. AGENCY USE ONLY (Leave blank)	2. REPORT DATE September 1991	3. REPORT TYPE AND DATES COVERED Final Report, July 1990 - March 1991		
4. TITLE AND SUBTITLE Evolution and Development of Hypersonic Configurations, 1958-1990		5. FUNDING NUMBERS Project 2404 Task Numbers: 240407 240416 Work Unit 93		
6. AUTHOR(S) Draper, Alfred C., and Sieron, Thomas R.				
7. PERFORMING ORGANIZATION NAME(S) AND ADDRESS(ES) Flight Dynamics Directorate, WL, AFSC WL/FIMG Wright-Patterson AFB OH 45433-6553 Thomas R. Sieron, (513)255-4613		8. PERFORMING ORGANIZATION REPORT NUMBER WL-TR-91-3067		
9. SPONSORING / MONITORING AGENCY NAME(S) AND ADDRESS(ES)		10. SPONSORING / MONITORING AGENCY REPORT NUMBER		
11. SUPPLEMENTARY NOTES				
12a. DISTRIBUTION / AVAILABILITY STATEMENT Approved for Public Release; Distribution Unlimited			12b. DISTRIBUTION CODE	
13. ABSTRACT (Maximum 200 words) This report traces the activities of the Flight Dynamics Laboratory in hypersonic configuration research from 1958 to 1990. Early efforts concentrated on simple configurations and progressed to more sophisticated lifting body point designs as analysis and design techniques became available. Several flight technology demonstration programs pioneered the exploitation of this new challenging flight regime and provided an extensive data base for the development of the Space Shuttle. Hypersonic air-breathing cruise vehicles are shown to be dominated by inlet and nozzles integration with the airframe. A list of "lessons learned" is compiled to provide a useful reference for the designer in the early formulation of configurations concepts.				
14. SUBJECT TERMS Hypersonics, Lifting Body, Flight Test Vehicles, Hypersonic Configuration Research			15. NUMBER OF PAGES 128	
			16. PRICE CODE	
17. SECURITY CLASSIFICATION OF REPORT Unclassified	18. SECURITY CLASSIFICATION OF THIS PAGE Unclassified	19. SECURITY CLASSIFICATION OF ABSTRACT Unclassified	20. LIMITATION OF ABSTRACT Unlimited	

FOREWORD

This report was prepared in-house by Mr Alfred C. Draper and Mr Thomas R. Sieron of the Aeromechanics Division, Flight Dynamics Directorate, Wright Laboratory at Wright-Patterson Air Force Base, Ohio 45433-6553. It represents a summary of the Flight Dynamics Laboratory technical contributions to the state of the art in the area of hypersonic configuration development from 1958 to 1990. The designation "Flight Dynamics Laboratory" is used throughout this report, instead of Flight Dynamics Directorate, in order to continue its' heritage and maintain recognition by other organizations and personnel. It was prepared during the period July 1990 to March 1991. The prime motivation for this report was a paper titled "The Air Force and Hypersonics 1963-1990" given by the authors at the History of Hypersonics symposium, sponsored by the National Air and Space Museum Smithsonian Institution in October 1990. The authors wish to acknowledge the contributions to this report by current and former members of the Aeromechanics Division, Flight Dynamics Laboratory. A large amount of data used throughout this report has been obtained from past technical reports and papers which are referenced in the report. Appreciation is expressed to the following individuals* for their contributions in the development of a comprehensive hypersonic configuration technology base:

Alexander, Grover
Benson, Burtis
Brigalli, Anthony J.
Buck, Melvin L.
Burke, Gerald L.
Bursey, Charles H.
Burnett, Duane R.
Cosenza, Charles J.
Dahlem, Valentine III
DeCamp, Ronald W.
Fehl, John E.

Flaherty, Jack I.
Gord, Peter R.
Hankey, Wilbur
Hayes, James R.
Johnson, David T.
Lane, Paul
Loptien, George W.
Martinez, Conrad Jr.
McLaughlin, Edward
Miller, Earl
Nash, Richard

Neumann, Richard D.
Norris, Richard B.
Patterson, Jerold L.
Rinn, Stephen W.
Selegan, David R.
Shang, Joseph J.
Shereda, Donald E.
Sliski, Neil J.
Stetson, Kenneth F.
Smith, Richard R.
Zima, William P.

* Apologies are offered to those individuals whose names were unintentionally omitted from this list.

CONTENTS

<u>SECTION</u>	<u>PAGE</u>
FOREWORD	ii
FIGURES	iv
SYMBOLS AND ABBREVIATIONS	vii
ACRONYMS	ix
1. SUMMARY	1
2. INTRODUCTION	3
3. CONFIGURATION RESEARCH	6
4. LIFTING BODY CONFIGURATION DEVELOPMENT	28
5. FLIGHT RESEARCH PROGRAMS	48
6. APPLICATION OF LIFTING BODY CONFIGURATION TECHNOLOGY	57
7. HYPERSONIC AIR BREATHING TECHNOLOGY DEMONSTRATORS	83
8. TWO STAGE REUSABLE LAUNCH VEHICLE CONCEPT	98
9. LESSONS LEARNED	106
REFERENCES	108

Accession For	
NTIS Grant	<input checked="" type="checkbox"/>
DTIC Tab	<input type="checkbox"/>
Unannounced	<input type="checkbox"/>
Justification	
by	
Distribution	
Availability Codes	
Avail and/or	
Dist	Special
A-1	



FIGURES

<u>FIGURE</u>	<u>TITLE</u>	<u>PAGE</u>
1	Chronology of Hypervelocity Vehicles	4
2	Classes of Configurations	7
3	Key Technology Factors	8
4	Force, Moment and Flow Visualization	10
5	Hypervelocity Vehicle Configuration	12
6	Aero Control and Auxiliary Drag Devices Summary	14
7	ASSET in Gliding Flight	16
8	ASSET Vehicle Configuration	17
9	PRIME SV-5D General Arrangement	19
10	Test of Recovered Prime Vehicle	21
11	Payoff of Aerodynamic Efficiency	22
12	Air Base Requirements	23
13	Maneuver Performance of Lifting Reentry Vehicles	24
14	Configuration Research	27
15	Lifting Body Configurations	29
16	High L/D Configuration Evolution	30
17	Configuration Aerodynamics for Lifting Bodies	32
18	Geometry Effects on L/D	33
19	Volume Increase Through Cross Section Changes	34
20	Rarefaction Correlation Parameter	36
21	Configuration Variations For Directional Stability	37
22	FDL-5 Compression Sharing Design	38
23	Full Scale Mockup of the FDL-5	40

FIGURES (CONT'D)

<u>FIGURE</u>	<u>TITLE</u>	<u>PAGE</u>
24	L/D for Typical Configuration Designs	41
25	Nose Temperatures	42
26	Leading Edge Temperatures	44
27	Boundary Layer Transition	46
28	Lower Surface Centerline Temperatures	47
29	X-24A Lifting Body Vehicle	49
30	Comparison of X-24A and X-24B	51
31	X-24A to X-24B Modification	52
32	X-24B Aerodynamic Design Features	53
33	X-24B Flight Envelope	55
34	Previous Lifting Body Research Vehicles	56
35	Vehicle Options and Stage and One-Half Evolution	58
36	Launch Vehicle Cost Comparison	60
37	Mock-Up of FDL-5 With External Tanks	61
38	Shuttle Reentry Temperature Distributions	63
39	Space Shuttle Configuration Development	64
40	Comparison of X-24B Shuttle/Landing Approach	65
41	X-24B Contributions To Shuttle Landing Phase	66
42	OMS Pod Heating	68
43	Maneuvering Reentry Research Vehicle	69
44	Representative Flight Corridors	70
45	Shuttle Packaging of MRRV Designs	72
46	MRRV Packaging With External Tanks	73

FIGURES (CONT'D)

<u>FIGURE</u>	<u>TITLE</u>	<u>PAGE</u>
47	MRRV Engineering Design Model	74
48	Candidate Structural Flight Experiments	76
49	Candidate Aerodynamic Flight Experiments	77
50	MRRV Technology Options	79
51	Synergetic Plane Change Capability	80
52	Aeroconfigured Orbital Transfer Vehicles	82
53	Configuration Design Trend	84
54	Advanced Manned Interceptor Test	86
55	Hypersonic Airbreathing Cruise Vehicles	87
56	Research Aircraft Configuration Comparison	88
57	X-24C Configuration	90
58	X-24C Hypersonic Propulsion Experiment	92
59	X-24C Hypersonic Structure Experiment	93
60	Navier-Stokes Results	94
61	Flying Wind Tunnel Experiments	96
62	Flying Wind Tunnel Flight Corridor	97
63	Two Stage Reuseable Launch Vehicle "BETA"	99
64	Booster Evolution	101
65	First Stage Booster Design	102
66	Orbiter Evolution	104
67	BETA Wind Tunnel Model	105

SYMBOLS AND ABBREVIATIONS

A	planform area
alt	altitude
C*	linear viscosity relation, $C^* = \left(\frac{\mu^*}{\mu_0} \right) \left(\frac{T_0}{T^*} \right)$
C _A	axial force coefficient
C _D	drag coefficient
C _L	lift coefficient
ft	feet
ft/s	feet per second
K	thousands
lb	pound
lb/ft ²	pound per square foot
L/D	lift-to-drag ratio
M	Mach number
nm	nautical mile
P	pressure
q	dynamic pressure
\dot{q}	heat transfer rate
Q	total heat
R _N	Reynolds number
s	second
S _w	wetted area
T	temperature
V	volume; velocity

SYMBOLS AND ABBREVIATIONS (CONT'D)

W weight
 $W/C_L A$ glide parameter

Greek

α angle of attack
 β angle of sideslip
 Γ body dihedral angle (Fig 17)
 ϵ emissivity
 θ_c body profile angle
 Λ leading edge sweepback angle
 μ viscosity
 \bar{V} rarefaction, parameter, $\frac{M}{\sqrt{R_N}}$
 Φ upper body roll-in angle (Fig 17)

Subscripts

∞ free stream conditions
 δ conditions at edge of boundary layer
 θ boundary layer momentum thickness
 w wall

Superscripts

*

value of quantity at reference condition

ACRONYMS

AEDC	Arnold Engineering Development Center
ALS	Advanced Launch System
AMSC	Advanced Military Spaceflight Capability
AOTV	Aeromaneuvering Orbital Transfer Vehicle
ASD	Aeronautical Systems Division
ASSET	Aerothermodynamics/Elastic Structural Systems Environmental Tests
BGRV	Boost Glide Reentry Vehicle
BTU	British Thermal Unit
FWT	Flying Wind Tunnel
GEO	Geosynchronous Earth Orbit
MRRV	Maneuvering Reentry Research Vehicle
NASA	National Aeronautics and Space Administration
NASP	National Aerospace Plane
NHFRF	National Hypersonic Flight Research Facility
OMS	Orbital Maneuvering System
OPT	Optimum
ORB	Orbit
PILOT	Piloted Low Speed Test
PNS	Parabolized Navier Stokes
PRIME	Precision Recovery Including Maneuvering Entry

ACRONYMS (CONT'D)

RD&E	Research, Development, Test & Engineering
RSI	Reusable Surface Insulation
S/HABP	Supersonic/Hypersonic Arbitrary Body Program
SORTIE	Super Orbital Reentry Test Integrated Environment
SSME	Space Shuttle Main Engine
STS	Space Transportation System
TAV	Trans-Atmospheric Vehicle
TPS	Thermal Protection System

1. SUMMARY

The Flight Dynamics Laboratory has played a pioneering role in the development of aerospace vehicles. A complete spectrum of programs have been investigated since 1958 through the current activities and projected into the 1990s. The Laboratory began its activities with participation in the precursor studies which led to Project Mercury. It was responsible for the aerodynamic, performance and aerothermodynamic tasks of the X-20 before the establishment of the Systems Program Office. The Laboratory was strongly involved with the X-7A, a ramjet test vehicle, where basic aerothermodynamic and structural information was obtained at Mach numbers in excess of four. This was followed by considerable configuration analysis and testing including significant involvement with the very successful flight testing of the Alpha Draco vehicle. The Alpha Draco was a precursor to the Boost Glide Reentry Vehicle later flown from the Western Test Range. The Laboratory and ASD were very active in the X-15 as well as the PRIME and ASSET programs. Concurrent with these high speed activities, the Laboratory, worked enthusiastically on the lifting body technology and was specifically assigned technical direction of the X-24A. Out of the Laboratory's earlier research and the X-24A results, the X-24B was conceived. The Laboratory technically directed, managed, and successfully pursued the complete flight and data analysis of this new generic class of lifting entry vehicle.

As early as 1967, the Laboratory was involved in the definition of what later would prove to be the Nation's Space Shuttle. It was an active member of the President's Space Task Group to define and identify the country's

next step in space beyond Apollo. Shortly after completion of the report of the President's Space Task Group, recommending a Space Transportation System or Shuttle, there was a temporary excursion with a straight wing orbiter which subsequently gave way to the recommendations of the FDL for the delta wing shuttle. The Laboratory made many contributions to the technology base used in the development of the Space Shuttle including lessons from the ASSET, the PRIME, the X-24A and the X-24B flight test programs. The Maneuverable Reentry Research Vehicle which was capable of being Shuttle launched or air launched from current jumbo jets, provided the impetus for the Military Spaceflight Capability investigations of advanced reusable launch vehicle concepts.

Strong interest in hypersonic air-breathing cruise vehicles propelled the Laboratory into defining a flight demonstration vehicle for the Mach range 5 to 7. The efforts converged to the X-24C vehicle which took maximum advantage of the X-24B technology. In the early 1980s there was renewed interest in transatmospheric vehicles and later the National Aerospace Plane because of major technology advancements in materials, propulsion and aerodynamics and the need to provide a future replacement for the Space Shuttle. Many concepts such as single-stage-to-orbit and two-stage-to-orbit vehicles were pursued to identify and evaluate critical technologies. Technology demonstration vehicles such as the Flying Wind Tunnel were conceived to flight demonstrate critical propulsion and materials technologies. In summary, the Flight Dynamics Laboratory has been a major contributor to the understanding of hypersonic flow and pioneered the development of many innovative hypersonic vehicle concepts.

2. INTRODUCTION

This report traces the Aeromechanics Division, Flight Dynamics Laboratory interest in hypersonic configuration research from 1958 to 1990 as depicted in Figure 1. Efforts are shown to have progressed from simple configurations through a rather comprehensive series of lifting body investigations for entry from both close proximity and high energy orbits. The Laboratory interest was not restricted to any one given class of vehicles, or any specific configuration concept, rather it was directed to many classes of hypersonic vehicles across the entire flight spectrum. Initially, the emphasis was placed on a broad configuration technology base, but evolved to more definitized lifting body configurations. It is indicated that Laboratory interest in lifting entry vehicle technology was motivated by sound technological reasons for achieving practical configuration designs with potential military applications. It will show emphasis was directed toward developing analysis and design techniques which could be employed for generalized configurations, and emphasized the necessity of assuring not only adequate generality in the techniques and methods developed, but also the necessity for encompassing the pragmatic constraints to assure acceptability.

This systematic approach was augmented with several flight test programs which explored this new flight regime. The FDL participated in many of these programs such as the X-7A, X-20, Alpha Draco, X-15 and the BGRV. These flight programs provided valuable data to confirm wind tunnel data and expand the data base to test conditions which could not be

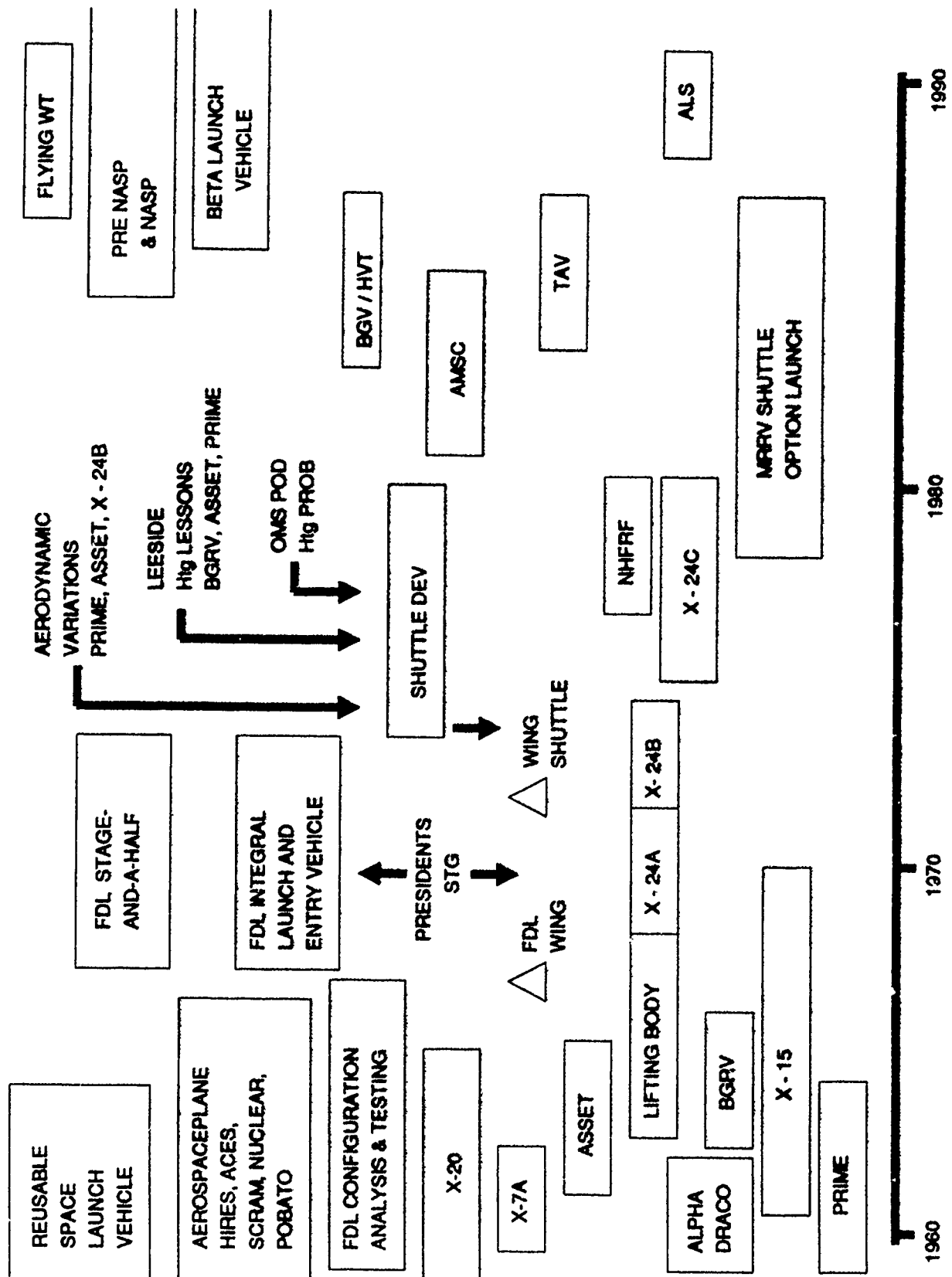


Figure 1. Chronology of Hypervelocity Vehicles

simulated in ground facilities. This data made it possible to determine which aerodynamic and aeroheating prediction techniques were accurate and which methods needed to be discarded and/or modified.

Aerospace technology demonstrators and flight testing were an integral part of the Flight Dynamics Laboratory program for transitioning emerging technologies to future operational systems. Several flight programs such as ASSET, PRIME, X-24A and X-24B are discussed as well as their technological contributions to the Space Shuttle. In addition, other attractive technology demonstration options are shown to offer exciting opportunities for expanding the flight corridor and opening the door to hypersonic airbreathing vehicles. Many of the lessons learned in these investigations were exploited in the design and development of the Space Shuttle, and incorporated in the formulation and definition of the National Aerospace Plane (NASP).

3. CONFIGURATION RESEARCH

The Flight Dynamics Laboratory established a comprehensive research program in the early 1960s to investigate fundamental elements of hypersonic configurations. This consisted of extensive parametric variations on simple geometries such as wing sweep, leading edge radii, nose radii, bluntness ratio, thickness, planform, cross section, body profile angles, and body classification; i.e., conoids, elliptical cones, etc. The procedure was to compare theoretical and analytical models with experimental data to determine the adequacy of correlation and to postulate techniques to better represent the characteristics of the configuration. Once a reasonably accurate representation was derived to handle simple geometries, then a consistent approach was employed for configuration "build-up" and shaping, which could satisfy the demands of trim, stability, and controllability. After confidence was achieved in our ability to handle generalized configurations, various point designs were developed which enabled the convergence and interaction of the aerodynamic, aerothermodynamic, structural concepts, and control requirements for vehicle concepts synthesized to fulfill specific performance, weight, and payload constraints. Figure 2 displays this process from parametric variations, configuration build ups, and point designs.

The results of these investigations produced three candidate classes of lifting reentry configurations which are illustrated in Figure 3. They were categorized as the winged/body, the lifting body, and the blended body. The winged vehicles or winged/body configurations were generally characterized with lower sweeps and higher aspect ratios. They also employ

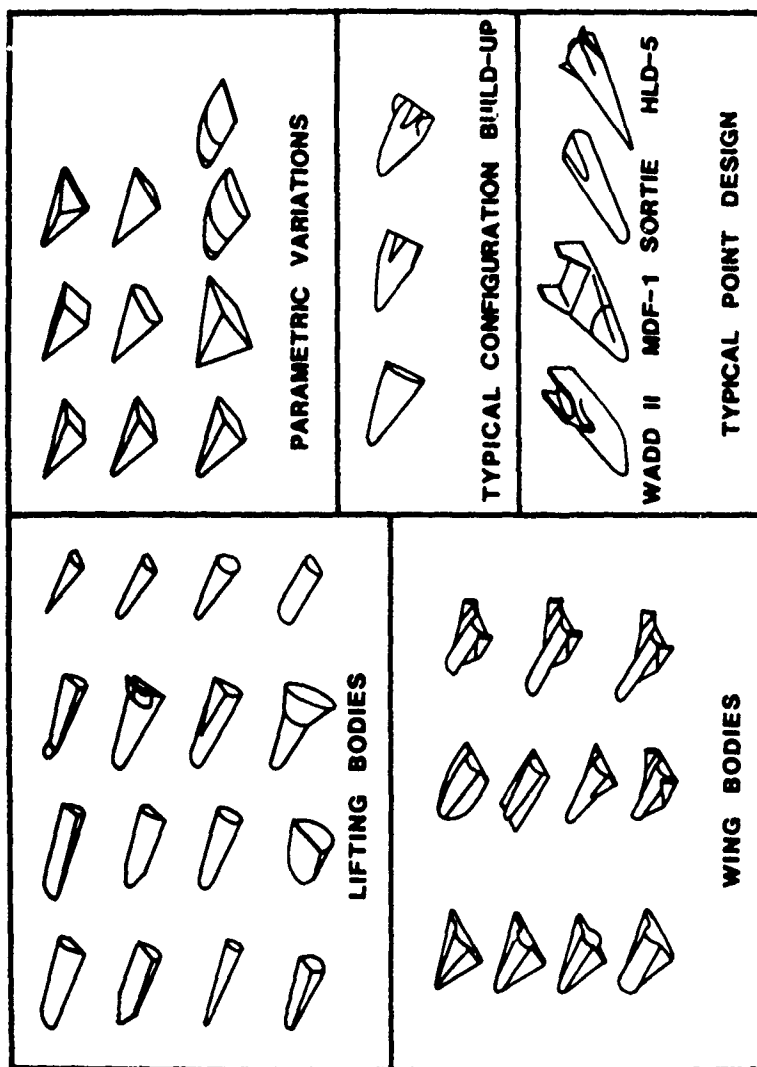
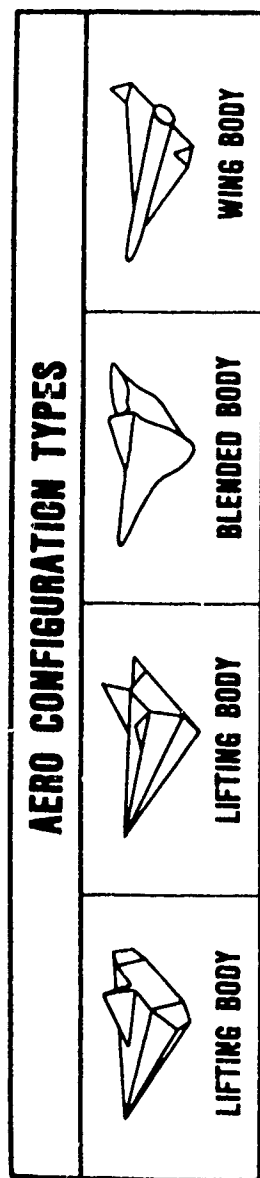


Figure 2. Classes of Configurations



CONFIGURATION SELECTION IS A CRITICAL DRIVER
CHOICE OF CONFIGURATION STABILIZING AND CONTROL SURFACES IS VITAL

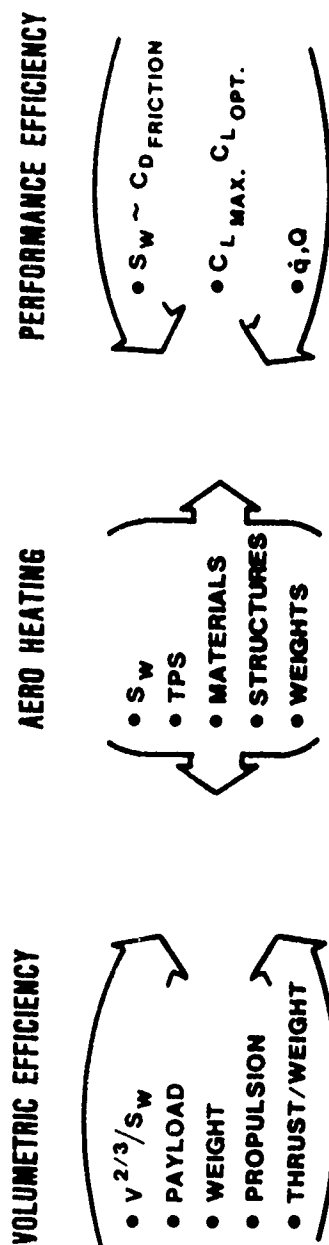


Figure 3. Key Technology Factors

more "conventional" leading edges and contoured surfaces with reduced base areas in order to improve the low and midspeed performance, including landing characteristics. Early in the investigations it became obvious that the lifting body vehicles offer substantial benefits in terms of volumetric efficiency which can be viewed as a first order indicator of payload carrying capability. High volumetric efficiency, $V^{2/3}/S_w$, also translates itself into reduced wetted area which means reduced skin friction drag; hence, a higher hypersonic lift-to-drag ratio which, in turn, results in higher levels of maneuverability both in terms of longitudinal and lateral range. Wetted area also is a first order indicator of the large surface areas which must be thermally protected; consequently, any reduction means a substantial dividend in terms of reduced thermal protection system weight. This, again, can be extended into reduced structural weight and total systems weight. In addition, the lifting body can generally be sized smaller for the same payload and mission requirements because of the increased volume. As a result of these benefits, increased emphasis was directed to the lifting body class of configurations by the Laboratory.

Configuration research covered a range of aerodynamic efficient vehicles from low to medium to high L/Ds over a wide range of Mach numbers (References 1-3). All the tools available were used to determine the technology sensitivities and drivers. Experimental data were obtained in both wind tunnels and aeroballistic ranges as shown in Figure 4. The wind tunnel tests were conducted across a complete Mach number range from subsonic through hypersonic speeds. The wind tunnel data were supplemented by tests conducted in the aeroballistic ranges. The test on ASSET shown in Figure 4 was run in the Naval Systems Weapon Center aeroballistic range. The results substantially added to the data base and confidence associated with the

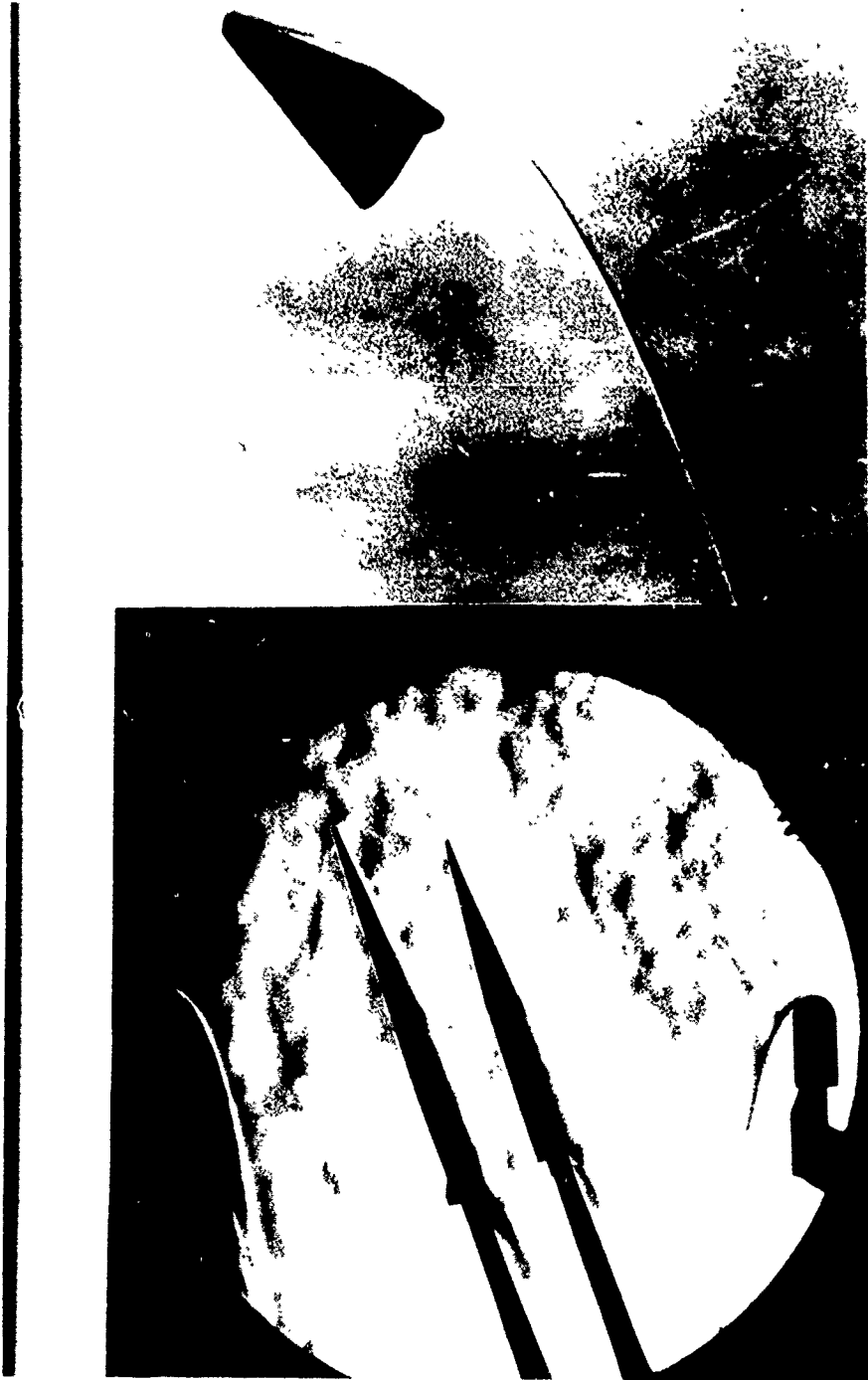


Figure 4. Force, Moment and Flow Visualization

aeromechanic and aerothermodynamic design of these configurations and represent one of the first series of successful lifting vehicles tested in an aeroballistic range.

Another generic family of lifting body configurations was developed and designated the MDF series. The approach used in these designs was to consider both the constraints demanded by hypersonic flight and those imposed by low speed performance. Nose and leading edge bluntness, sweep, and lower surface geometry were established, but the designs were carefully developed for shaping, contour, and camber of the upper surface to achieve improved low speed performance. A complete family of these configurations employing this dual design approach was addressed and actually employed classical airfoil sections molded into lifting bodies. The hypersonic lift-to-drag ratios generally spanned the range from 1.0 to approximately 1.6, but with substantially improved subsonic L/Ds and characteristics. The MDF-1 configuration, which molded a Clark Y airfoil into the lifting body, can show a lineage with the SV-5 configuration used in both the PRIME and PILOT programs. The MDF-1 configuration is shown in Figure 5.

An additional series investigated was postulated as potential configurations for entry at supercircular velocities (References 4-5). This was essentially a series of modified elliptical cones designated as the Super Orbital Reentry Test Integrated Environment (SORTIE) family of configurations. The lift-to-drag ratios achieved were between 0.75 and 1.2 with near neutral stability to facilitate large modulations in the lift coefficient. This configuration series focused primarily on the technologies which required solution for reentry from high energy orbits, including geosynchronous. Reentry velocities of approximately 34,000 ft/s from orbital altitudes of 20,000 nm were considered. There are many

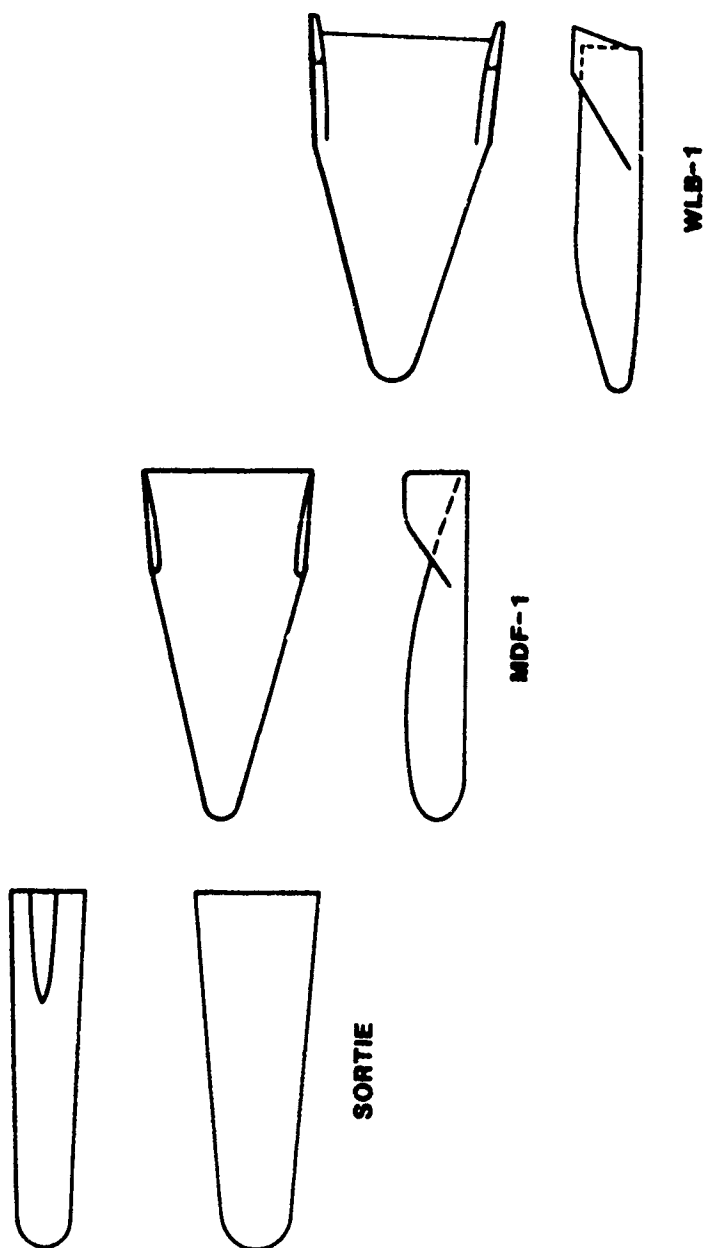


Figure 5. Hypervelocity Vehicle Configuration

problems associated with flight at velocities from 25,000 to 34,000 ft/s. The most critical problems are heating and stability. At supercircular reentry velocities the gas encountered is highly dissociated, partially ionized, and at twice the enthalpy levels as that encountered during low earth orbital reentry. Hot gas radiation of the shock layer becomes important and significant deficiencies in predicting heating values may occur depending on the prevailing state of equilibrium. The heat transfer rates will be substantially higher than from low earth orbital lifting reentry. The lateral, directional, and longitudinal stability and control characteristics of these high energy reentry vehicles at angle of attack became extremely challenging.

The SORTIE lifting body configuration shown in Figure 6 employed flat surfaces on the upper surface and on each side primarily for directional stability. Various control devices were investigated, including canards, elevons, flaps, cambered bodies/nose, and jet spoilers. The delta canards and elevons were evaluated separately, and in combination. Flaps mounted on the trailing edge proved to be quite effective and permitted the vehicle to be trimmed across the speed range. They were the preferred control device based on a combination of effectiveness and minimum heating. The combination of canards and elevons yielded the greatest trim power and highest trim L/Ds, but caused excessive aerodynamic heating. Aerodynamic drag devices, to independently modulate the drag relative to the lift also appeared to offer promise. Two techniques evaluated were the ejectable drag brake and the slide-trolley drag break which would be used during the initial portions of supercircular reentry. Many control and drag devices were tested as part of a comprehensive configuration/control surface research program.

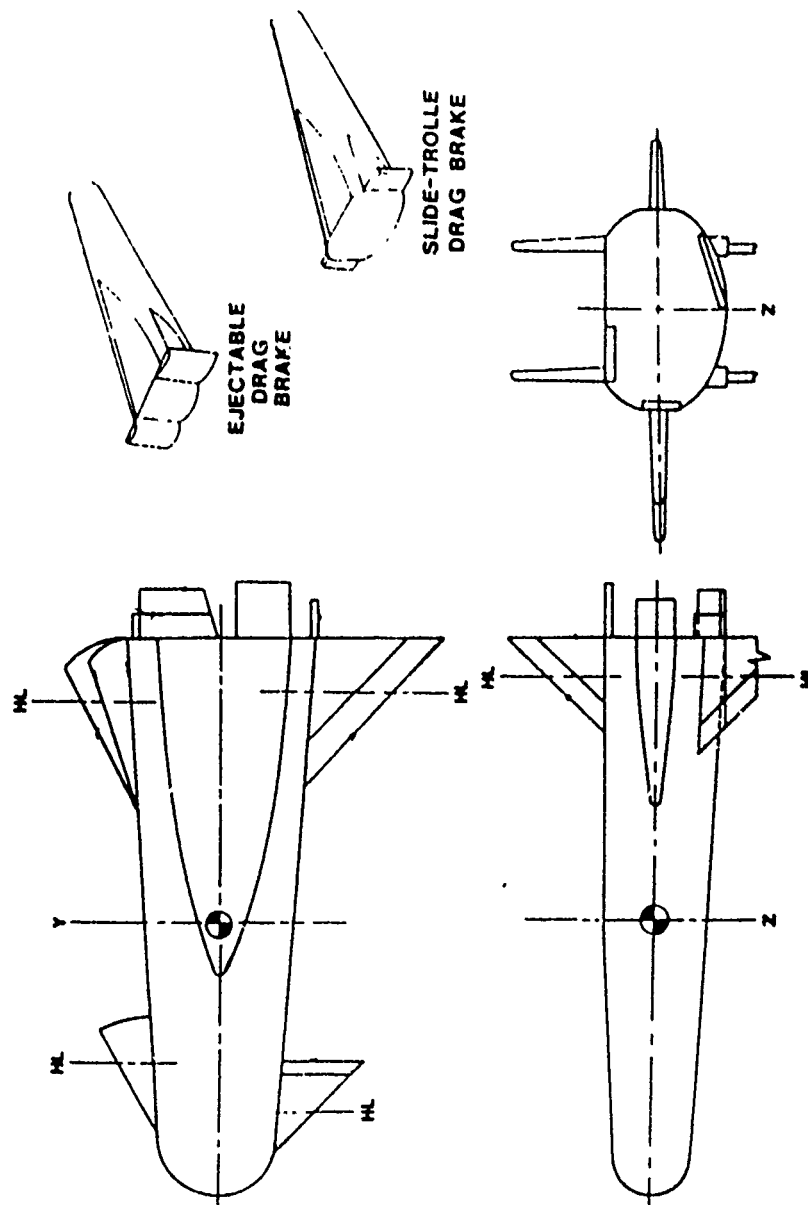


Figure 6. Aero Control and Auxiliary Drag Devices Summary

In 1961, the Air Force Flight Dynamics Laboratory initiated a flight test program designed to assess the applicability and accuracy of analytical methods and experimental techniques in the areas of structures, aerodynamics, aerothermodynamics, and aerothermoelasticity for a hypersonic glide re-entry vehicle (References 6-7). Much of this data could not be obtained in existing ground test facilities. Hence, a research step was essential to provide a higher degree of assurance in the design and development of future manned and unmanned, hypervelocity glide reentry and cruise vehicles. The name of this program was Aerothermodynamic/Elastic Structural Systems Environmental Tests (ASSET).

The ASSET Program objectives can be summarized as: (1) the correlation of data from hypersonic flight test with ground facility data, (2) the verification of analytical theories and prediction techniques, and (3) the evaluation of structural concepts and materials for hypersonic vehicles. The actual vehicle configuration took advantage of, and evolved from, a research configuration, WLB-1, included within the Laboratory's program. The ASSET configuration, with a $L/D = 1.25$, consisted of a flat bottom, 70° swept delta with a planform area of 14 ft^2 blended with a cone cylinder lifting body. Figures 7 and 8 illustrate the relatively simple vehicle configuration and its characteristics which were deliberately selected to simplify analysis, provide a relatively large volume, and allow the maximum use of available wind tunnel data. The vehicles' wing loading was about 85 lb/ft^2 and the angle-of-attack range varied from 20 through 40 degrees. Six vehicles were launched to altitudes ranging from $166,000$ to $212,000 \text{ ft}$ and at velocities of $13,000$ to $19,500 \text{ ft/s}$.

The ASSET flight program provided the first significant hypersonic flight information applicable to lifting reentry technology. The

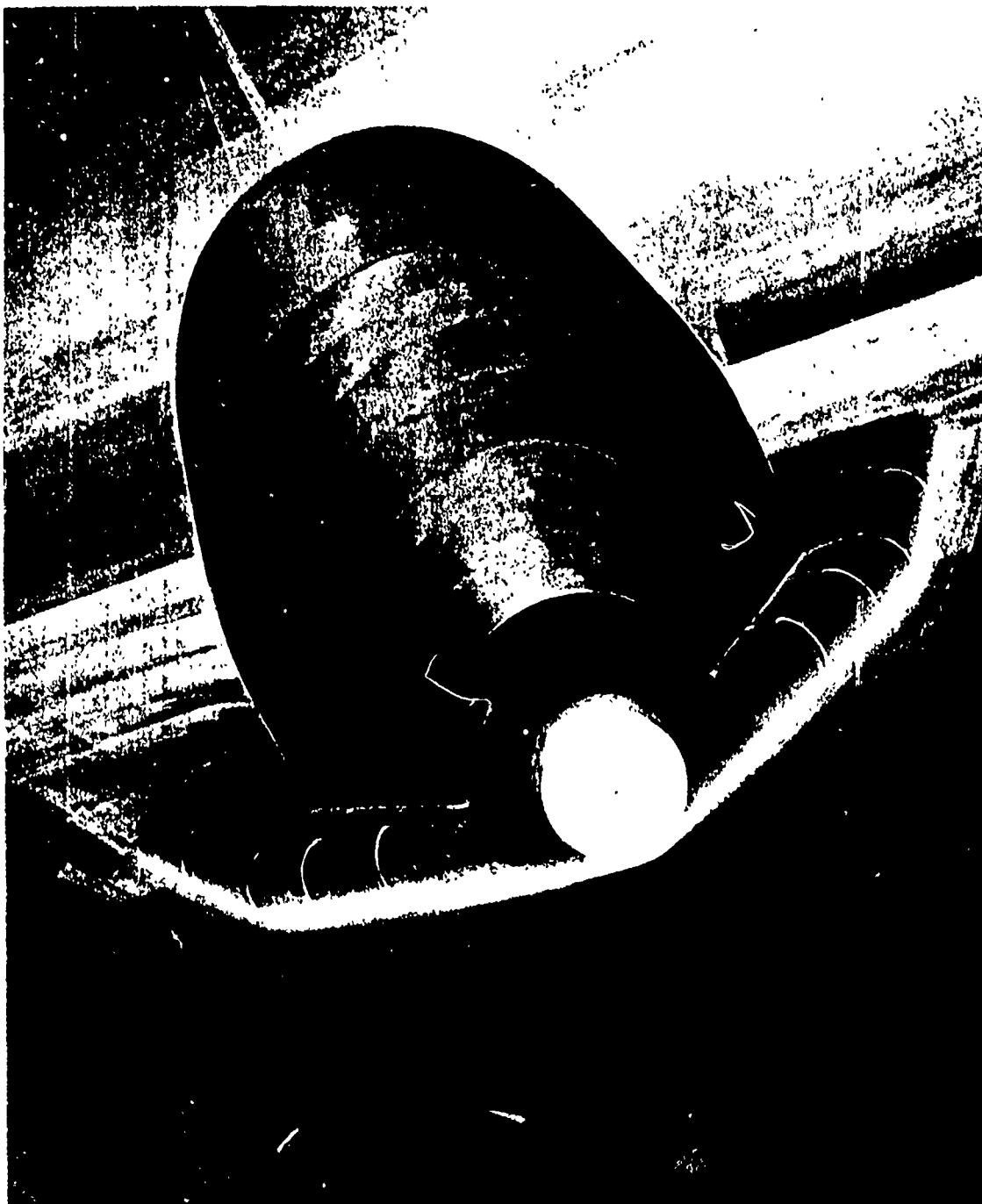


Figure 7. ASSET in Gliding Flight

Length	68.82 Inches
Span	54.88 Inches
Height	32.79 Inches
Wing Sweep	70 Degrees (True)
Wing Area	14 Square Feet
Nose Tip Radius	3 Inches
Leading Edge Radius	2 Inches
Average Weight	
Aerothermodynamic	
Structural Vehicle	1130 Pounds
Aerothermodynamic	
Elastic Vehicle	1225 Pounds

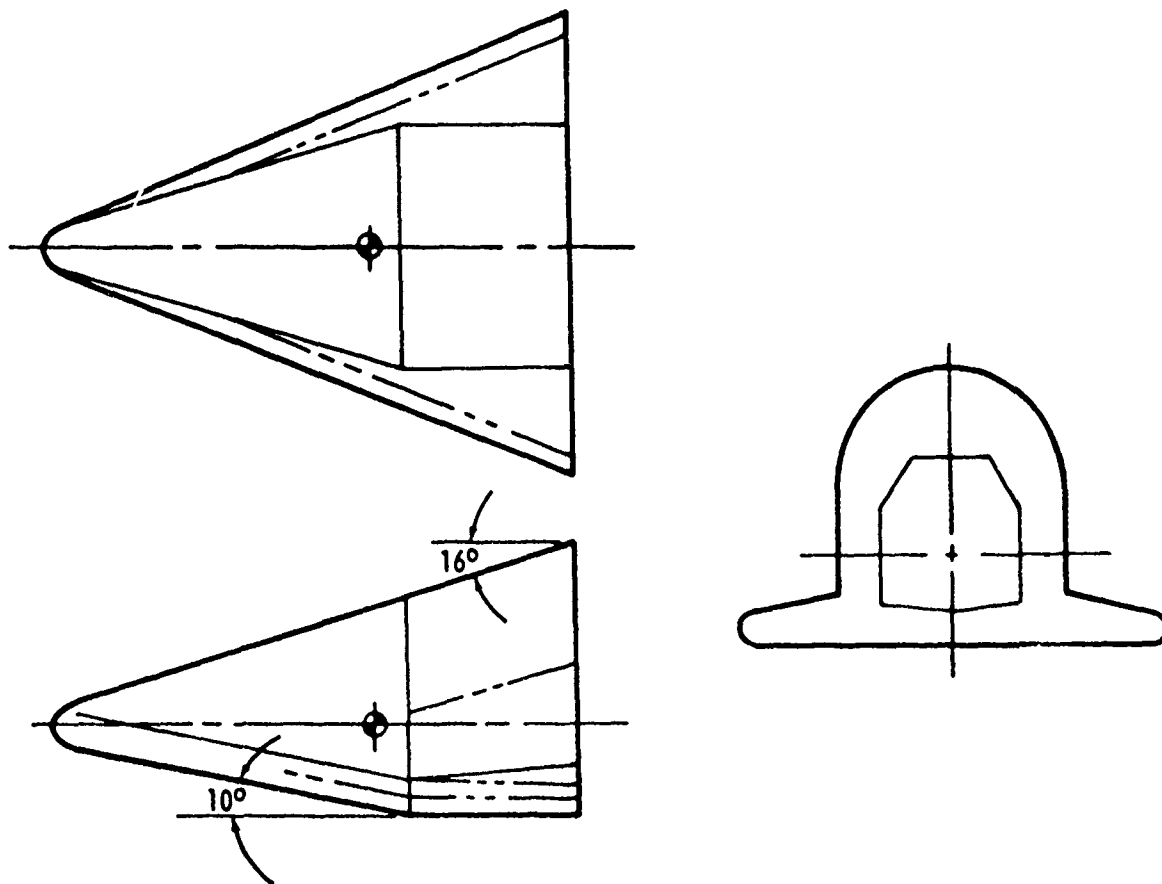


Figure 8. ASSET Vehicle Configuration

aerodynamic pressures, temperatures, heat transfer, material, and structural information obtained proved especially beneficial in the evaluation and understanding of the data obtained from subsequent programs, including ground test. The thermal protection system employed was metallic and reradiative and has proved to be particularly valuable relative to the understanding of the material capabilities and the evolution of structural concepts.

Another important Air Force lifting reentry flight test program was designated Precision Recovery Including Maneuvering Entry (PRIME). The PRIME and Piloted Low Speed Test (PILOT) programs have been designated the X-23 and X-24A programs, respectively. The programs had a component relationship with the PRIME being the hypersonic unmanned vehicle and the PILOT being its manned trisonic counterpart. The objectives of the PRIME program can be summarized as: (1) the acquisition of ablative heat shield and aerodynamic data, (2) the demonstration of accurate guidance to the recovery point, (3) the demonstration of cross range maneuvering, (4) demonstration of vehicle recovery system, and (5) a design for performance with minimum weight.

The PRIME configuration, designated the SV-5 is shown in Figure 9. It was a lifting body with a sweep back of 77° and a hypersonic lift-to-drag ratio of approximately 1.3. Its lower surface was flat and its wing loading was approximately 67 lb/ft². It operated at angles of attack from 21° to 52° , at a maximum velocity of 25,600 ft/s and a maximum altitude of 400,000 ft. It weighed approximately 860 lb and was boosted to orbital speeds on ATLAS boosters. Three flights were flown from the Pacific Missile Range with a primary thermal protection system which was ablative; however, stable shape geometry was maintained since the temperature levels achieved were

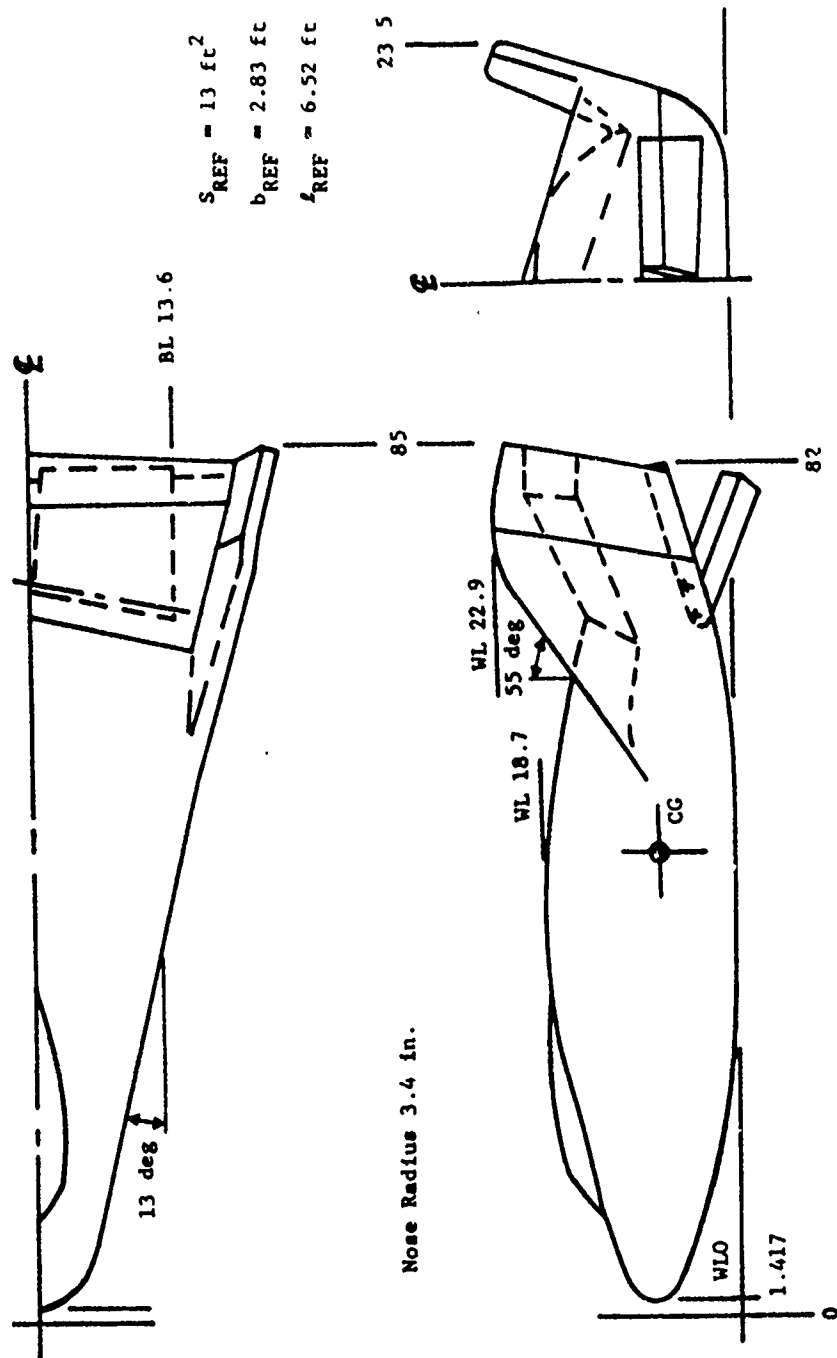


Figure 9. PRIME SV-5D General Arrangement

generally alleviated by the reradiative properties of the materials used. Pressure, force, temperature, heat transfer, hinge moments, and stability information were obtained from the flight test, as well as the integrity of the thermal protection system and structural concept for the Mach range 26 to 2 (Reference 8). Post-flight wind tunnel tests, Figure 10, were conducted with a recovered vehicle in order to assess any effects on the aerodynamic characteristics after the ablative thermal protection system had charred. Based on these tests and data acquired, a simple method was devised to simulate ablative effects on sub-scale wind tunnel models (Reference 9).

There evolved an intense interest in highly efficient lifting body vehicles because of inherent operational advantages. The performance advantages (Figures 11, 12, 13) associated with increased hypersonic lift-to-drag ratio are significant for many operational factors such as increased longitudinal and lateral range capability, rapid recall and response time (References 10-17). Figure 12 indicates the large reduction in number of bases required for recovery as a function of lift-to-drag ratio. Maneuvering within the atmosphere by proper combinations of angle of attack and bank angle can produce the range capabilities shown in Figure 13 in terms of maneuvering landing footprints.

The configurations capable of achieving a $L/D \sim 3$ at a velocity of 20,000 ft/s and altitude of 200,000 ft were designated high L/D vehicles. The high lift-to-drag ratio vehicle shapes are generally characterized by highly swept configurations possessing low bluntness ratios and high fineness ratios. These configurations tend to operate at reduced angle of attack to achieve their maximum lift-to-drag ratios. Obviously, the leeward or upper surface, with its expansion pressures, must be treated

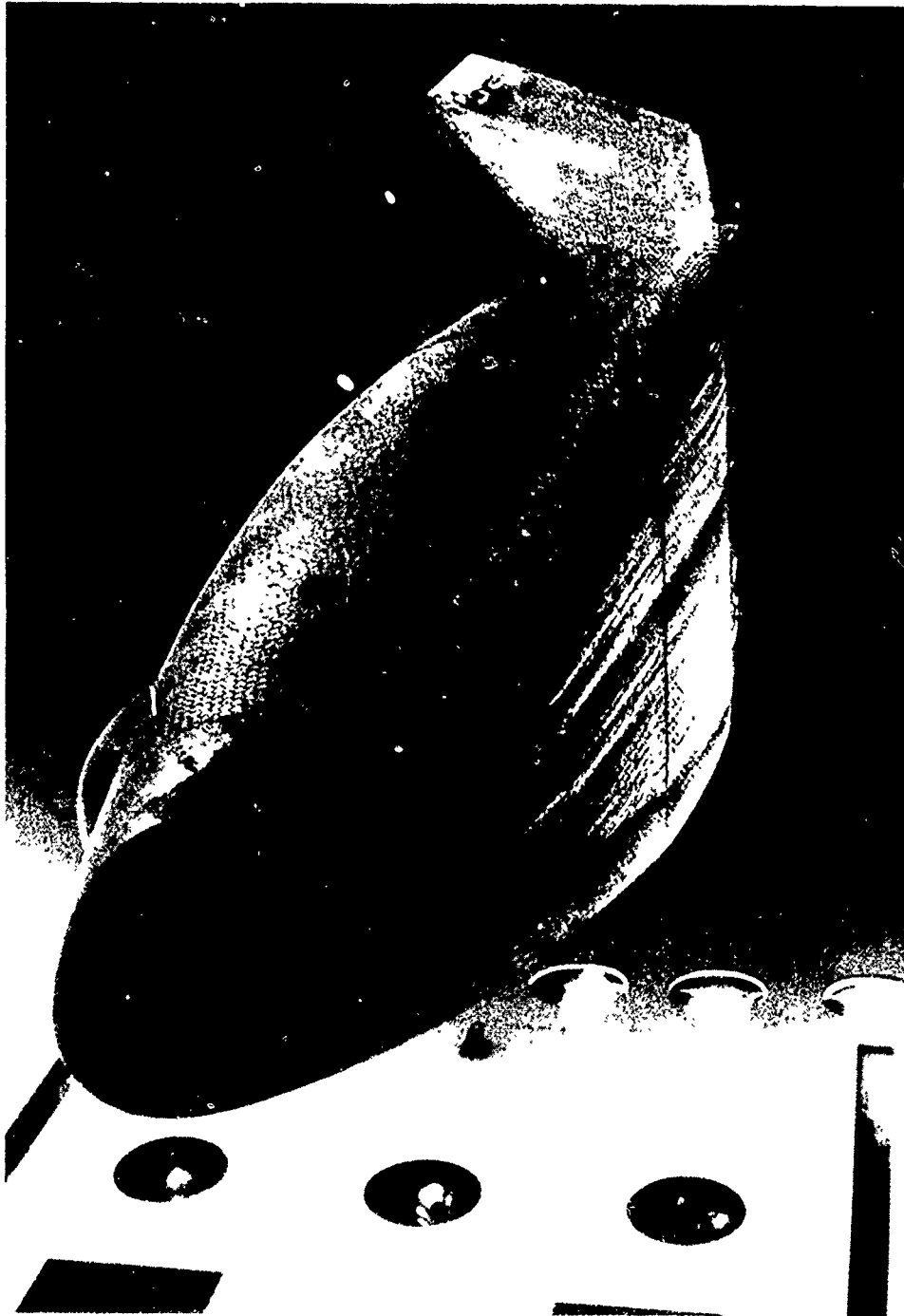


Figure 10. Test of Recovered Prime Vehicle

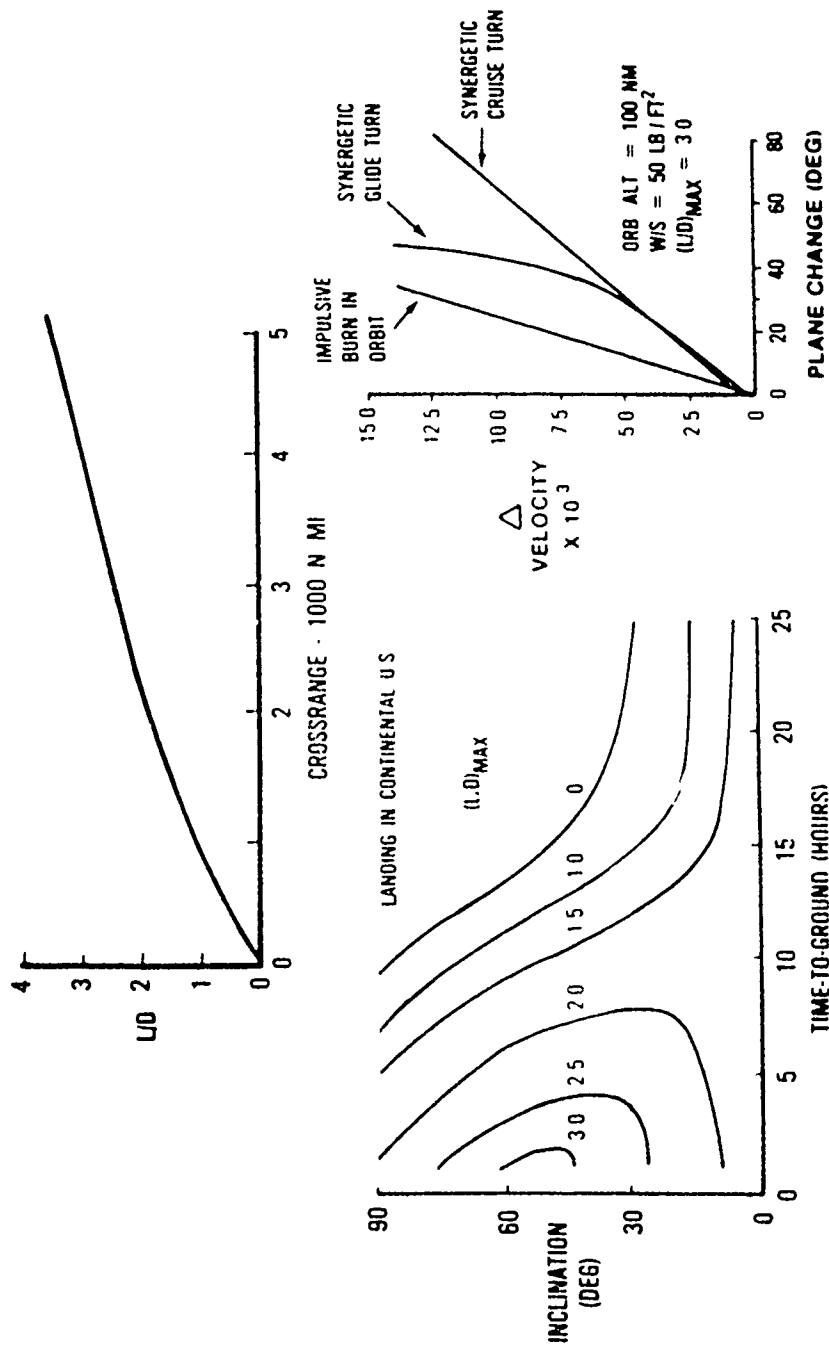


Figure 11. Payoff of Aerodynamic Efficiency

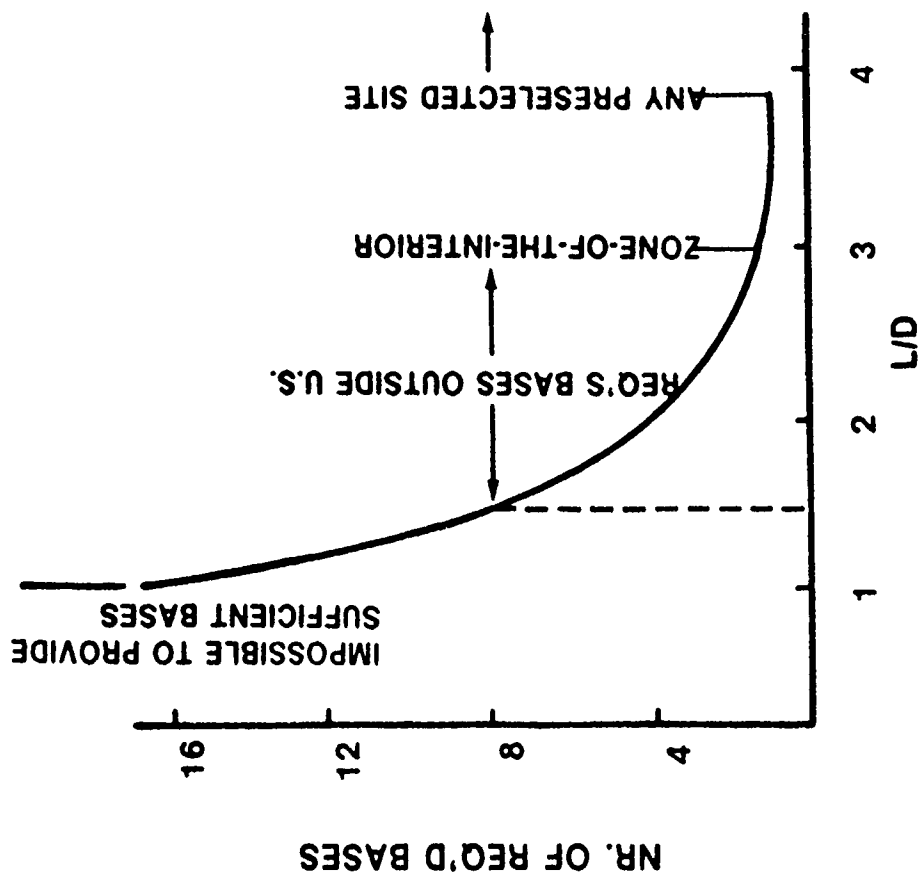


Figure 12. Air Base Requirements

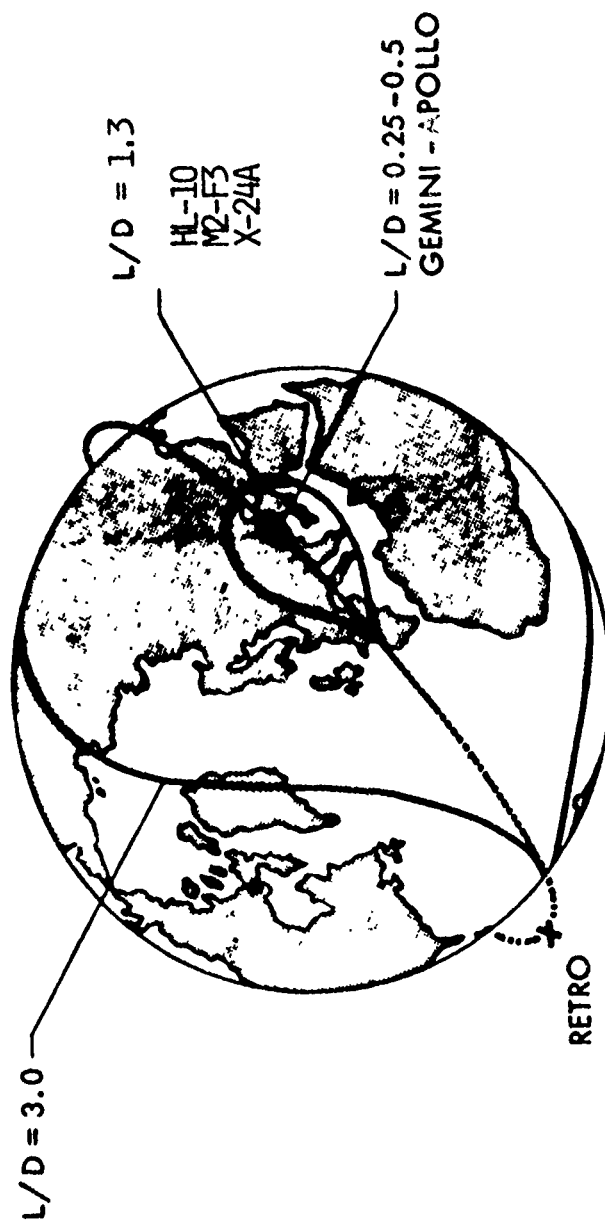


Figure 13. Maneuver Performance of Lifting Reentry Vehicles

more accurately with deliberate tailoring to improve aerodynamic efficiency. Viscous effects, as reflected in skin friction force terms, are critical, and wetted area becomes important. Viscous interaction and boundary layer transition were identified for more precise treatment. Interaction effects can be masked by blunt leading edges, but become more important for consideration in the slender designs.

Aerodynamic heating, because of the changes in angle of attack and sweep back conditions, was also indentified for more in-depth assessment. This, of course, was also aggravated by the increase in flight times and could likely necessitate advanced cooling techniques. Further, because of the nature of not only the flight path, but also the generic configurations considered for increased performance efficiency, extensive use of aerodynamic control surfaces appeared to be desirable. This then enabled the focusing of research not only on control effectiveness and design, but also on the aerothermodynamic problems encountered with such deflected surfaces.

The initial efforts with high lift-to-drag ratio configurations were characterized with cautious optimism and approached the feasibility question both analytically and experimentally. Both fixed and variable geometry configurations were investigated with the intent of making the designs amenable to both high speed and low speed flight. The objective was to achieve high aerodynamic efficiency at hypersonic speeds with acceptable low speed performance. Favorable interference configurations were also assessed, but for the most part, were discontinued because of the added complexities associated with localized heating problems, increased TPS, and added weight.

A chronology of configuration research by the Laboratory is presented in Figure 14. The initial efforts were concentrated on low L/D vehicles and winged configurations similar to high speed aircraft. Heavy emphasis was placed on understanding the fundamentals of hypersonic flow and proceeding to the development of simple and then complex configurations.

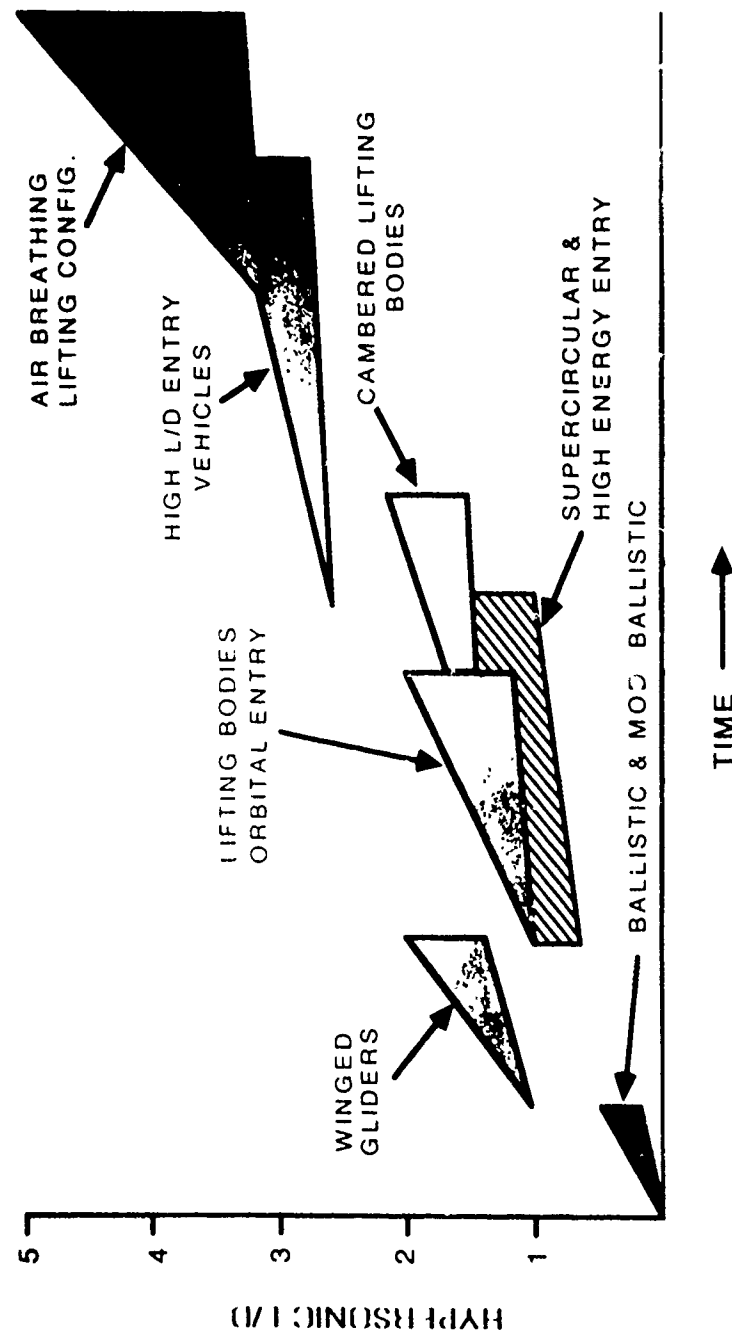


Figure 14. Configuration Research

4. LIFTING BODY CONFIGURATION DEVELOPMENT

A generic family of configurations shown in Figure 15 evolved from the early parametric configuration data base which were characterized by high volumetric efficiency. The high L/D configurations were assessed for aerodynamic feasibility, aerothermodynamic acceptability, performance flexibility, volumetric efficiency, size and comparative weights, thermal protection system and structural concepts. The validated analytical results indicated that high L/D configuration technology had progressed to the point where stable, controllable vehicles, with large volume, could be designed for specific missions and survive the heating environment. The program in the Flight Dynamics Laboratory was converged in the mid-1960s into four highly acceptable designs; i.e., the FDL-5, FDL-6, FDL-7, FDL-8 configurations, the latter of which evolved into the X-24B and X-24C configurations (References 18-26). These configurations are displayed in Figure 16 with a pictorial representation of their evolution.

The technology which permitted this advancement to point designs was the development of accurate pressure and skin friction prediction methodologies (References 27-29). The Supersonic/Hypersonic Arbitrary Body Program, often abbreviated S/HABP is the backbone of the prediction techniques. The heart of the program is an arbitrary body surface integrator. In this case, pressure and shear stress are integrated to evaluate aerodynamic forces and moments. The shape is described by a set of three dimensional/space coordinates, and the smooth surface is reduced to a number of planar facets. The local pressure on each increment is evaluated using Newtonian, tangent cone, tangent wedge, or some similar theory. Shear



Figure 15. Lifting Body Configurations

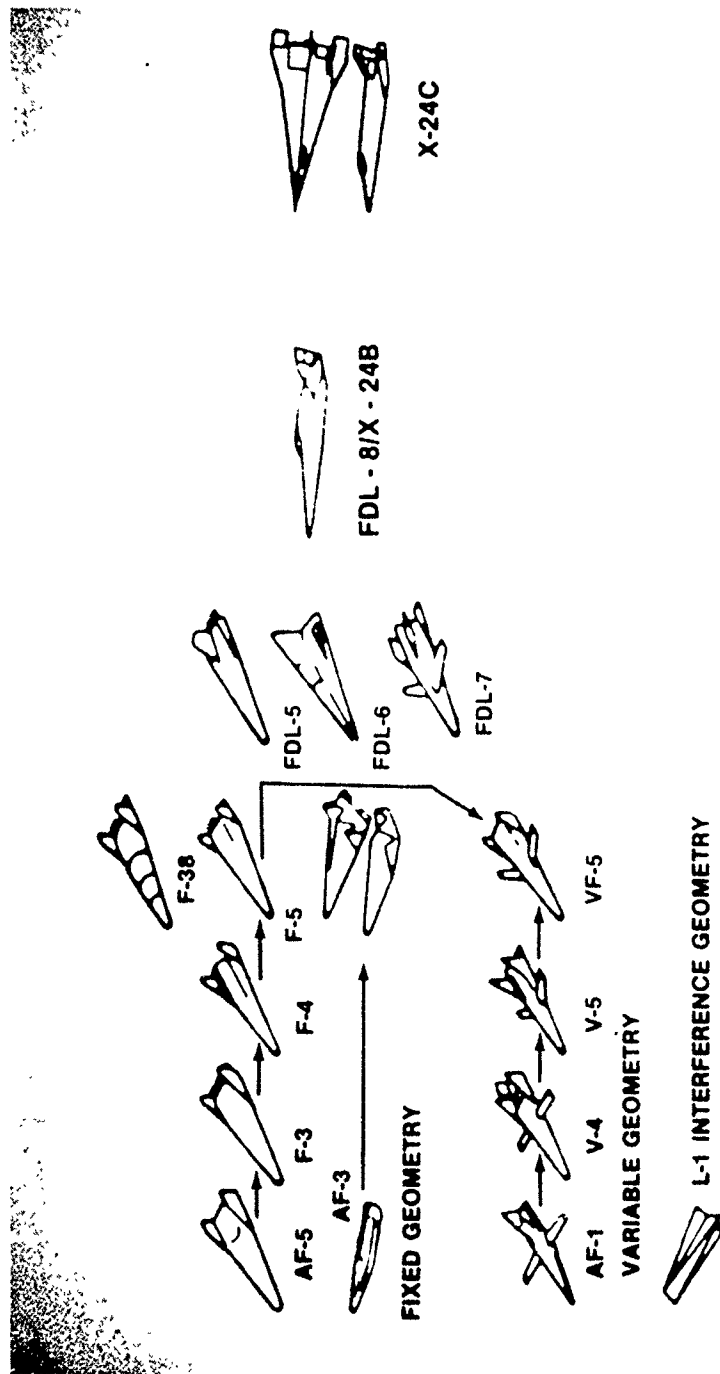


Figure 16. High L/D Configuration Evolution

stress is evaluated using algebraic relations, such as the reference temperature method for laminar and turbulent cases (Reference 30). The S/HABP is a powerful tool for evaluating hypersonic aerodynamic characteristics. It has been used to develop guidelines for leading edge sweep, nose and leading edge radii, cross section contours, fore and aft ramp angles, pitch and yaw stability, and control effectiveness. Figures 17, 18, and 19 show the type of parametric investigations conducted. The skin friction methods have been verified by wind tunnel data, and the methods are used to extrapolate sub-scale test results to full scale flight. The S/HABP was used in the development of the Flight Dynamics Laboratory high lift-to-drag ratio vehicles.

In the early years of hypersonic technology development, a major limitation was the simulation capability of wind tunnel facilities at high Mach numbers over a range of Reynold's numbers. This created a major obstacle in understanding the influence of viscous interaction on the skin friction drag, i.e. interaction of the leading edge shock wave with the boundary layer. As experimental facilities became available, the accuracy of the theoretical methods could be evaluated. This rapidly led to modifications of the methodology based on wind tunnel data. Two major correlation parameters evolved to predict the influence of low density flow on the aerodynamic characteristics. They were designated the viscous interaction parameter $\frac{M^3}{\sqrt{R_{N_L}}}$, and the rarefaction parameter, $\frac{M}{\sqrt{R_{N_L}}}$. A

modification of the rarefaction parameter, Reference 31, based on the Chapman-Rubesin solution for uncoupling the momentum and energy equations at a reference temperature condition within the boundary layer permitted a correlation of wind tunnel data from several facilities and the

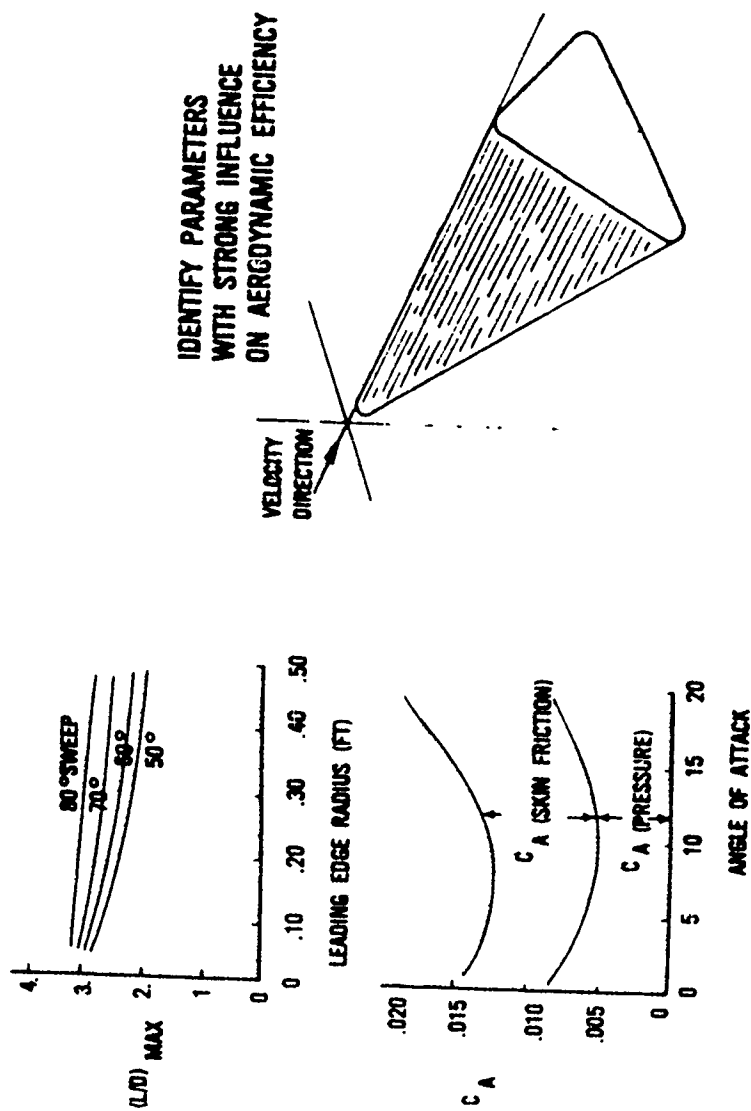


Figure 17. Configuration Aerodynamics for Lifting Bodies

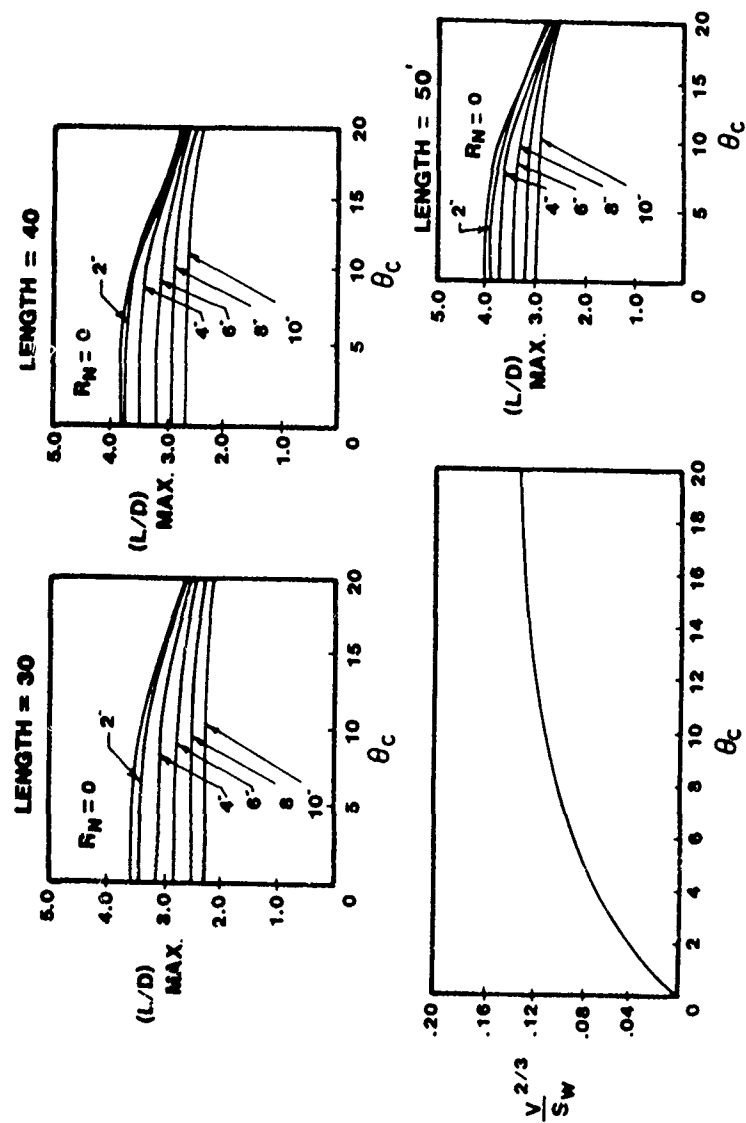


Figure 18. Geometry Effects on L/D

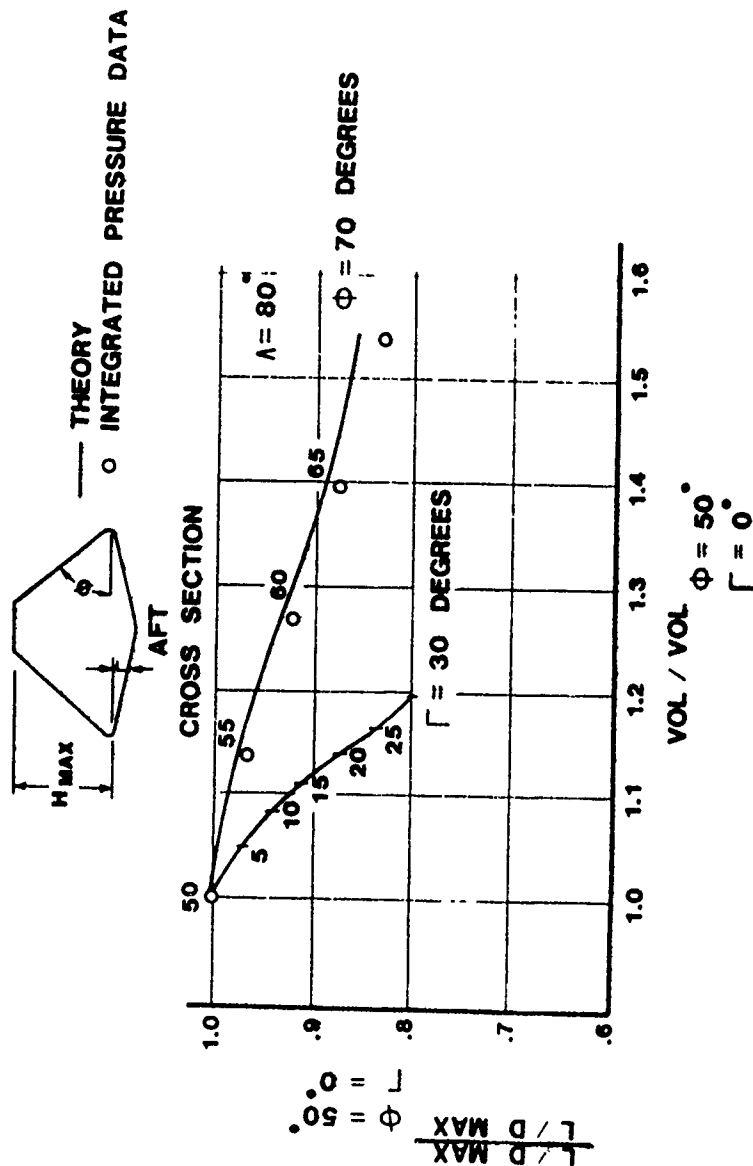


Figure 19. Volume Increase Through Cross Section Changes

extrapolation of data to free flight conditions. In Figure 20, the modified rarefaction parameter $\frac{M \sqrt{C^*}}{\sqrt{R_{N_L}}}$ is shown to provide excellent correlation with

wind tunnel data obtained on the FDL-5 configuration. The value of $\frac{M \sqrt{C^*}}{\sqrt{R_{N_L}}}$

at the flight condition of $V = 20,000$ ft/s and an altitude of 200,000 ft for a 35 ft vehicle is 0.0106. This corresponds to a trimmed flight hypersonic L/D max of 2.84.

The next hurdle involved shaping the lifting body configurations for adequate longitudinal, lateral, and directional stability (References 32-35). The lifting body lends itself to many options for providing directional stability. Several approaches are depicted in Figure 21 including the complete elimination of the vertical fins. The configurations chosen for more complete assessment were generally those with the higher aerodynamic performance efficiency as well as geometric compatibility with the payload bay of the space shuttle. One of the more unique configurations developed was the FDL-5 series illustrated in Figure 22. The basic problem addressed in this design was to eliminate the fins of the vehicle without degrading the hypersonic L/D, the subsonic L/D and the hypersonic directional stability. The large aerodynamic fins usually located in the outboard aft portions of the high speed vehicles have consistently presented design problems associated with unpredictable flow phenomena, high aerodynamic heating, dynamic instabilities and high structural weight.

The design approach conceived by the Air Force Flight Dynamics Laboratory and modified by the Lockheed Aircraft Company involved a new approach to configuration shaping called compression sharing. Compression

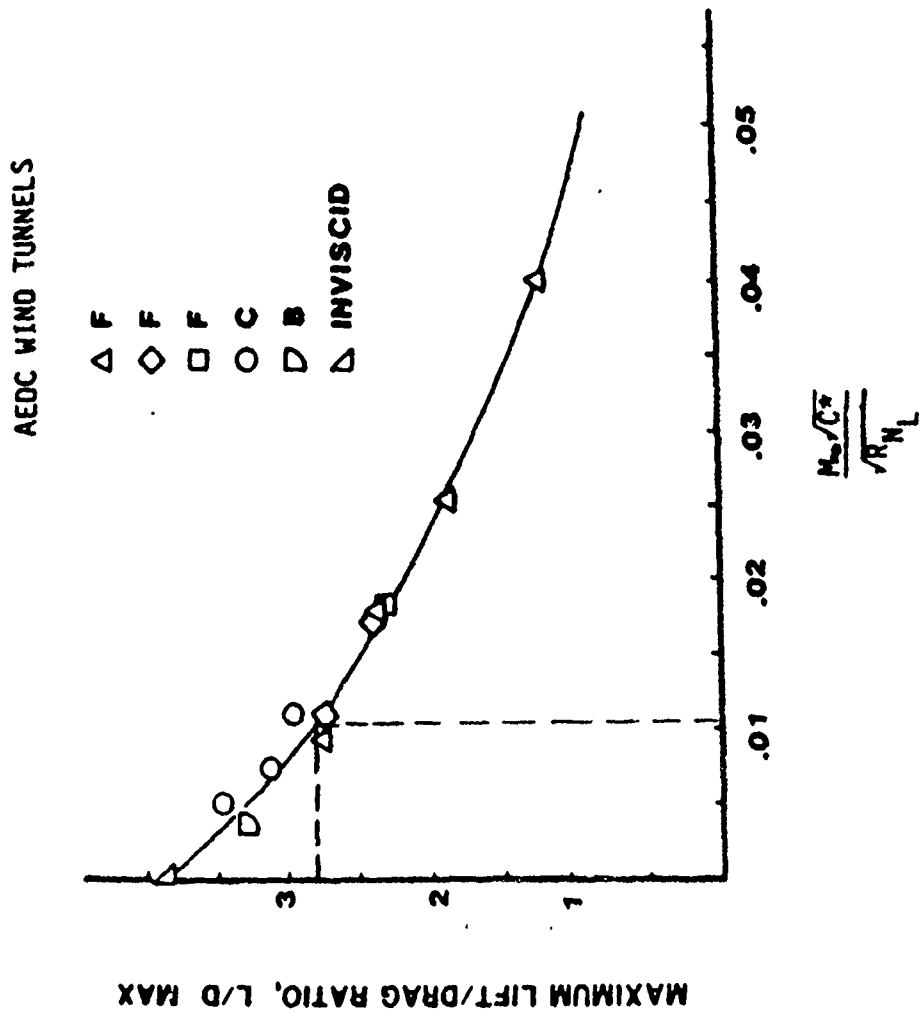


Figure 20. Rarefaction Correlation Parameter

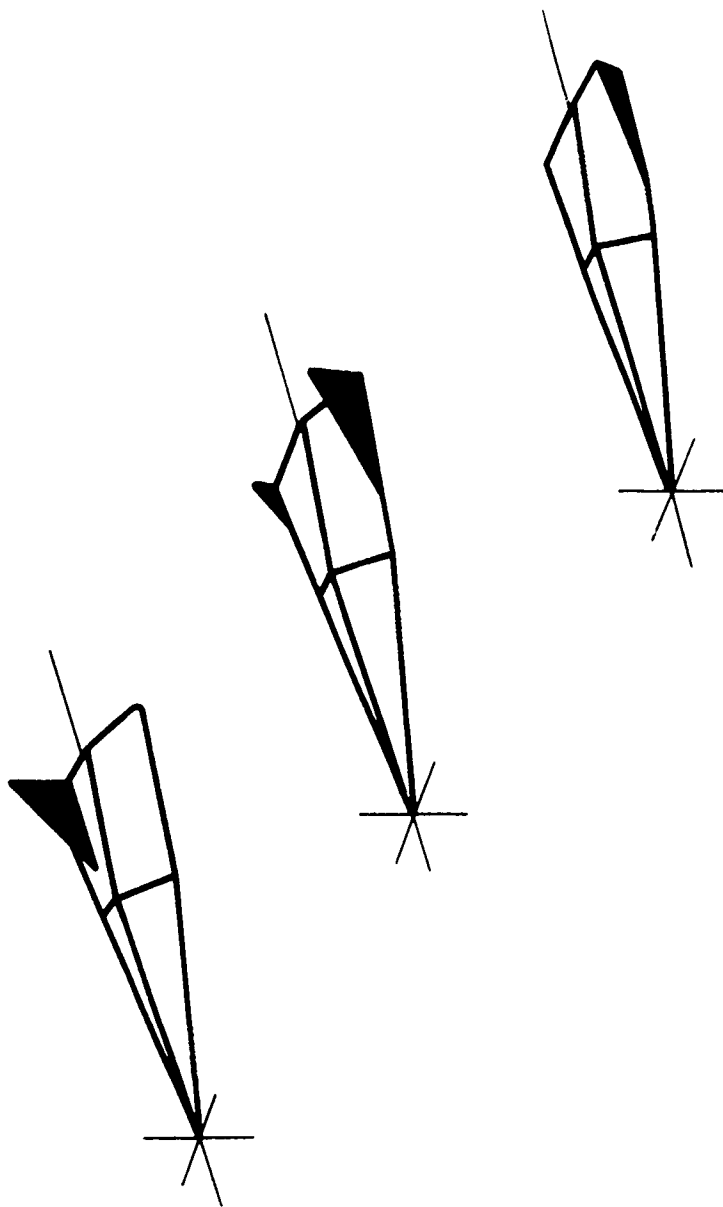


Figure 21. Configuration Variations For Directional Stability



Figure 22. FLL-5 Compression Spring Design

sharing is the precise contouring of the aft body that distributes directionally stabilizing pressures at hypersonic speeds to provide maximum effectiveness and the lowest drag. This compression sharing concept has been successfully demonstrated in wind tunnels from Mach numbers of 2 to 19 (References 23-26). Experimental data indicated a center upper vertical fin was required for lower speed flight. The Laboratory designed and fabricated a full scale mock-up of the FDL-5 lifting body configuration to assess the volume distribution and the location and arrangement of various subsystems. This mock-up is shown in Figure 23 sitting on a ramp at Wright Field.

In the development of a comprehensive data base for the FDL-6, FDL-7 and FDL-8, extensive force, moment, pressure and temperature tests were conducted across the complete Mach number range from subsonic through hypersonic speeds (References 36-41). The lateral or cross range performance capabilities of these high L/D configurations are shown in Figure 24, along with the variation in hypersonic lift-to-drag ratio.

To assess the viability of a configuration, major consideration must be given to the impact of aerodynamic heating (References 42-52). Extremely high temperatures on configuration components or interference regions can easily cause a configuration to be discarded. Temperatures at the stagnation point of a configuration have been evaluated parametrically as a function of the glide parameter $W/C_L A$ as shown in Figure 25. These calculations were made assuming an equilibrium glide trajectory at the velocity where peak laminar heating occurs (21,000 ft/s). Both a spherical nose and an ellipsoidal nose made of refractory material having 0.8 emissivity were considered. Also shown in this figure is the range of maneuverability of a nominal $W/A = 60 \text{ lb/ft}^2$ configuration operating at maximum

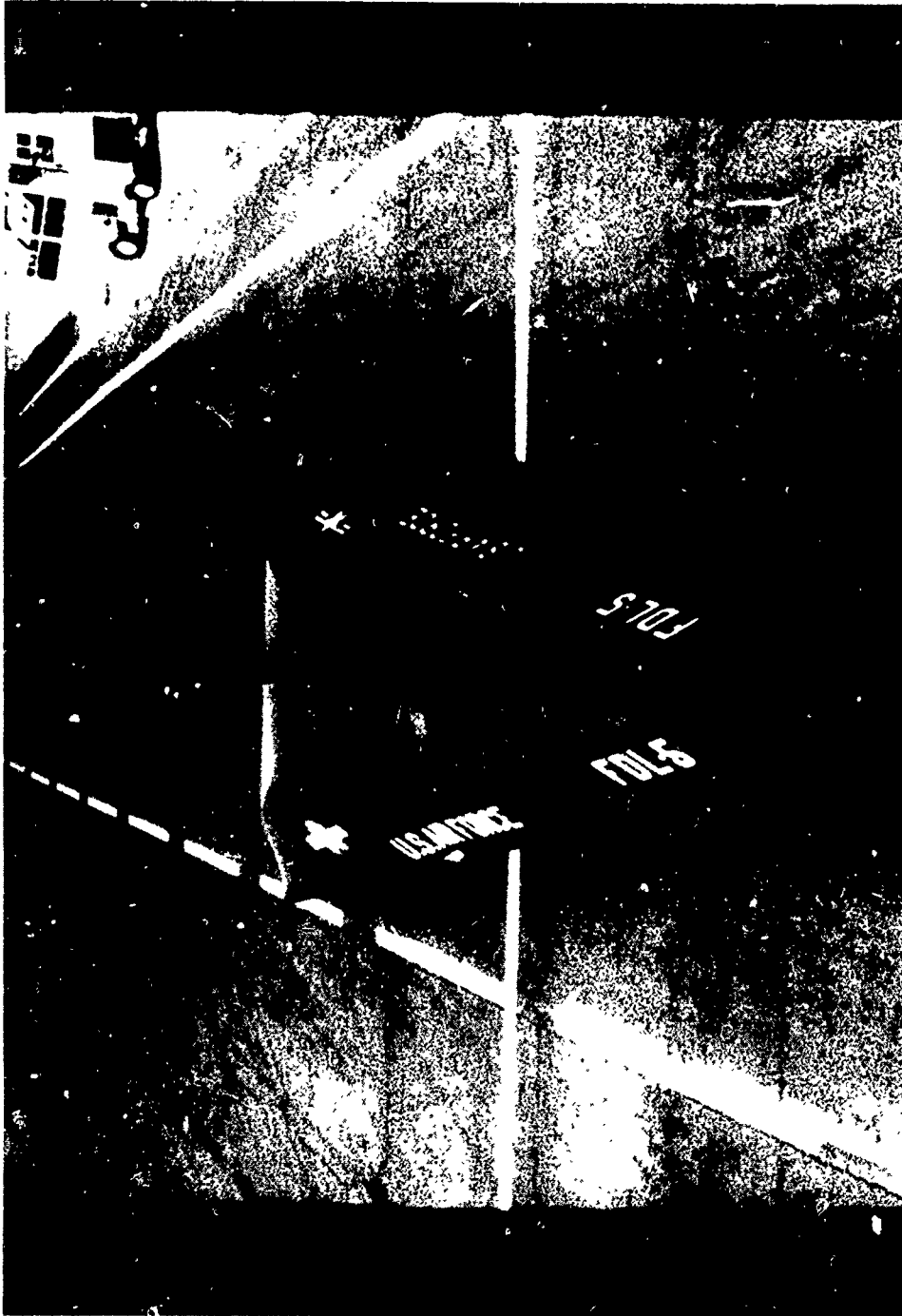


Figure 23. Full Scale Mockup of the FUL-5

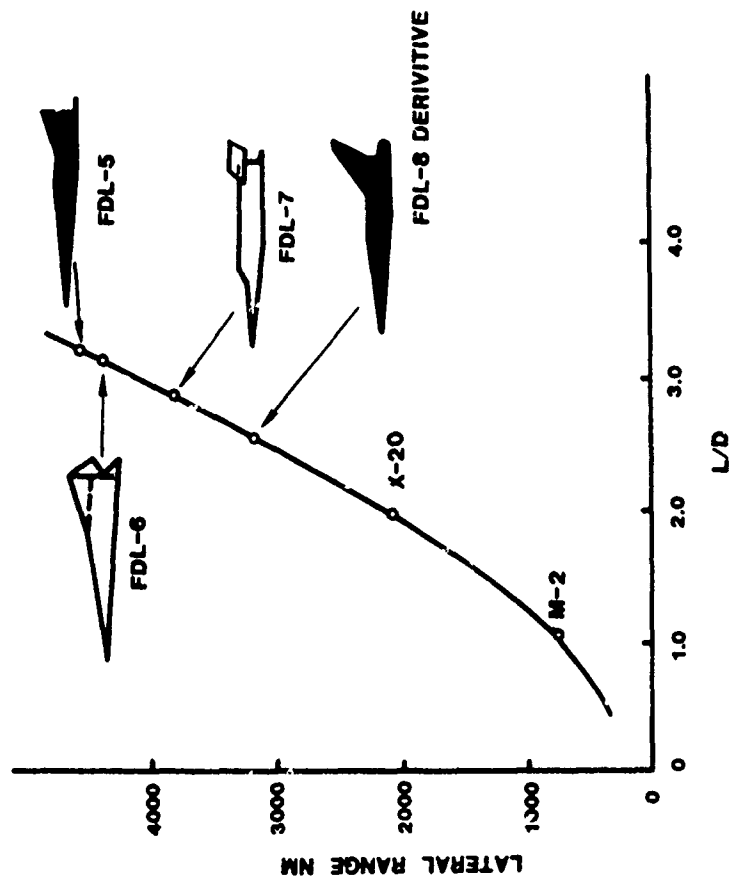


Figure 24. L/D for Typical Configuration Designs

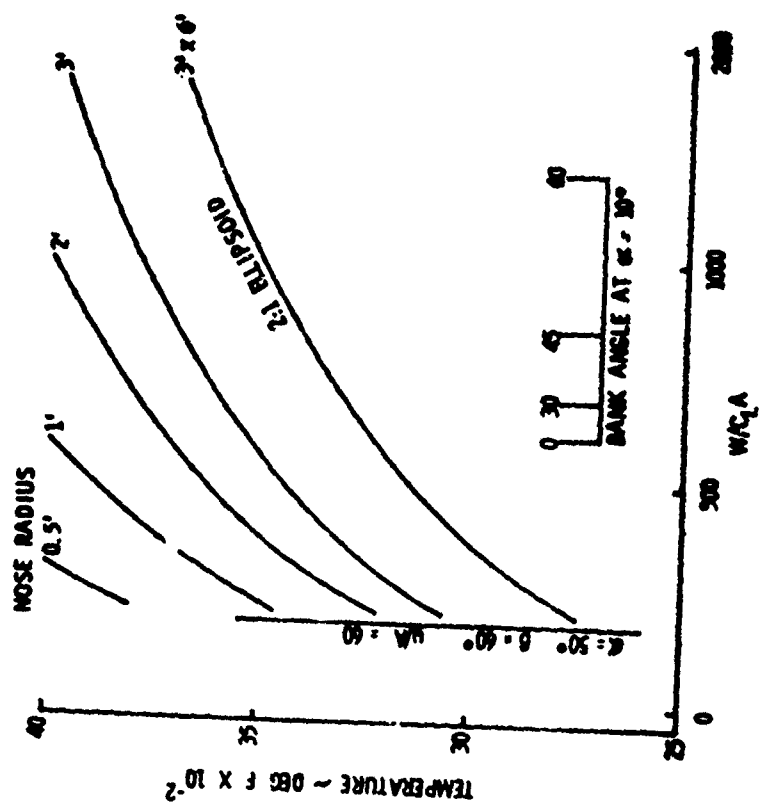


Figure 25. Nose Temperatures

lift-to-drag ratio ($\alpha \sim 10^\circ$). This attitude both maximized maneuvering cross range and represents the maximum heating condition to which the nose cap will be subjected. Operations at higher angles of attack will substantially reduce the nose temperature as the glide parameter is reduced through increases in C_L . Information for a reduced time entry trajectory corresponding to an angle of attack of 50° and a bank angle of 60° is also shown. The temperature levels bracketed by these limiting trajectories can be sustained by existing refractory materials and are substantially below temperature levels substantiated in flight materials. The use of optimized nose contours can further reduce temperatures through enlarging the "effective nose radius." Optimization leads to heating rate reductions of the order of 0.7 of the corresponding spherical value. The 2:1 ellipsoidal nose shown is an example of such a heating rate reduction which has been demonstrated through appropriate wind tunnel investigations. Leading edge stagnation line calculations and supporting data are similarly presented in Figure 26.

The mechanism and magnitude of boundary layer transition and the resulting effect of turbulent flow on the skin friction drag and surface temperature is of considerable consequence both on the aerodynamic performance and thermal protection system efficiency. A typical high fineness ratio lifting entry vehicle, on the order of 100 ft long, has an axial force coefficient composed of approximately half pressure forces and half skin friction forces at a design point of Mach 20 and 200,000 ft altitude. A large spacecraft vehicle could potentially experience transition at altitudes of approximately 200,000 ft. When this occurs, the turbulent skin friction contribution will be twice that of laminar skin

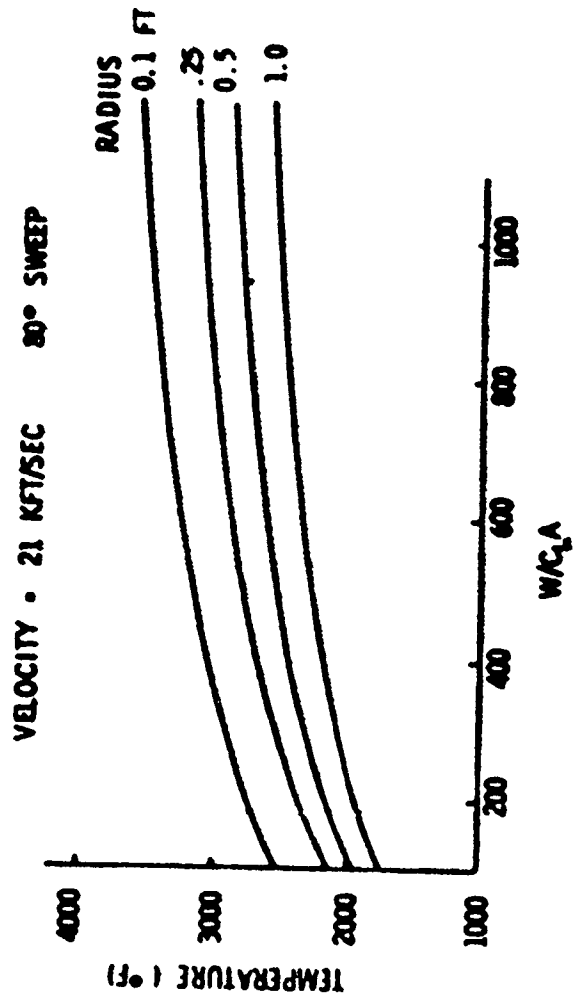


Figure 26. Leading Edge Temperatures

friction with a resultant decrease in L/D . Figure 27 shows the effect of transition criteria for vehicles of different lengths. Figure 28 indicates the heating to the lower surface centerline for the condition of $\alpha = 10^\circ$ to 50° . Both laminar flow with and without outflow (sweep effects) and turbulent flow conditions are shown at 10° with the maximum shown as a function of velocity.

The upper figure of this pair shows peak laminar, transitional and turbulent temperatures as a function of length. The two lower curves are for laminar flow with and without outflow effects due to sweep angle. The dashed line shows the heating through the transitional region for an assumed transition criterion of Re_0/M_L of 150 at the beginning of transition. The length of the transition region has apparently been assumed as 1.25 times the length of the laminar run. For vehicle lengths less than approximately 120 ft, transition has not occurred at the 19,000 ft/s velocity, so the peak turbulent temperature line is continued, indicating the various velocity points at which transition would be complete and the local peak temperature would be realized.

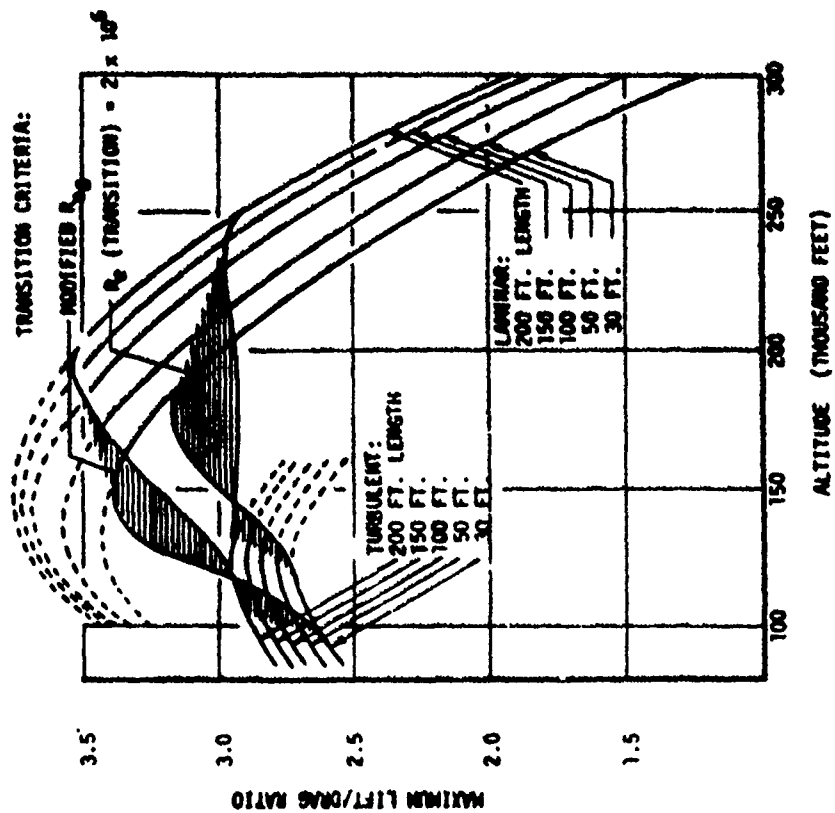


Figure 27. Boundary Layer Transition

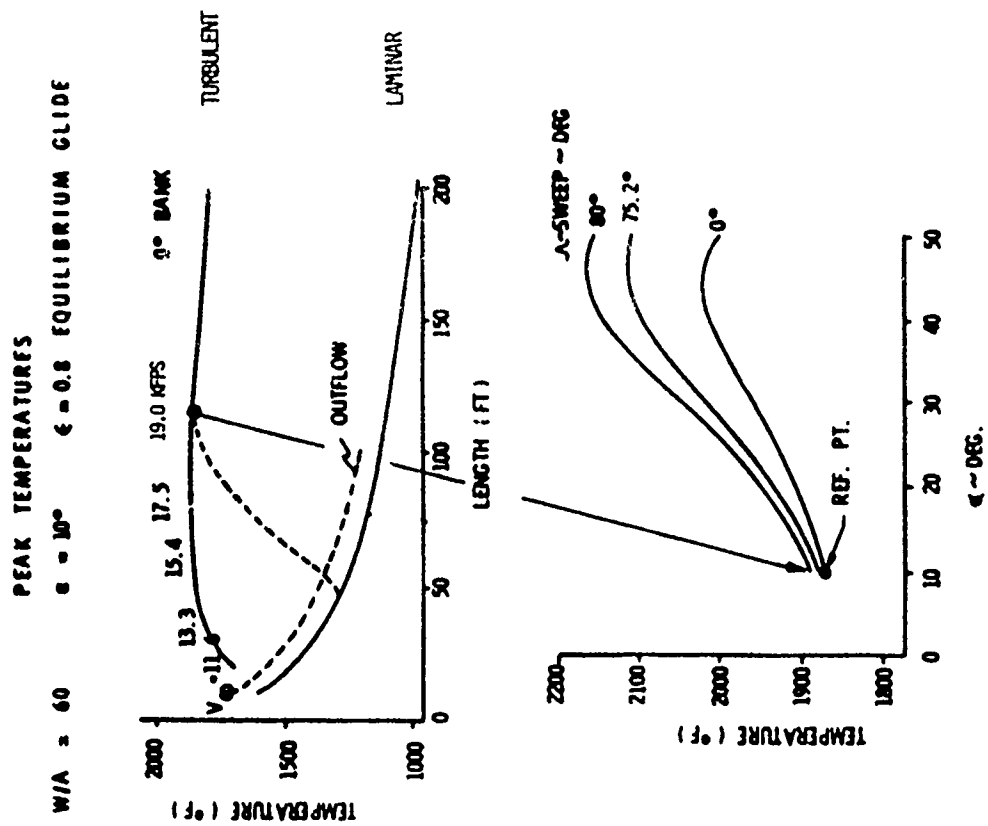


Figure 28. Lower Surface Centerline Temperatures

5. FLIGHT RESEARCH PROGRAMS

There was strong interest in both the Air Force and NASA to flight demonstrate the low speed flight characteristics of lifting reentry vehicles in the mid 1960s for application to future space reentry vehicles. Many of the early configuration concepts had to be discarded because of poor low speed characteristics. The X-24A project was the second Air Force flight test project to use the lifting body reentry configuration. The first project titled PRIME was previously discussed. The purpose of the X-24A PILOT project was to investigate maneuverable lifting body flight from the low supersonic speed range to touchdown. One of the main objectives was to gather data and prove that the configuration could be maneuvered to a safe horizontal unpowered landing at a preselected landing site. Twenty-eight successful X-24A landings were accomplished to fulfill this objective. The X-24A flight vehicle is shown in Figure 29. The vehicle demonstrated good landing characteristics and achieved a maximum subsonic L/D of 4, a very respectable subsonic L/D for such a low aspect ratio vehicle. Handling qualities were excellent. The completion of the X-24A flight test program presented a rare opportunity to flight demonstrate a high lift-to-drag configuration.

High L/D configuration technology had advanced to the point where extensive efforts were being directed to improving the low speed aerodynamic characteristics (Reference 53). The very low aspect ratio and high leading edge sweepback characteristic of these vehicles severely handicapped this class of configurations. Intensive investigations were carried out to

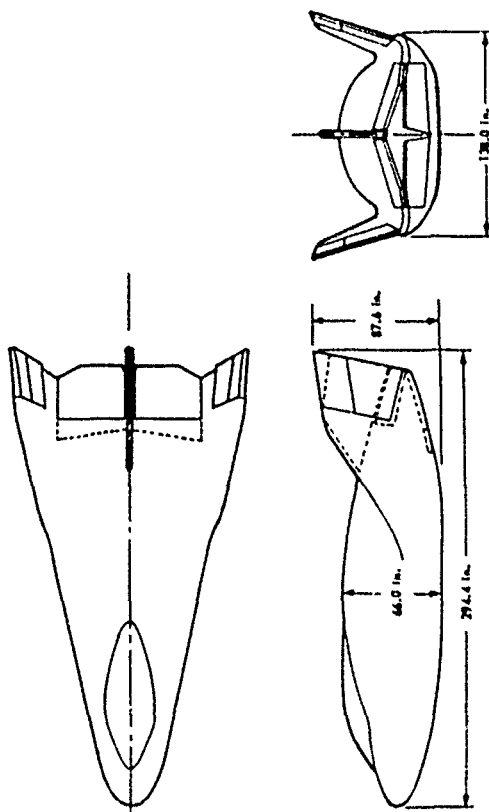


Figure 29. X-24A Lifting Body Vehicle

modify the aft portion of these configurations for acceptable low speed performance without compromising the hypersonic characteristics. This was the basis for the evolution and development of the FDL-8 which later became the X-24B. It was characterized by a double delta planform and a boattailed upper aft body to enhance lift and reduce base drag (Reference 54).

The X-24A flight test vehicle was then modified and designated the X-24B. The fineness ratio was increased by extending the body approximately 14 ft and blending the body into aft strakes. The similarity is apparent in Figure 30 where the X-24A and X-24B are shown together. The structural modifications to the X-24A are shown in Figure 31 as it is converted to the X-24B.

The design features of the X-24B are shown in Figure 32. The flat bottom and high sweep angle contributed to the high hypersonic L/D while the 3° nose ramp provided the proper hypersonic trim conditions. The 3 inch leading edge radius and 60° side body angle were the result of aerodynamic reentry heating considerations. Flared out upper and lower flaps provided stability necessary at high speed. Boattailing these surfaces toward the faired position increased the subsonic L/D for acceptable landing performance. The double delta planform was necessary for the X-24B application in order to move the center of pressure aft. This was required because of the aft center of gravity resulting from the location of the test aircraft systems rocket engine, propellant tanks, propellant, existing main landing gear position, etc. Considerable wind tunnel testing in the subsonic and transonic regime was conducted to meet the above hypersonic constraints and provide good low speed characteristics.



Figure 30. Comparison of X-24A and X-24B

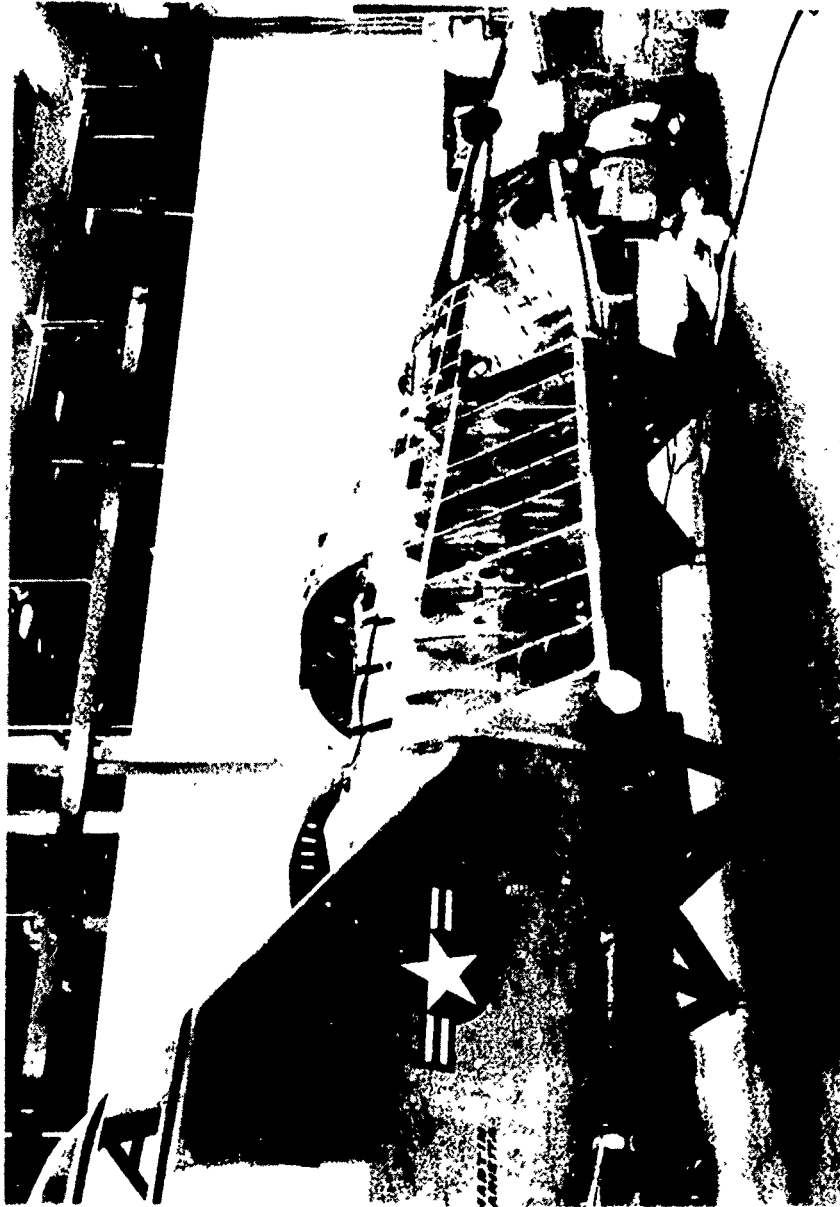


Figure 31. X-24A to X-24B Modification

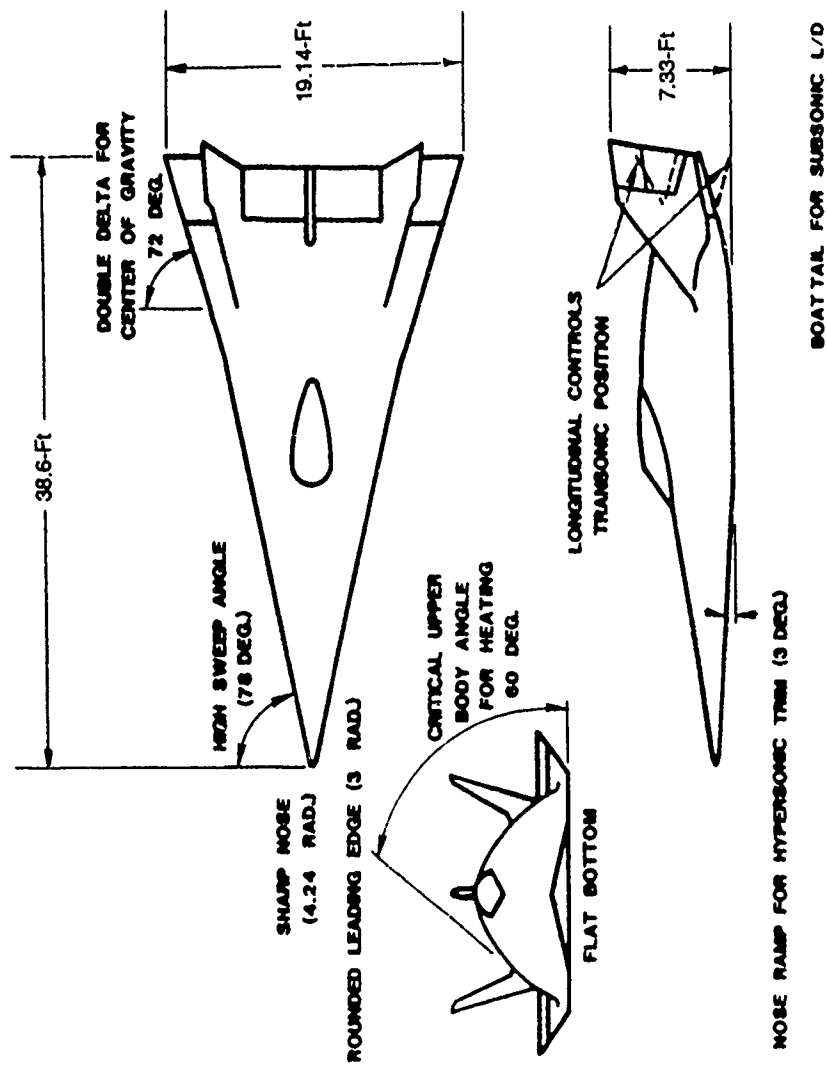


Figure 32. X-24B Aerodynamic Design Features

The flight research program was very successful and consisted of 6 glide flights and 24 powered flights. At the completion of these flights, six additional glide flights were flown for checkout of three new pilots. The 36 flights were flown between August 1973 and November 1975 gathering data to determine performance, handling qualities and stability and control from subsonic, transonic and supersonic Mach number up to a maximum Mach number of 1.76 (References 55-56). Predictions of flight characteristics were based on wind tunnel data; therefore, verification of these data were a primary objective of the program. In general, the wind tunnel data was in agreement with flight test results. Subsonically the maximum L/D was 4.5 and the vehicle exhibited good handling qualities over much of the flight envelope. There were some instabilities when the rocket motor were fired but well within the available control power.

The X-24B program was very successful and produced a significant number of flights in a short time. This was attributed to using the X-24A vehicle and the experienced engineering and flight test team from the X-24A program. A summary of the flight program with a synoptic display of the lessons learned is presented in Figure 33. The X-24B yielded important information from all phases of its flight and was the most efficient aerodynamic vehicle of the lifting body series as attested to by the flight test pilots.

A summary of Air Force and NASA lifting body research vehicles which have been flight tested is presented in Figure 34. Shown are the recovered ASSET and PRIME vehicles as well as the lifting bodies tested at transonic speeds; the HL10, M2F2, the X-24A, and the highly efficient X-24B.

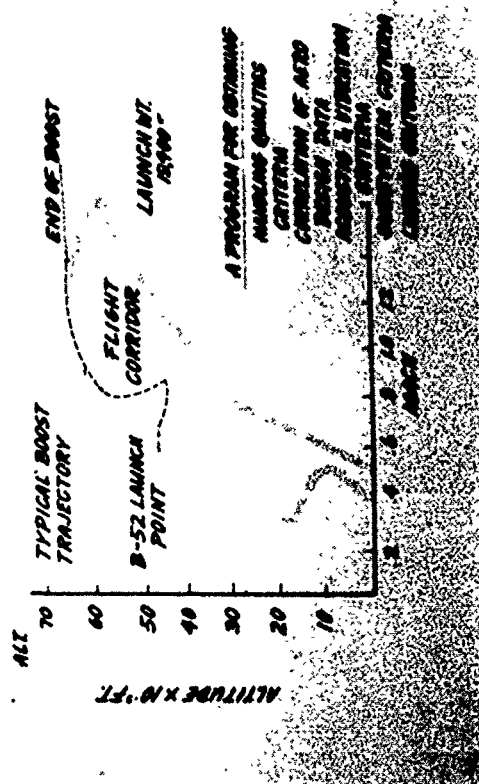


Figure 33. X-24B Flight Envelope

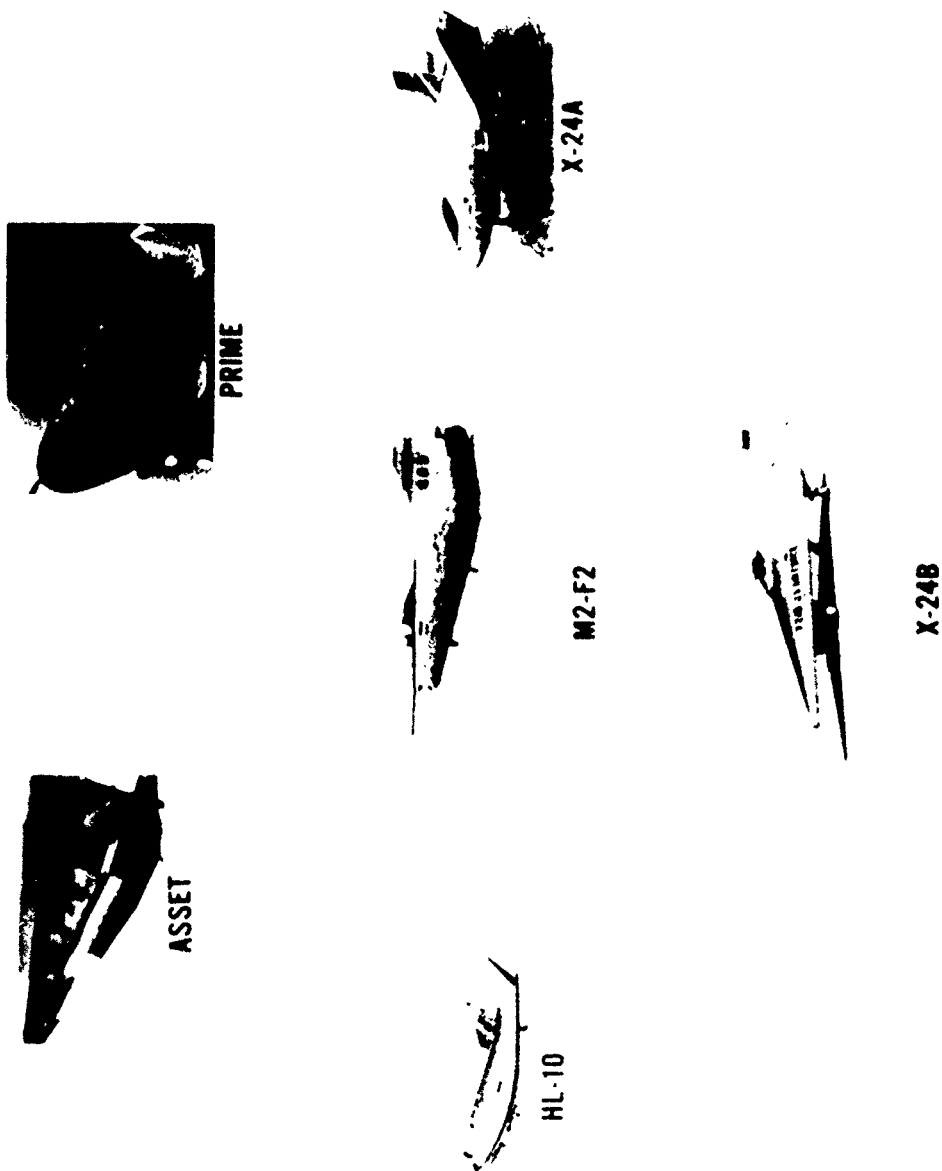


Figure 34. Previous Lifting Body Research Vehicles

6. APPLICATION OF LIFTING BODY CONFIGURATION TECHNOLOGY

Efforts in the early 1960s to couple reusability in launch vehicles with the payload carrier generally concentrated on highly sophisticated recoverable vehicles. A substantial number of these investigations were focused on complex horizontal takeoff air-breathing systems which utilized very advanced propulsive schemes such as in-flight air collection or supersonic combustion ramjets. Other studies included vertically launched rocket systems with a horizontal landing capability. These concepts eventually were converged into self-contained fully integrated vehicles such as aerospace plane concepts. Unfortunately because of the large RDT&E costs necessary to initially acquire these complex systems, their relative cost-effectiveness compared to the expendable systems was such as to reduce their attractiveness for launch applications. Considerable interest developed in the mid 1960s on the "Tip Tank Concept" or stage and one-half launch vehicle system (References 57-58). This approach of integral launch/reentry vehicles employed low cost light-weight throw-away propellant tanks attached to the sides of the spacecraft with main engines integrated with and returned with the spacecraft, Figure 35. The vehicle sizes were generally much larger than those considered in the X-20 and other spacecraft design studies. Factors which influenced the size were the incorporation of integral propulsion within the vehicle and significantly higher discretionary payloads.

The cost requirements for various programs directed toward reusable, recoverable vehicles are normally delineated into three subdivisions. These

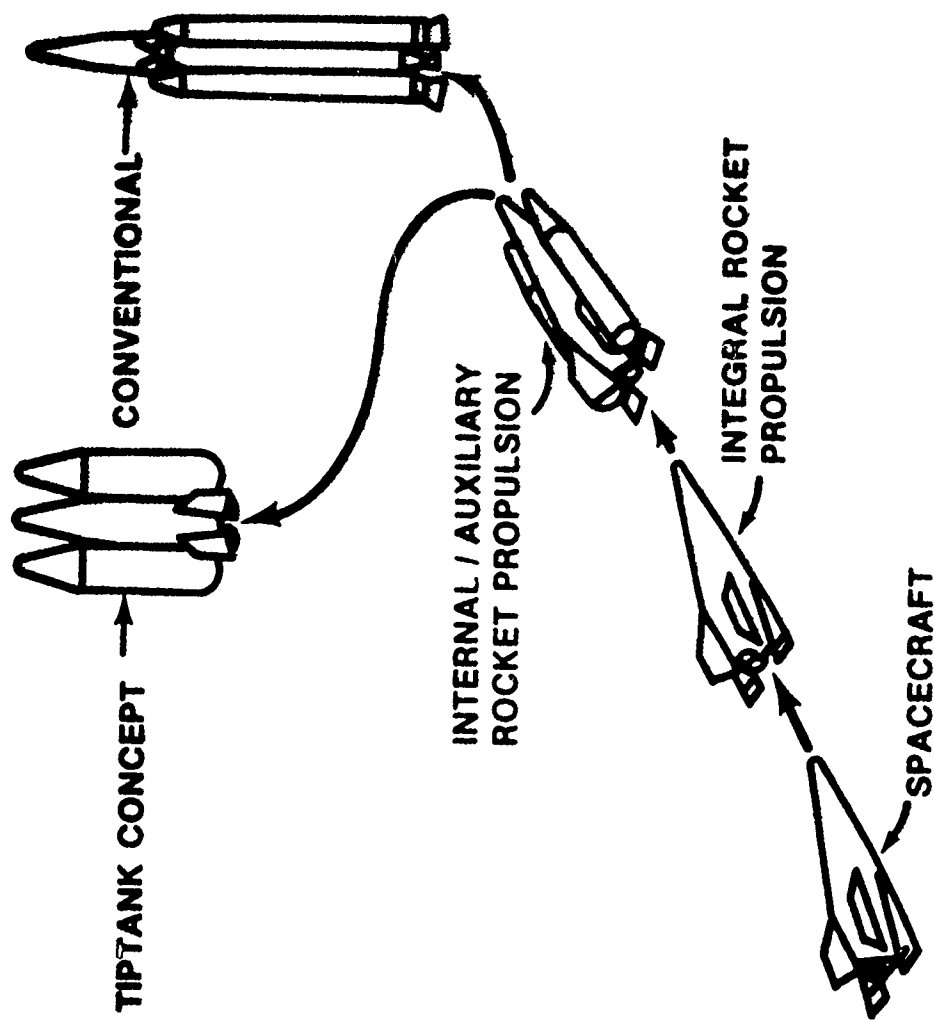


Figure 35. Vehicle Options and Stage and One-Half Evolution

are RDT&E costs, expendable costs, and the cost associated with the operations. Total program costs were grossly estimated as a function of the number of launches for several reusable concepts and the trends are shown in Figure 36. Several factors worth noting in selecting a concept were the initial RDT&E cost to achieve the system, the "crossover" point with expendable systems relative to the number of launches, and the slope of the curve with successive launches. The stage and one-half system offered particularly attractive potential for each of these considerations. This concept consisted of a slender, lifting reentry vehicle which carried all launch and reentry subsystems including engines for reuse, in addition to expendable fuel tanks. These tanks had no specially required heat protection and contained a high fuel fraction. The structural weight of the tanks was a very low percentage of the total system's weight. The FDL-5 mock-up is shown in Figure 37 with the expendable tanks. During these investigations, considerable information was obtained on the mating of tanks. Various tank schemes were evaluated but the "V" tank was selected because of low drag and minimal interference heating. The "V" tank also integrates well with the high fineness ratio lifting body configuration.

In the early definition of the Space Shuttle configuration, NASA expressed strong interest in evaluating a straight wing orbiter based upon its good low speed performance characteristics. This prompted an intensive effort by FDL to define the impact of aerodynamic heating on straight wing configurations. Aerodynamic heating not only influences configuration shape, but also dictates the heat-protection system, and ultimately the reusability (References 59-60). Hence, it is necessary to have an accurate

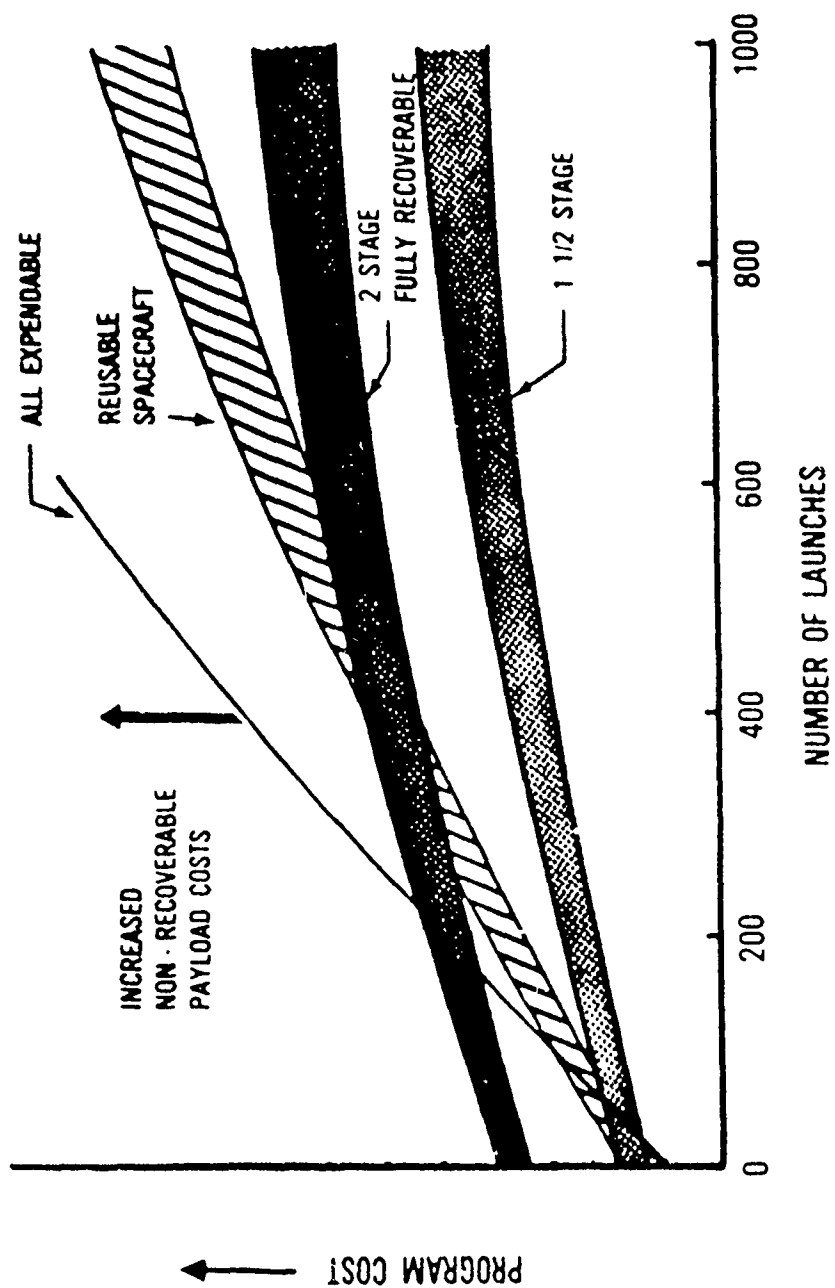


Figure 36. Launch Vehicle Cost Comparison



Figure 37. Mock-up of FDL-5 With External Tanks

knowledge of the heating level and an understanding of the factors which affect the aerodynamic heating. Interference heating represented a significant problem with the straight wing orbiter, consequently several candidate delta wing configurations were also investigated. Based on experimental results the straight wing configuration experiences higher skin temperatures than the delta. Also, temperature increases less with angle of attack for the delta than the straight wing configuration. The results shown in Figure 38 compare the isotherms at $\alpha = 40^\circ$ and $\alpha = 60^\circ$ for the two configurations. The delta has a uniform distribution and no interference regions at both angles of attack. The straight-wing configuration, however, has areas of higher temperatures at both angles of attack and regions of interference heating at $\alpha = 40^\circ$. This in-depth technical data and analysis was instrumental in the selection of a delta wing configuration for the Space Shuttle.

The Laboratory also provided a solid technology base for the development of the Space Shuttle. This included, as shown in Figure 39, the flight technology demonstration programs of ASSET, PRIME and the X-24A and B. The X-24B was a major contributor to the landing and approach patterns used by the Space Shuttle as depicted in Figure 40. The X-24B further contributed to the Shuttle landing phase (Figure 41) by demonstrating the first landing of an unpowered lifting body vehicle on a paved runway. The handling qualities of the X-24B and its ability to fly a precise track were demonstrated on this first concrete runway landing. Flying an alternate flight card because only three of the four rocket chambers worked, the pilot was able to glide from an altitude of 57,000 ft to a precise landing on the runway by touching down on either side of a white stripe, which was the

SHUTTLE RE-ENTRY TEMPERATURE DISTRIBUTIONS

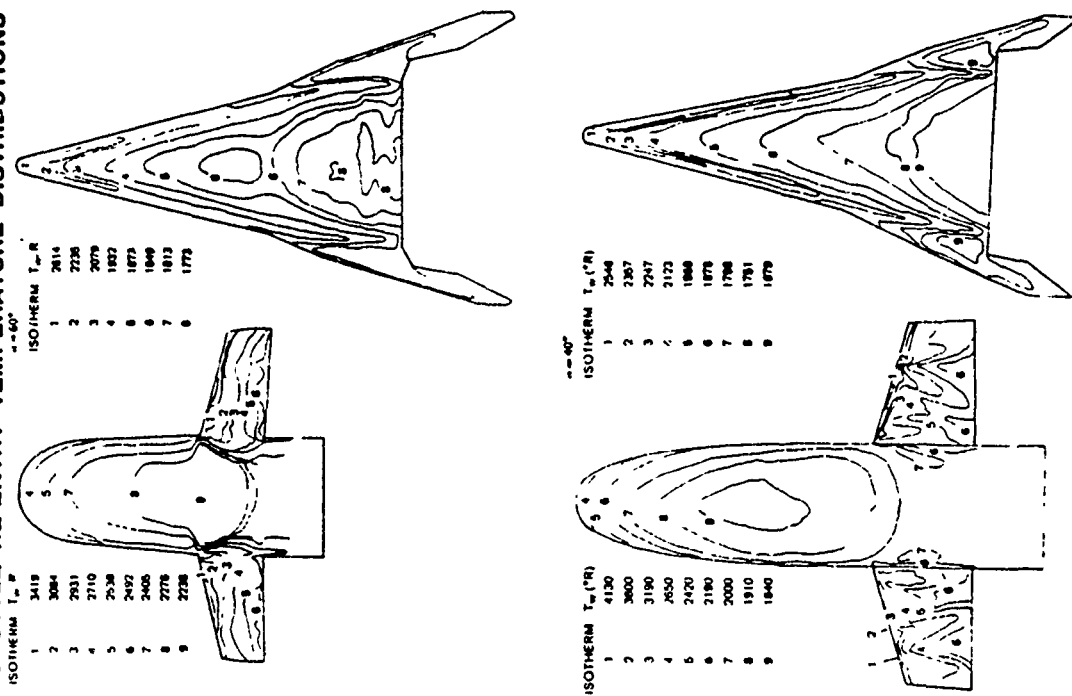


Figure 38. Shuttle Reentry Temperature Distributions

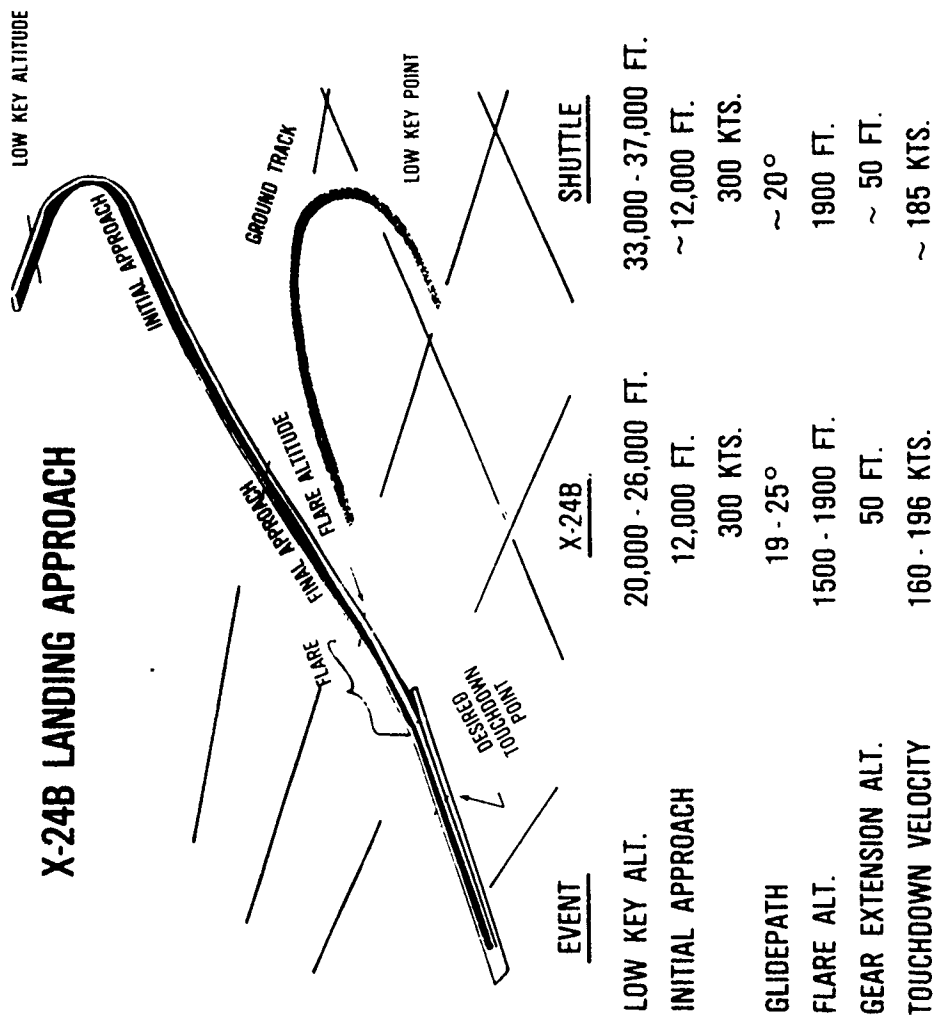


Figure 40. Comparison of X-24B Shuttle/Landing Approach

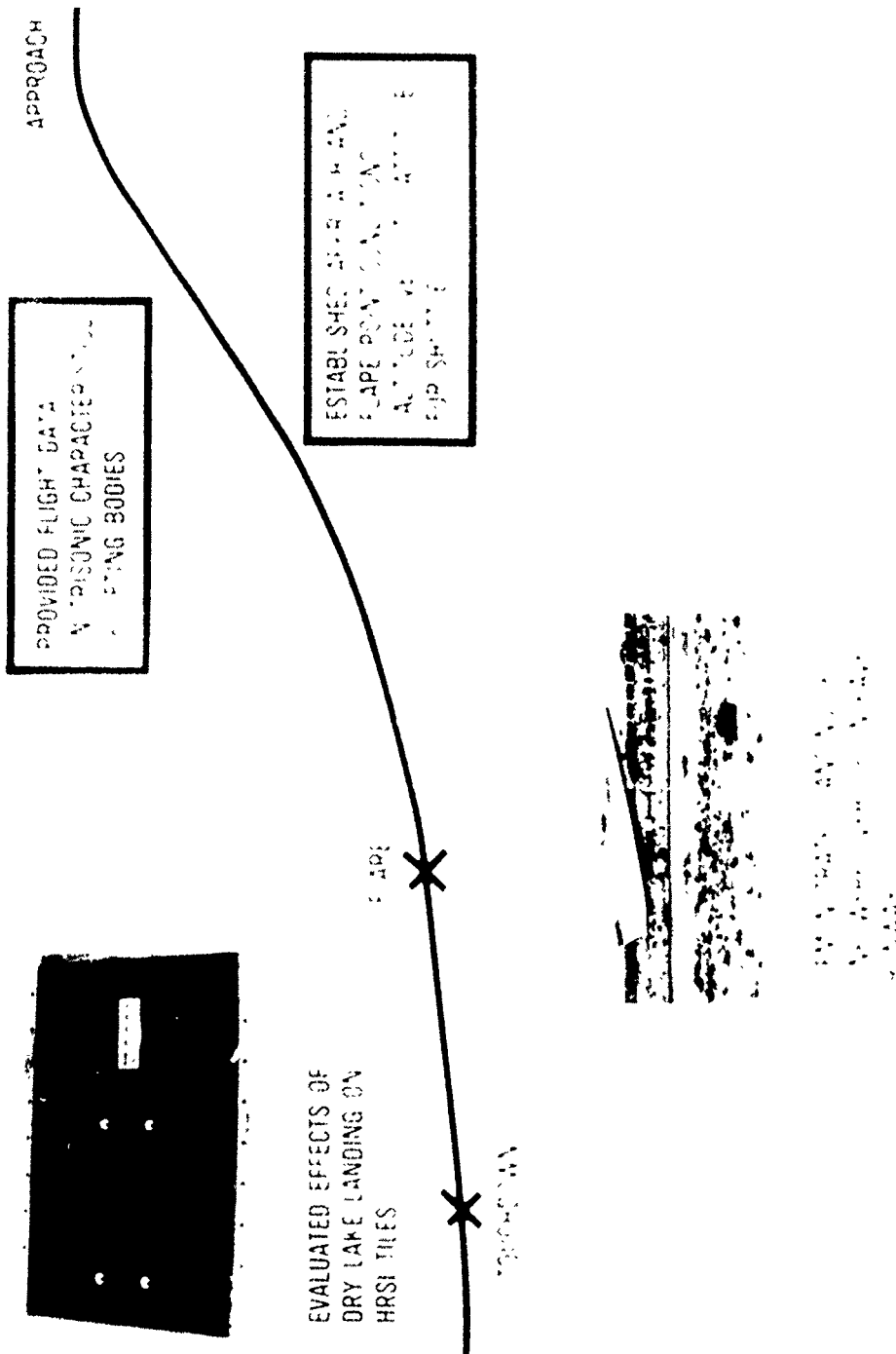


Figure 41. X-24B Contributions To Shuttle Landing Phase

preselected touchdown point, with the left and right gear, respectively. The X-24B also evaluated some of the principal thermal protection systems to be used on the Shuttle. Reuseable Surface Insulation (RSI) panels were subjected to thermal testing and then flight tested on the X-24B to determine the effects which might impact the aerodynamic and performance characteristics during the terminal portions of the flight. The evaluation of sand effects on the RSI panels was also assessed to determine any adverse effects as a result of operational landings in the desert environment.

The nature of the OMS pod heating on the Space Shuttle is illustrated in Figure 42, The FDL actively participated in the evaluation on this critical technical issue. Particular emphasis was given to the body side heating and the OMS pod heating. Attention was directed toward the heating associated with reduced angle of attack with some degree of yaw as well as increased entry velocities associated with retrograde orbits.

The FDL initiated the concept of the Maneuvering Reentry Research Vehicle (MRRV) depicted in Figure 43 to take advantage of the Space Shuttle and demonstrate critical interdisciplinary technologies in a more demanding flight corridor for future transatmospheric vehicles. This concept is a high L/D lifting body carried aloft within the payload bay of the Space Shuttle. The vehicle can be manned or unmanned and can carry its own propulsion system both internally or externally. The FDL also initiated a program designated X-24C which was primarily intended to flight demonstrate air-breathing propulsion systems, such as Scramjets, for the Mach range 5 to 7.

Typical flight corridors are presented in Figure 44 for the Shuttle, MRRV and the X-24C (References 61-62). The space shuttle flies at very high altitudes since it employs a high angle of attack reentry ($\alpha = 30^\circ$) and

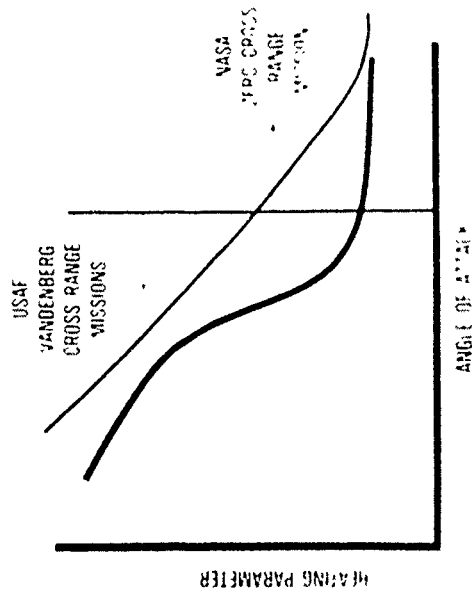
OMS POD HEATING



AFFDL ISOLATED OMS POD
HEATING PROBLEM IN JAN 1979



AFFDL SPONSORED HEATING TESTS A NASA TUNNEL
AEDC TUNNEL B AND OIL FLOW TEST IN AFFDL



G

Figure 42. OMS Pod Heating



Figure 43. Maneuvering Reentry Research Vehicle

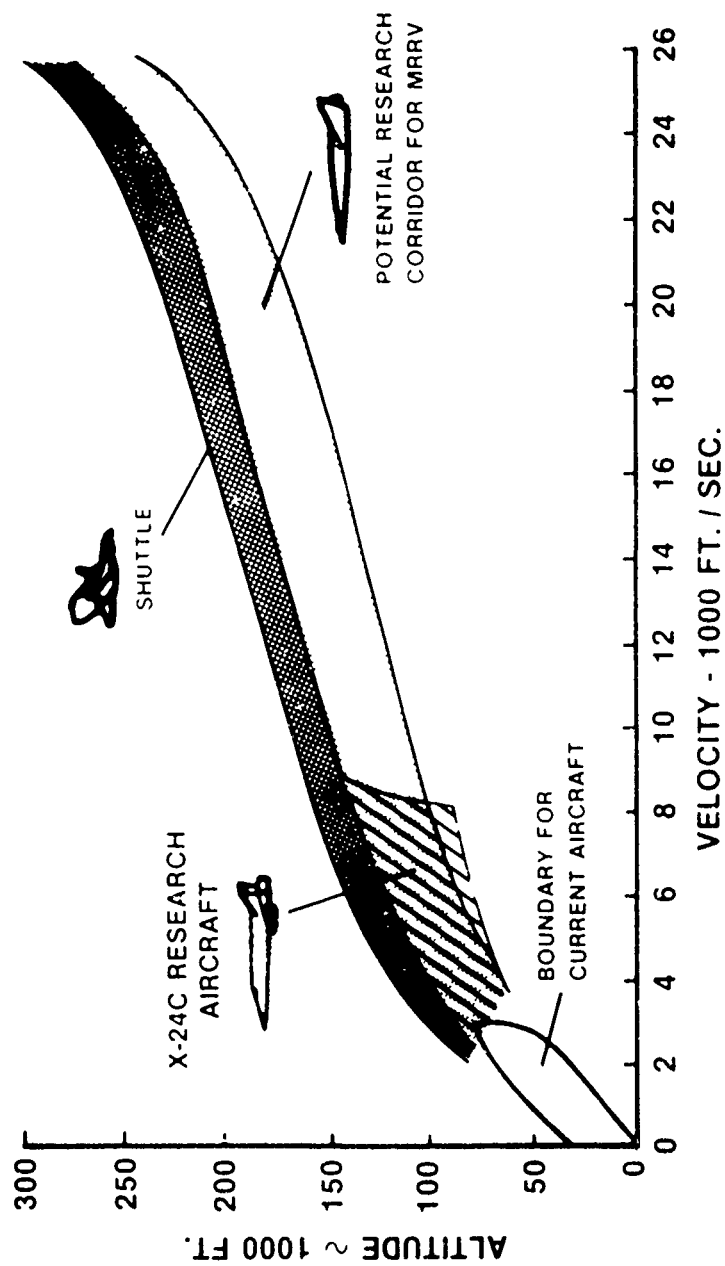
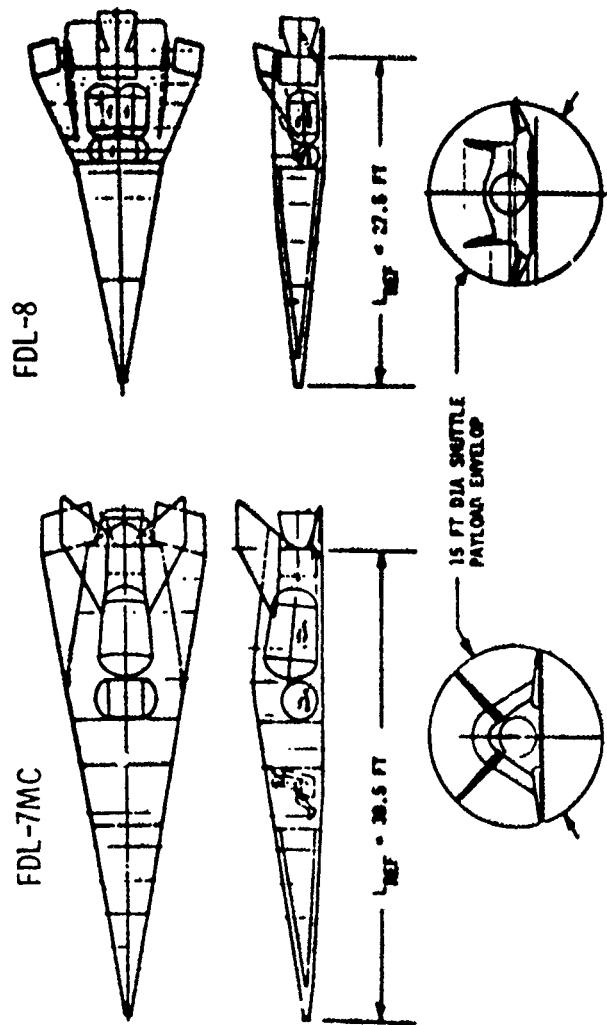


Figure 44. Representative Flight Corridors

maintains this relatively high altitude until it pitches over at a Mach number of 8.0. The high L/D MRRV operates at relatively low angles of attack ($\alpha = 10^\circ$) and penetrates much deeper into the atmosphere as it returns from orbit. The MRRV corridor represents the typical flight of a single stage to orbit aerospace plane. Thus it could be used to demonstrate critical aerodynamic, structures and materials technology for NASP type vehicles. The flight envelope of the X-24C is representative of future hypersonic airbreathing systems for reconnaissance and continental defense.

Various high L/D configuration options were investigated for the MRRV concept. These included the FDL-5, FDL-6, FDL-7 and FDL-8. The maximum L/D for the MRRV configurations ranged from 2.7 to 3.0 for a nominal vehicle length of 39 ft. Figure 45 compares a manned FDL-7 MC configuration with an unmanned FDL-8 design. Payload packaging was also compared for these configurations both with and without external propellant tanks, shown in Figure 46. Some internal propellant was provided in most of the vehicle designs; however, different levels of external propellant were assessed relative to packaging and performance constraints and requirements. The large manned vehicles (FDL-7MC) could package a maximum propellant weight of 8,820 lb while the unmanned modified FDL-8 system increased the maximum propellant weight to 13,000 lb. Engineering working models, as shown in Figure 47 were fabricated to assist in-house evaluations of subsystem arrangements, locations and packaging. They also provided a clear perspective of the external configuration geometry and aided in making modifications.

Some experiments which could be conducted by the MRRVs include: low density plume/airframe interaction tests; communication through the plasma sheath; effects of manufacturing and design on boundary layer transition;



NOTE: MAXIMUM SIZE VEHICLES WITHOUT FOLDING AERODYNAMIC SURFACES TO FIT WITHIN SHUTTLE PAYLOAD ENVELOPE

Figure 45. Shuttle Packaging of MRRV Designs

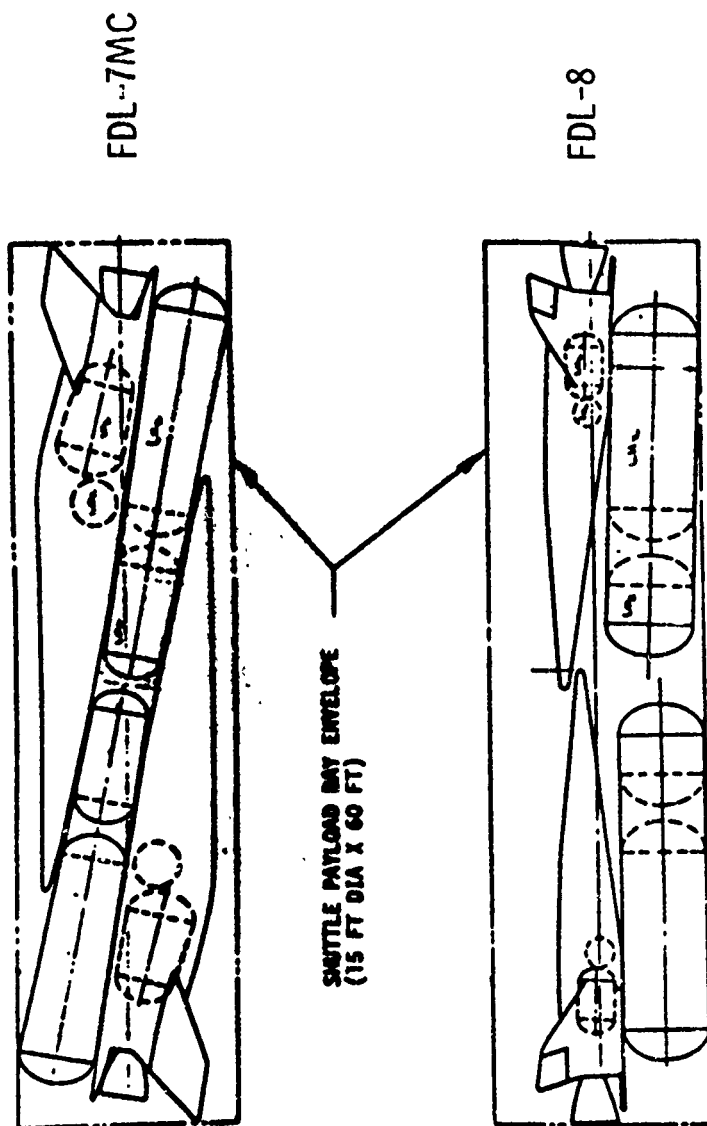


Figure 46. MRRV Packaging with External Tanks



Figure 47. MRRV Engineering Design Model

experimentation of active or passive cooling of metallic and nonmetallic materials; acoustic/dynamics experiments related to structural design criteria establishment; and sensor suitability during reentry including airdata (α , β , V , etc.) and electromagnetic and/or optical distortion through the plasma sheath. The MRRVs could be designed to uniquely function at variable Reynold's number, $W/C_L A$ and high Mach numbers. Dedicated experiment bays can be configured to perform a variety of experiments in much the same way that a test cart is prepared for a test in a wind tunnel, then inserted for the test with a minimum of installation time. Candidate areas for TPS, structures and material experimentations are shown in Figure 48. Three aerodynamic experiments which can be conducted in this flight environment are shown in Figure 49. The transverse jet has the potential for use in controlling reentry vehicles, and for cooling localized structural areas. Porous wall tests would provide design data for advanced vehicles which could profit from an active cooling method. Skin friction data could also be obtained in the presence of gases which would be representative of the ablation process. Non-uniform blowing experiments would define the effects on the turbulent boundary layer properties.

In the early 1980s there was a renewed interest in the exploration of hypersonic systems based on advances in aerodynamic, structures and materials technology. A thrust known as the Advanced Military Spaceflight Capability (AMSC) identified potential systems and associated technologies required to provide reliable access to space in an economical and timely manner (References 63-66). The MRRV type of technology demonstrator was suited ideally for leading the way to this military spaceflight capability in terms of technology options and investigations. It possessed the

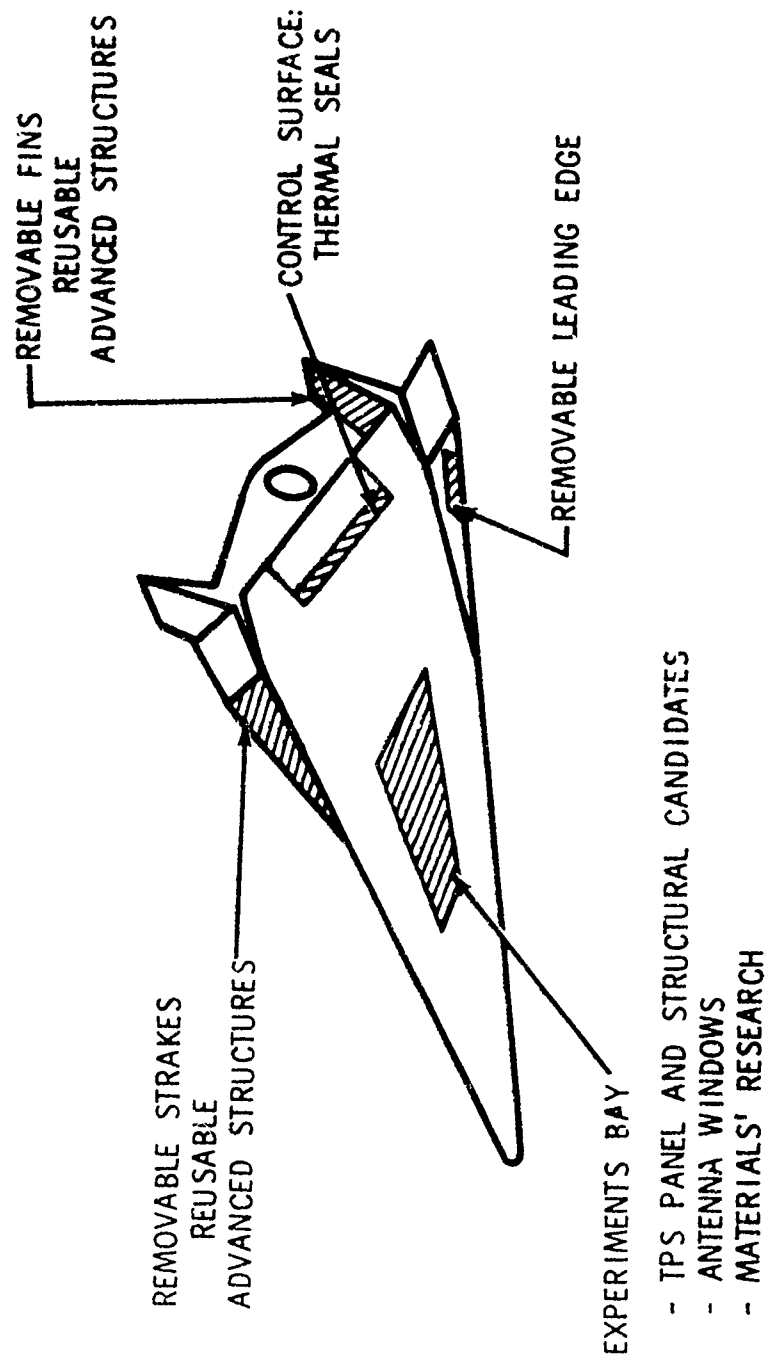


Figure 48. Candidate Structural Flight Experiments

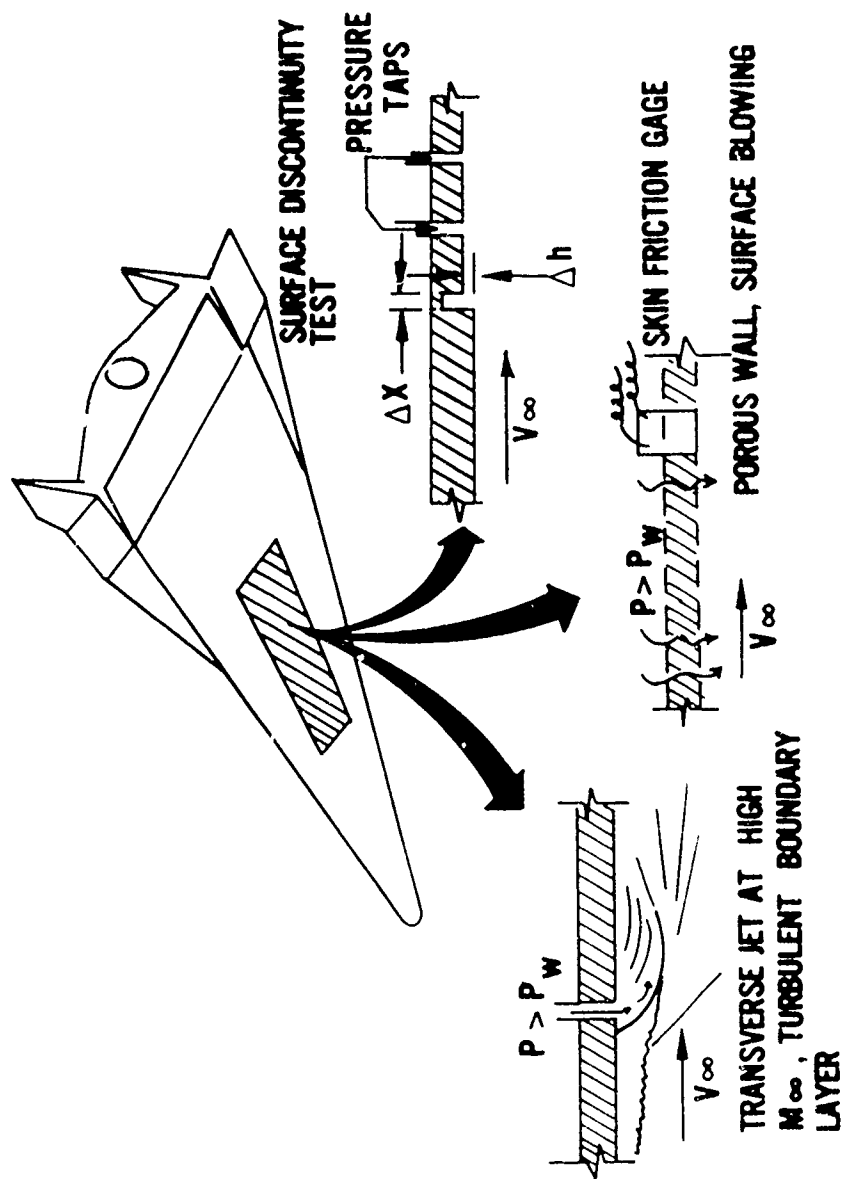


Figure 49. Candidate Aerodynamic Flight Experiments

capability to flight demonstrate the majority of the AMSC critical technologies, and some of its desired operational characteristics such as reusability, performance, flexibility and maneuverability. It also was envisioned to be launched by either the space shuttle or a large existing transport as shown in Figure 50.

To broaden the spectrum for application of lifting bodies, configurations and performance potential for orbital plane change vehicles were also investigated, not only to identify the benefits, but to also highlight some of the technology problems and areas which could profit from future research. The lifting body configuration is ideal for application to Aeroconfigured Orbital Transfer Vehicles (AOTV) (References 67-68). The prime advantage of AOTVs are the large orbital plane changes which can be achieved (Figure 51). At hypersonic lift-to-drag ratios near 1.0, no significant advantages are apparent at the lower inclination angles but as the lift-to-drag ratio increases to 3.0, performance benefits are clearly evidenced. Orbital transfers, or inclination angle changes, can be made either purely propulsively or by use of aerodynamic forces to change the plane. As the plane change angle increases, the pure impulse propulsive requirements become excessive, even to the point where moderate to large plane changes are not practical. If orbital transfer vehicles are designed to achieve a reasonable value of hypersonic lift-to-drag ratio, then a combination between the propulsive and aerodynamic forces make not only large plane changes practical, but by the use of this synergetic maneuver, moderate plane changes can be effected at substantially reduced velocity as shown in Figure 11. Synergetic cruise maneuvering is accomplished by blending the aerodynamic and propulsive forces in an optimal manner. The

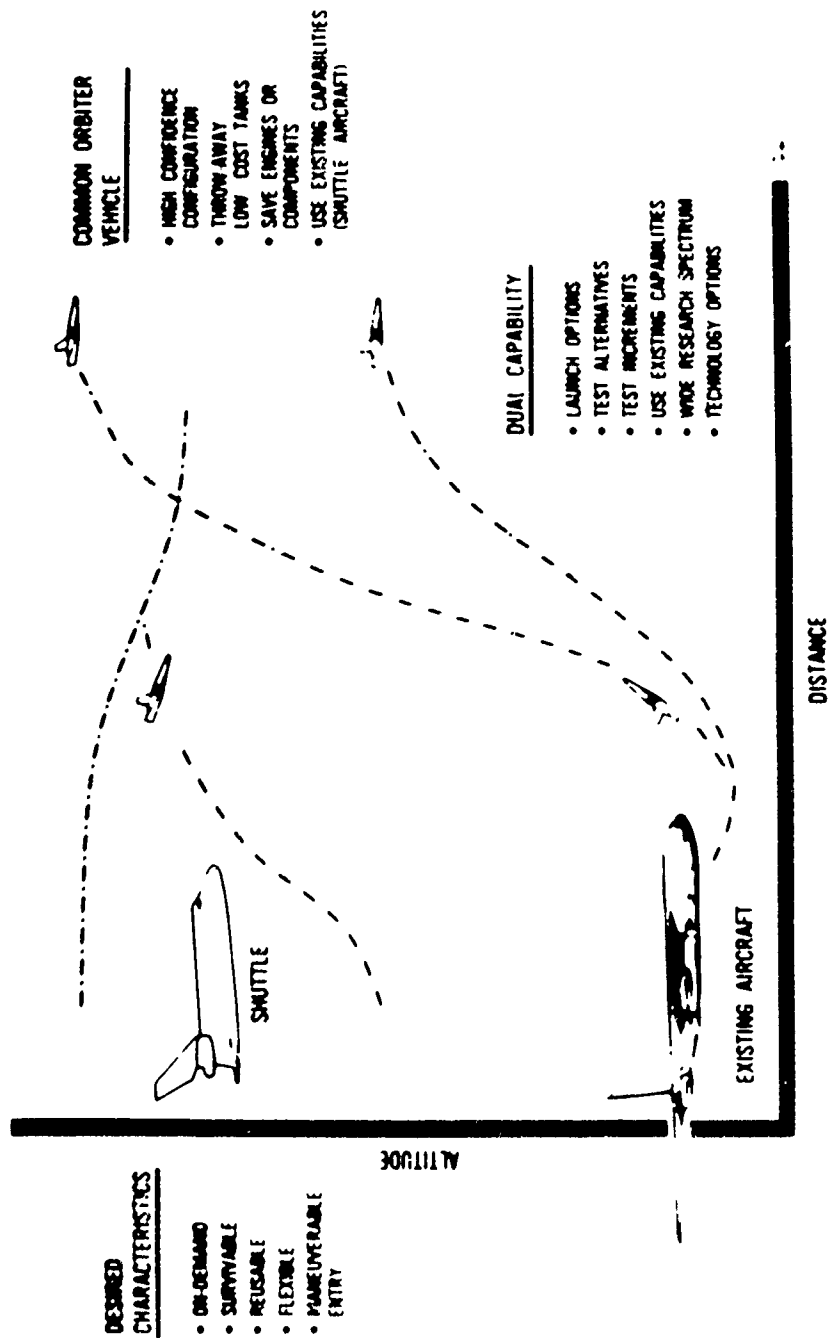


Figure 50. MRRV Technology Options

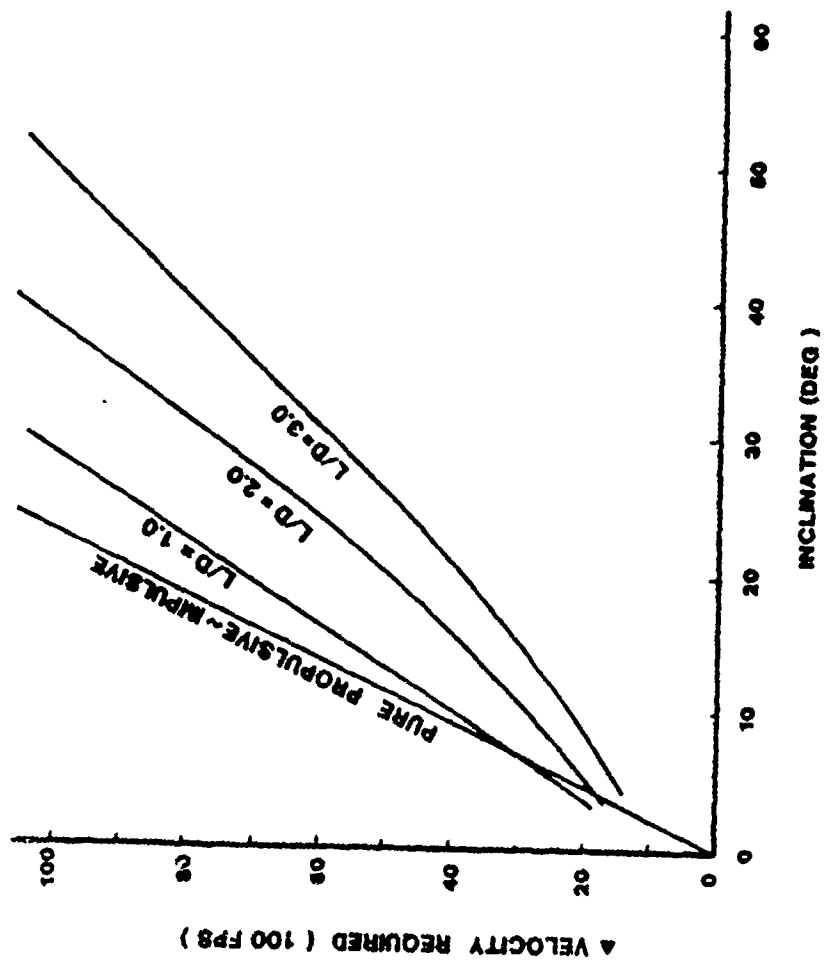


Figure 51. Synergetic Plane Change Capability

AOTV is decelerated to drop out of orbit and the rocket engine is pulsed or burned in a throttled condition at a high altitude (225,000 ft) and in combination with the aerodynamic forces produces efficient large plane changes. The AOTV is then boosted back into its new orbit using the rocket engine. Several ground based and space based AOTVs were formulated and analyzed for orbital plane changes from Low Earth Orbit (LEO) to LEO and High Earth Orbit (HEO) to LEO. Representative configurations are displayed in Figure 52. It was envisioned the ground based AOTVs would be deployed by the space shuttle and the space based AOTVs deployed from a future space station.

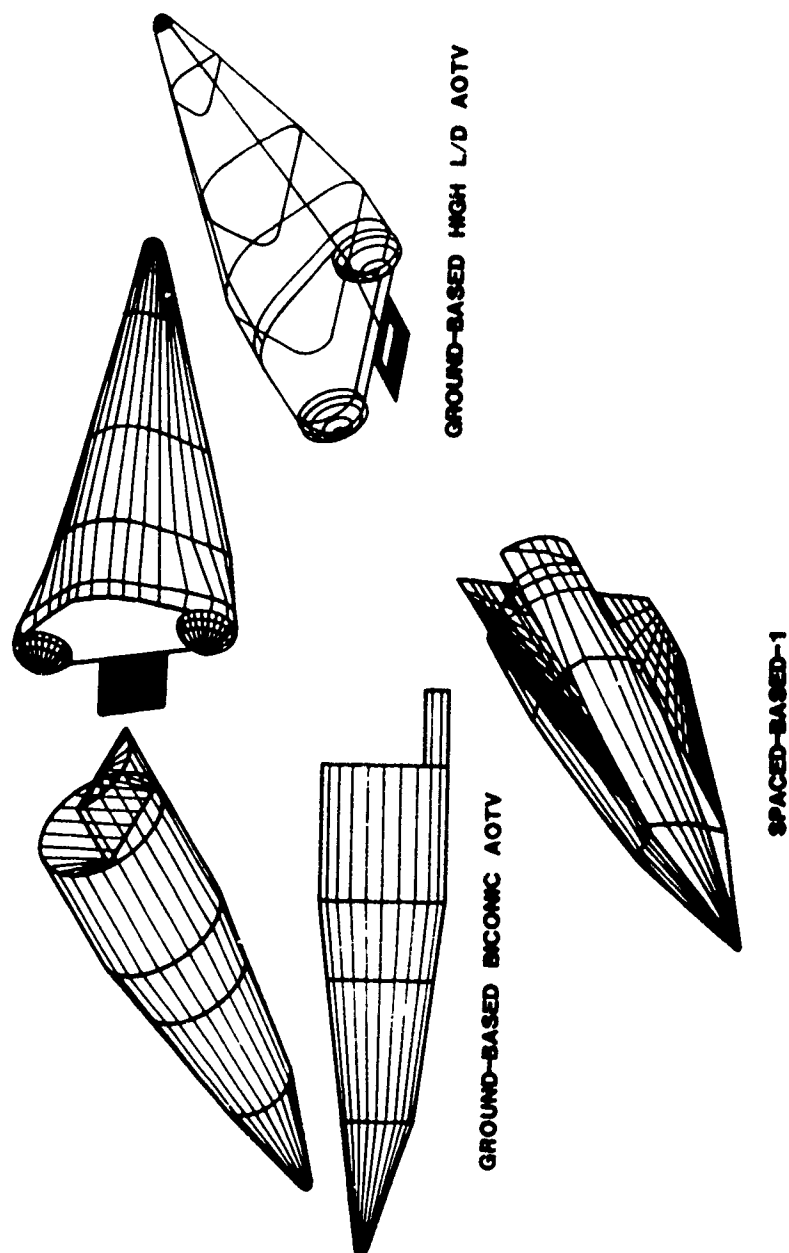


Figure 52. Aeroconfigured Orbital Transfer Vehicles

7. HYPERSONIC AIR-BREATHING TECHNOLOGY DEMONSTRATORS

There was strong interest in hypersonic air-breathing vehicles in the mid-1960s for various types of military applications. The primary technology limitation at this point in time was reusable high temperature materials, computational fluid dynamics, supersonic combustion engine technology and lightweight structures. Results from numerous studies indicated there appeared to be a convergence of aircraft and spacecraft configurations based on certain parameters associated with internal volume, compactness, aerodynamic efficiency and speed. The aero-performance parameter $M(L/D)_{MAX}$ is an indicator of a configurations aerodynamic efficiency and speed requirement. Various aircraft and spacecraft configurations are presented in Figure 53. The spacecraft, such as, Mercury, Apollo and Space Shuttle are characterized by high volumetric efficiency. This is because of the emphasis on compactness to maximize volume and minimize wetted area in order to reduce the impact of aerodynamic heating and thermal protection system weight. Aircraft configurations tend to have low volumetric efficiency and emphasize aerodynamic efficiency. This tends to drive the configuration towards high aspect ratios and large wing areas at subsonic speeds and slenderized fuselages at supersonic/hypersonic speeds. The two configuration classes tend to merge for transatmospheric vehicles such as the aerospace plane. This results from attempting to maximize internal volume, for fuel storage, minimize wetted area for reduced TPS weight and at the same time maintain high aerodynamic efficiency throughout the flight envelope.

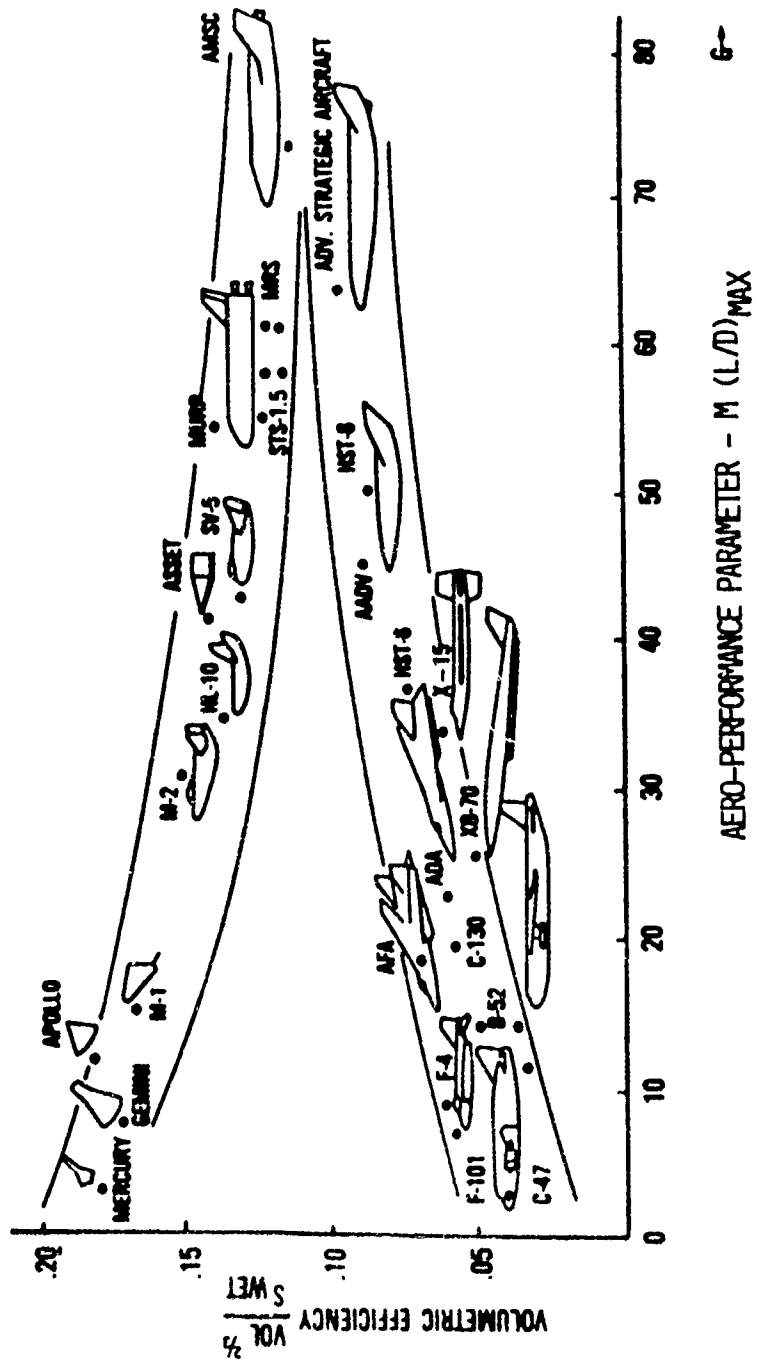


Figure 53. Configuration Design Trend

Hypervelocity air-breathing cruise vehicles tend to be lifting body configurations with a small distinct wing at the aft end for aerodynamic center control and good low speed efficiency. This is shown in Figures 54 and 55 for vehicles which cruise at Mach numbers between 5 and 14. These configurations evolved from intensive Flight Dynamics Laboratory investigations to establish a creditable configuration data base for use in system planning studies to evaluate future hypersonic manned systems. The advanced manned interceptor (Figure 54) was extensively tested at subsonic, transonic and high supersonic speeds at Arnold Engineering Development Center. Detailed analysis were performed on the configurations presented in Figure 55 to determine the impact of supersonic combustion propulsion engines (scramjets) on the configurations. It is apparent at Mach numbers 10 and 14 that the scramjets strongly impact the configuration. In fact, the entire lower body surface serves as the inlet and nozzles for these configurations. These efforts prompted FDL to define candidate technology demonstrator vehicles to explore the hypersonic environment for this class of configurations.

The configuration characteristics for two generic families of research aircraft are compared in Figure 56. The X-15 wing/body configuration demonstrated the technology for aircraft type configuration such as the F-16 and the F-104. The X-24 highly swept configuration is representative of future high speed vehicle designs such as for aerocruise, suborbital vehicles, high speed cruise aircraft, advanced aerospace configuration, and the emerging transatmospheric vehicles. The design evolutionary trend is clearly in the direction of the delta configuration.

The last configuration in the X-24 series was the X-24C. The limited rocket thrust and the aluminum construction of the X-24B prevented the

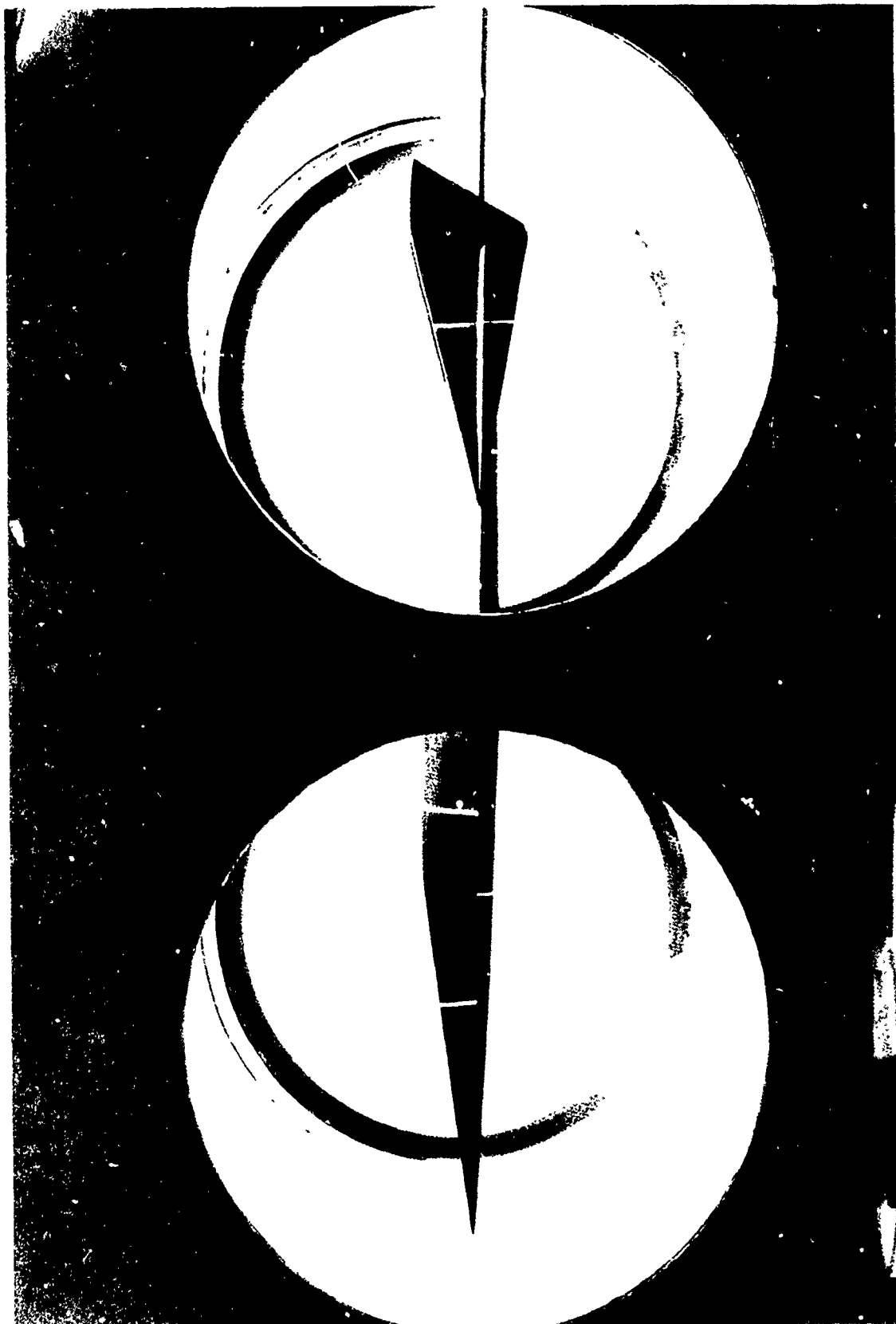


Figure 54. Advanced Manned Interceptor Test

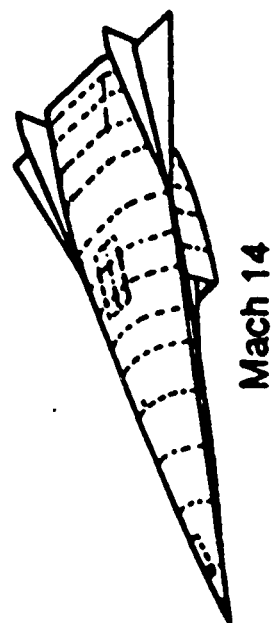
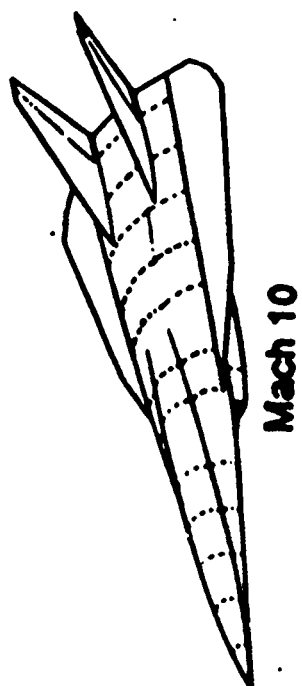
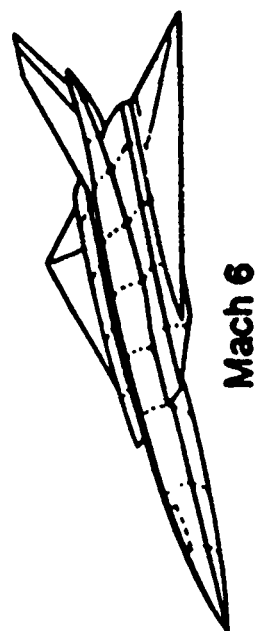


Figure 55. Hypersonic Airbreathing Cruise Vehicles

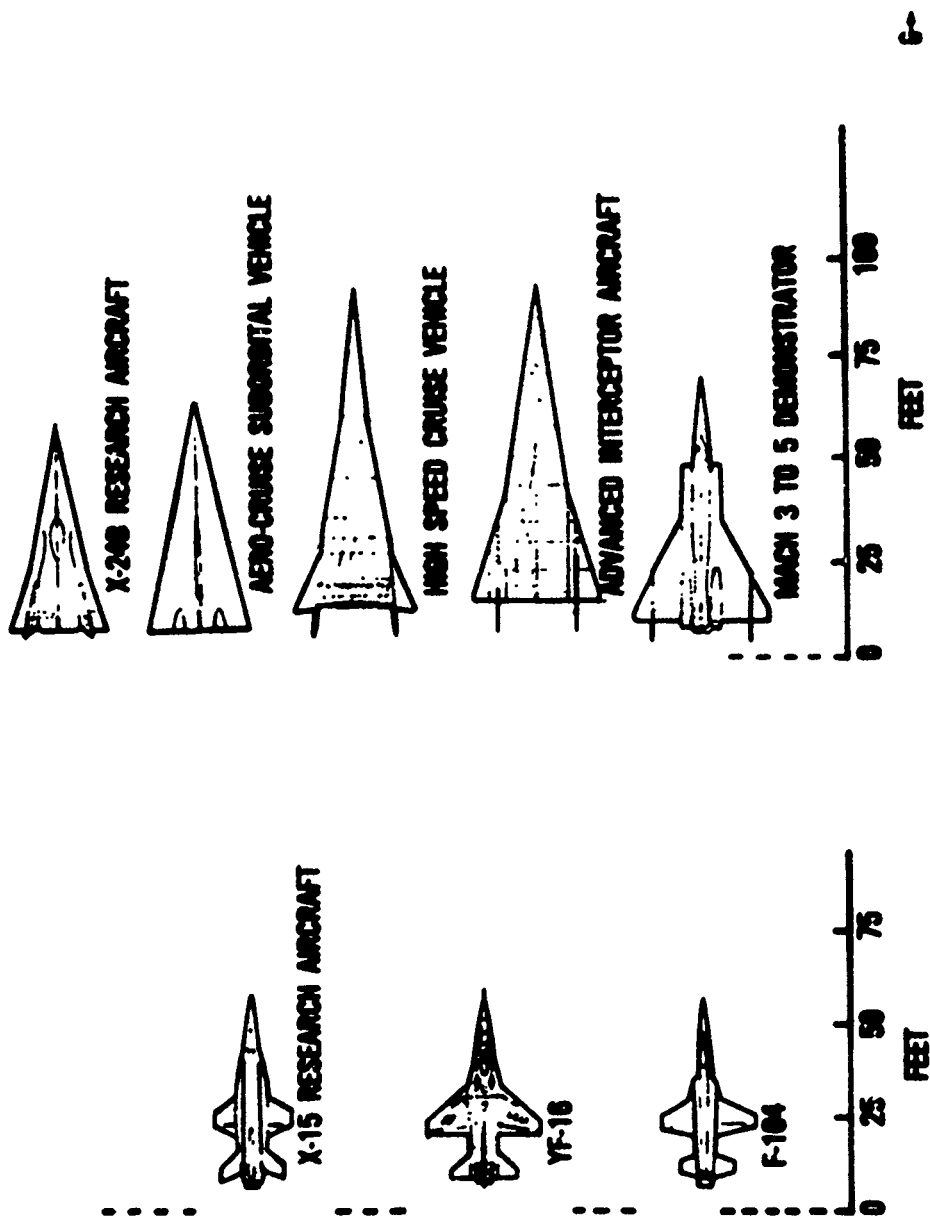


Figure 56. Research Aircraft Configuration Comparison

realization of the hypersonic flight potential of the configuration. Before the X-24B was completed in late 1972, it was recognized that the X-24B represented one of three elements that already existed, and needed only to be brought together to comprise a truly hypersonic research vehicle. These elements were: (1) the X-24B airframe; (2) the LR-99 rocket engine which had been used in the X-15; and (3) the insulative qualities of a low-density heat shield material that had been developed for the Mars atmosphere entry of the Viking Spacecraft. With moderate enlargement, sufficient propellant could be accommodated in the airframe for the rocket to accelerate it to hypersonic speeds, while the bond-on heat shield would insulate the aluminum structure from aerodynamic heating, and would itself be unaffected by the relatively benign environment when compared with the planetary entry conditions for which it had been developed. A modified X-24B vehicle, called the X-24C, was to be a low-cost low-risk testbed for research and development in hypersonic flight (References 69-71). The performance required was a speed of Mach 6 at 1000 lb/ft² operational dynamic pressure, using a LR-99 rocket engine, a B-52 launch, and a direct bond thermal protection system. The X-24C was to be an experimental testbed and a detailed 3-view drawing is presented in Figure 57.

Thirty-four experiments were defined as possibilities for flight on this research vehicle. These were reduced to 15 generic classes for purposes of evaluating experiment requirements related to the X-24C design. However, primary emphasis was placed on establishing a minimum length of vehicle that could accelerate a specified supersonic-combustion ramjet experiment to Mach 6, start the scramjet, throttle the rocket engine, and deploy a speed brake so that a minimum of 40 seconds of steady or

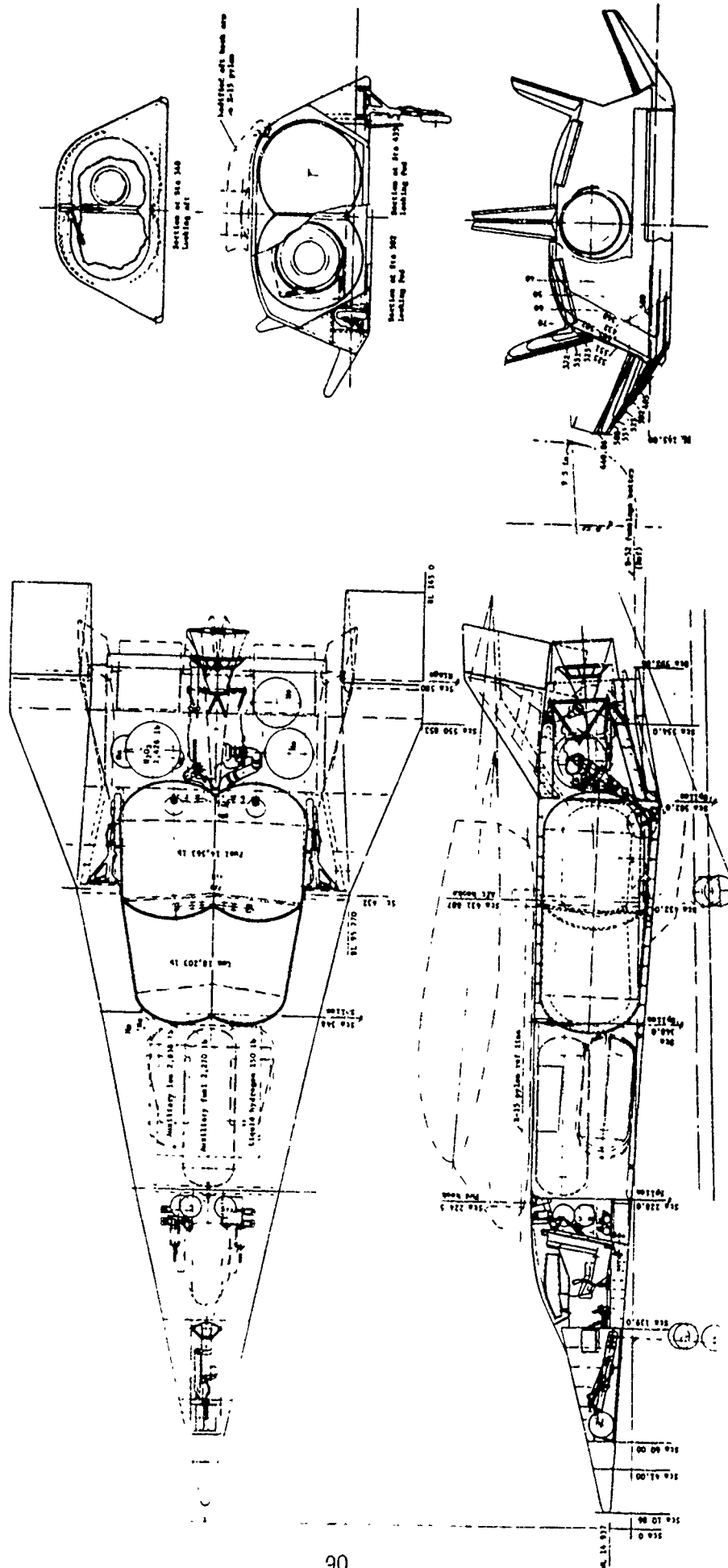
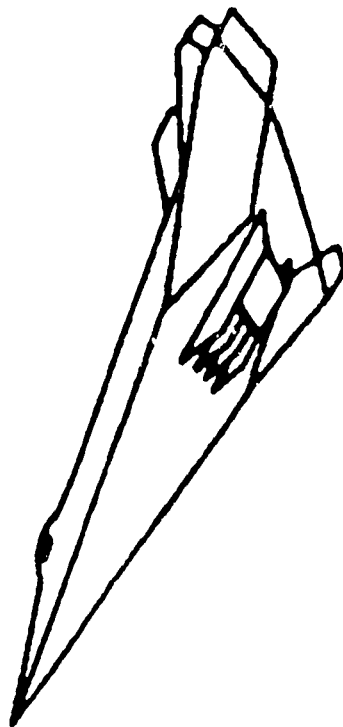


Figure 57. X-24C Configuration

quasi-steady flight could be obtained (Figure 58). In addition to the external scramjet attachments, a dedicated payload bay was provided in a 10-foot long replaceable, structural fuselage section as displayed in Figure 59. The X-24C investigations did not result in a flight test article, but were the center of extensive analytical and experimental investigations which focused toward a flight test article.

Applications of the Navier-Stokes equations for vehicle design were limited by the computational efficiency of the system of nonlinear partial differential equations and the accurate modeling of turbulence, laminar-turbulent transition, and finite rate chemical reaction. These limitations were common to all the numerical simulations (PNS, Euler) and were an area of intensive research. In spite of the difficulty encountered, this methodology was used for supersonic/hypersonic vehicle design. In 1985, engineering insight and computer power allowed J. Shang to determine the complete flow field about the X-24C hypersonic lifting body. Figure 60 presents the code and experimental results for the X-24C configuration (References 72-73).

The next air-breathing technology demonstrator investigated was to explore the Mach number speed regime of 8 to 16. The Flying Wind Tunnel (FWT) vehicle concept was designed to be as simple as possible to reduce development, manufacturing, launch, and operations costs. To keep the vehicle size and complexity down, the propulsion system was not designed to accelerate the vehicle. Instead, the propulsion performance would be assessed by measuring the change in the vehicle deceleration rates with the engine turned on and off. This approach required that the vehicle be accelerated to the desired test conditions by an external booster system,



FEATURES

- MACH 6 CRUISE FOR 30 SECONDS
- H₂ TANK AND SYSTEMS
- ACCOMMODATE 3 SCRAMJET MODULES
- AERO CONTROL

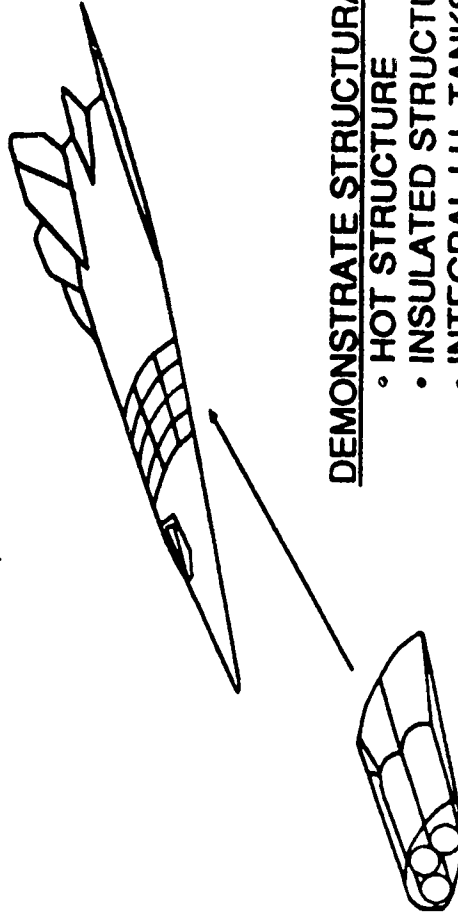
DEMONSTRATE AIRBREATHING PROPULSION TECHNOLOGIES

- SCRAMJET MODULES
- HYDROGEN FUEL
- VEHICLE INTEGRATION

Figure 58. X-24C Hypersonic Propulsion Experiment

FEATURES

- REPLACEABLE 10 FOOT FUSELAGE SECTION
- QUASI STEADY TEST TIME
- HYPERSONIC HEATING AND LOADS



REPLACEABLE
TEST ARTICLE

DEMONSTRATE STRUCTURAL TECHNOLOGIES

- HOT STRUCTURE
- INSULATED STRUCTURE
- INTEGRAL LH₂ TANKS
- METALLIC TPS
- SEALS, GAPS, EXPANSION JOINT

Figure 59. X-24C Hypersonic Structure Experiment

SURFACE STREAMLINE PATTERN

M=5.95
REYNOLDS NUMBER 1.64×10^7
 $\alpha=6$ DEGREES

	C_L	C_D	L/D
EXPERIMENTAL DATA	3.876×10^{-2}	3.173×10^{-2}	1.158
NUMERICAL RESULT	3.502×10^{-2}	2.900×10^{-2}	1.183
ERROR (%)	4.71	6.71	2.16



Figure 60. Navier-Stokes Results

removing any reliance on the propulsion efficiencies of the air-breathing propulsion system. The vehicle was designed to be as small as was practical for the propulsion module. The criteria for sizing the vehicle was driven by the minimum length required for the flow to naturally transition to a turbulent boundary layer just before reaching the inlet. It was determined that a forebody length of 10 ft was near the minimum allowable to obtain satisfactory propulsion data (References 74-76).

The driving technologies to be tested and evaluated in high speed flight are the supersonic combustion ramjet (scramjet) and associated aerodynamics and aerothermodynamics for both the propulsion system and the flight research vehicle. Subscale scramjet engines have been tested and are currently being tested in ground facilities up to Mach 8. Although inlet performance at speeds above Mach 8 can be reasonably predicted, there is no experimental design and performance data base for combustion and nozzle expansion characteristics at the higher Mach numbers above Mach 8. Limited data exists for boundary layer transition, shock behavior, catalytic wall effects, species concentrations, nonequilibrium chemistry, and many other high speed flow phenomena. This versatile research vehicle illustrated in Figure 61 will be able to fly an integrated scramjet engine and measure airbreathing propulsion, aerodynamic, and aerothermodynamic phenomena. The vehicle was designed to fly at dynamic pressures up to 1500 lb/ft² and its proposed flight corridor is shown in Figure 62.

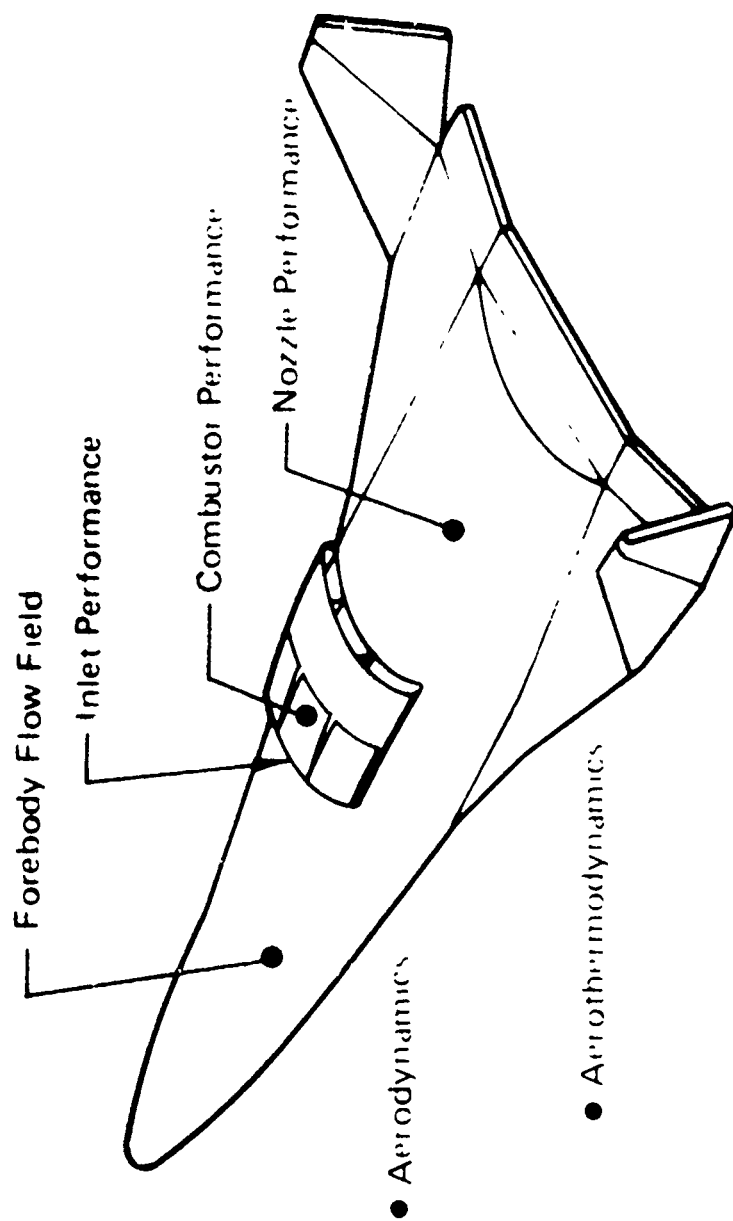


Figure 61. Flying Wind Tunnel Experiments

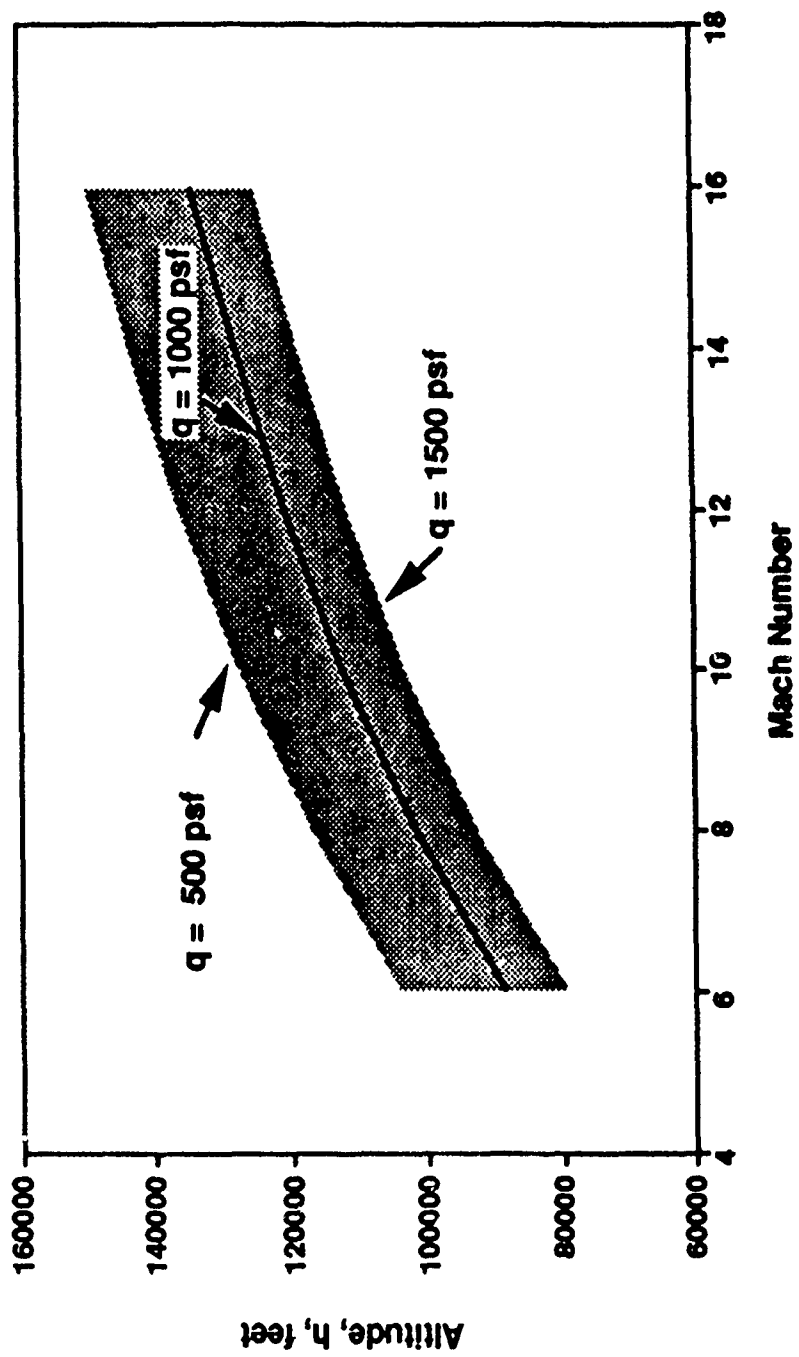
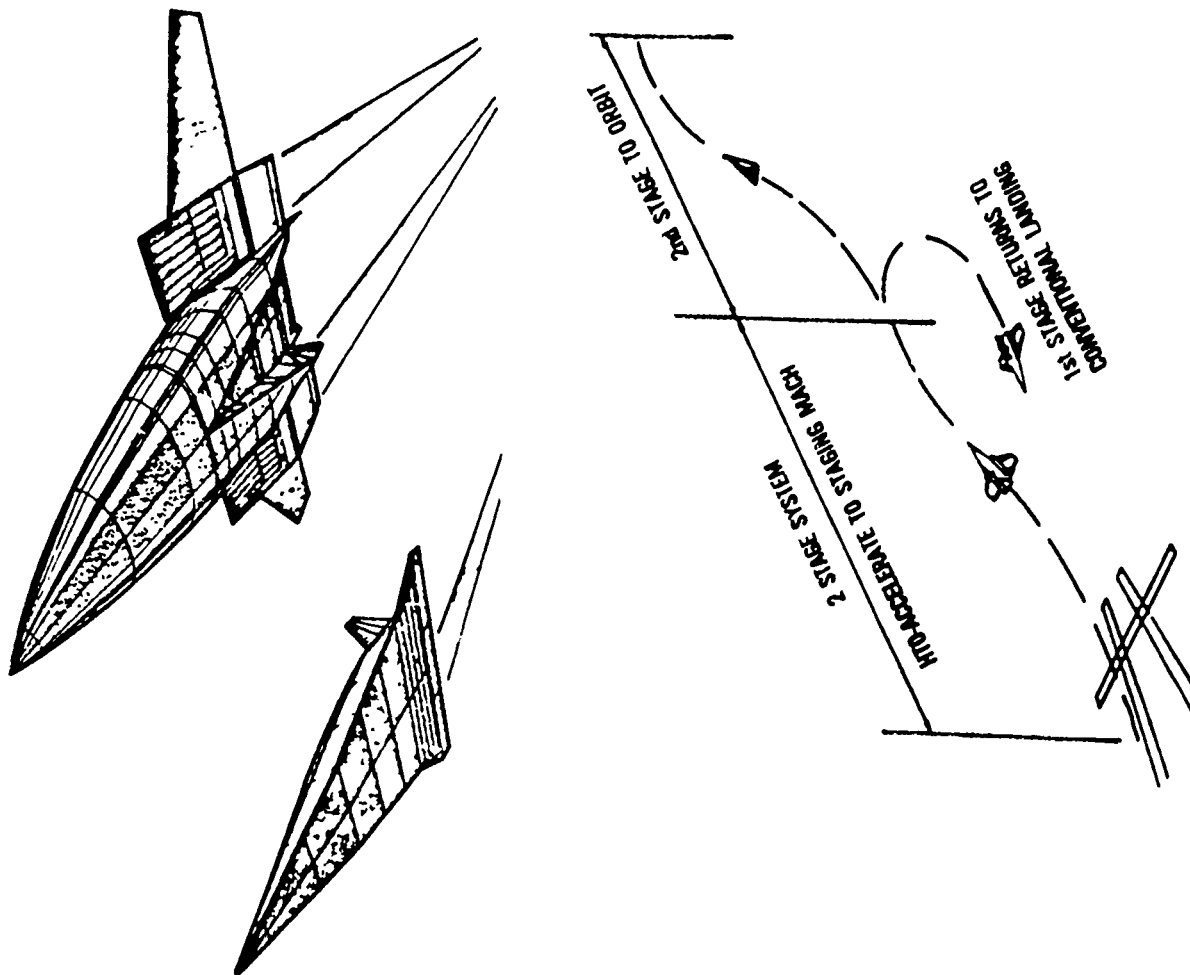


Figure 62. Flying Wind Tunnel Flight Corridor

8. TWO-STAGE REUSABLE LAUNCH VEHICLE CONCEPT

A two-stage fully reusable, horizontal takeoff and landing system was investigated as an interim, high confidence solution to meet the requirement of affordable access to space. The first stage booster was designed to employ air-breathing propulsion, while the second stage orbiter utilized an existing Space Shuttle main engine rocket system mated to a highly efficient, hypersonic aerodynamic shape. This arrangement tended to maximize the propulsion efficiency within the limits of near term/available technology levels. A bottom drop mode was selected for mating the orbiter to the booster. This arrangement minimized ground handling and logistic problems, ensuring the maximum number of available launch and landing sites. Incorporation of a viable air-breathing propulsion system, in conjunction with the bottom drop launch mode, proved to be a particularly challenging aspect of the configuration evolution. An innovative arrangement of advanced technology turbofans and 2-D subsonic combustion ramjets, shoulder mounted beneath a high elevation wing, provide an acceptable propulsion integration scheme. The engine concept included fully integrated turbofan engines within the ramjet nacelle, variable combustor and nozzle areas for the ramjet system, and even an element of thrust vector capability for pitch control (References 77-81).

This two-stage vehicle concept designated as "BETA" offers an alternate, near-term technology option which may be evaluated against competitive designs for possible concept development and production. The design shown in Figure 63 is fully reusable, features all-azimuth launch capability, has a horizontal takeoff and landing capability, can operate



- NEAR TERM STAGED SYSTEM
- DOABLE TECHNOLOGY LEVELS
- AIRBREATHING FIRST STAGE
- ROCKET SECOND STAGE
- SHUTTLE CLASS PAYLOADS
- FULL REUSEABILITY
- ALL AZIMUTH LAUNCH
- HORIZONTAL TAKE-OFF AND LANDING
- BOTTOM DROP STAGING MODE

Figure 63. Two Stage Reusable Launch Vehicle "BETA"

from numerous military/commercial sites, includes ferry capability to retrieve the orbiter, and has a payload capability into polar orbit nearly twice that of the Space Shuttle for only about one-half the initial lift-off weight. From its inception, it was intended to utilize air-breathing propulsion in the first stage booster and rocket propulsion in the second stage orbiter. Horizontal takeoff and landing was a ground rule, as was the maximum use of existing propulsion systems. To minimize ground handling and logistics, staging was to occur using a bottom drop mode. Staging Mach number was limited by near term propulsion requirements to a maximum Mach number of 8. The booster evolution is illustrated in Figure 64.

The BETA "4" concept was a refinement of the earlier BETA "3" and is illustrated in Figure 65. To improve transonic drag, the fuselage cross-sectional area was reduced, and to improve cross-sectional area distribution, the booster engine nacelles were moved forward. Attempts to reduce base drag with some form of fairings were not successful, due mainly to difficulties incorporating the fairings into the design. As a direct result of the higher than expected subsonic/transonic drag, the final booster design was forced to include a single SSME rocket engine on the booster (as was the case with BETA "2"). This unit operated in concert with the orbiter SSME rocket engine up through approximately $M = 3$. The in-house BETA configuration achieved closure at a gross takeoff weight of approximately 2.3×10^6 lb. The booster had a body length of 240 ft and a span of 180 ft. The orbiter had an overall length, including body flap, of 150 ft and a span of 60 ft. This configuration then served as the baseline for subsequent development of the BETA concept.

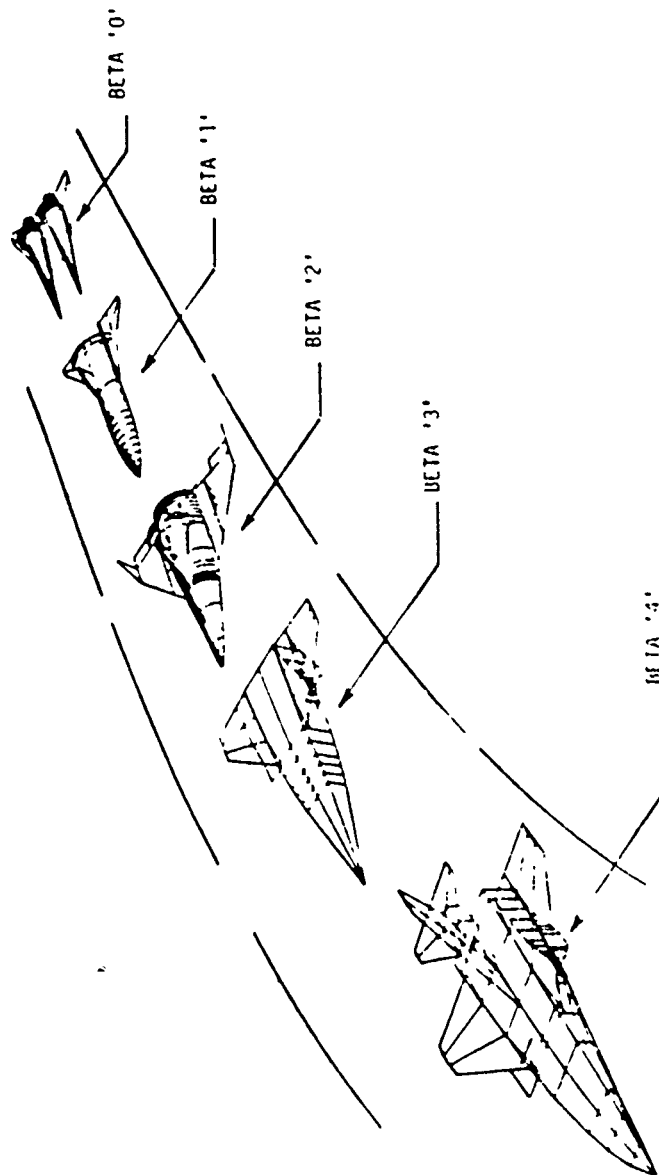


Figure 64. Booster Evolution

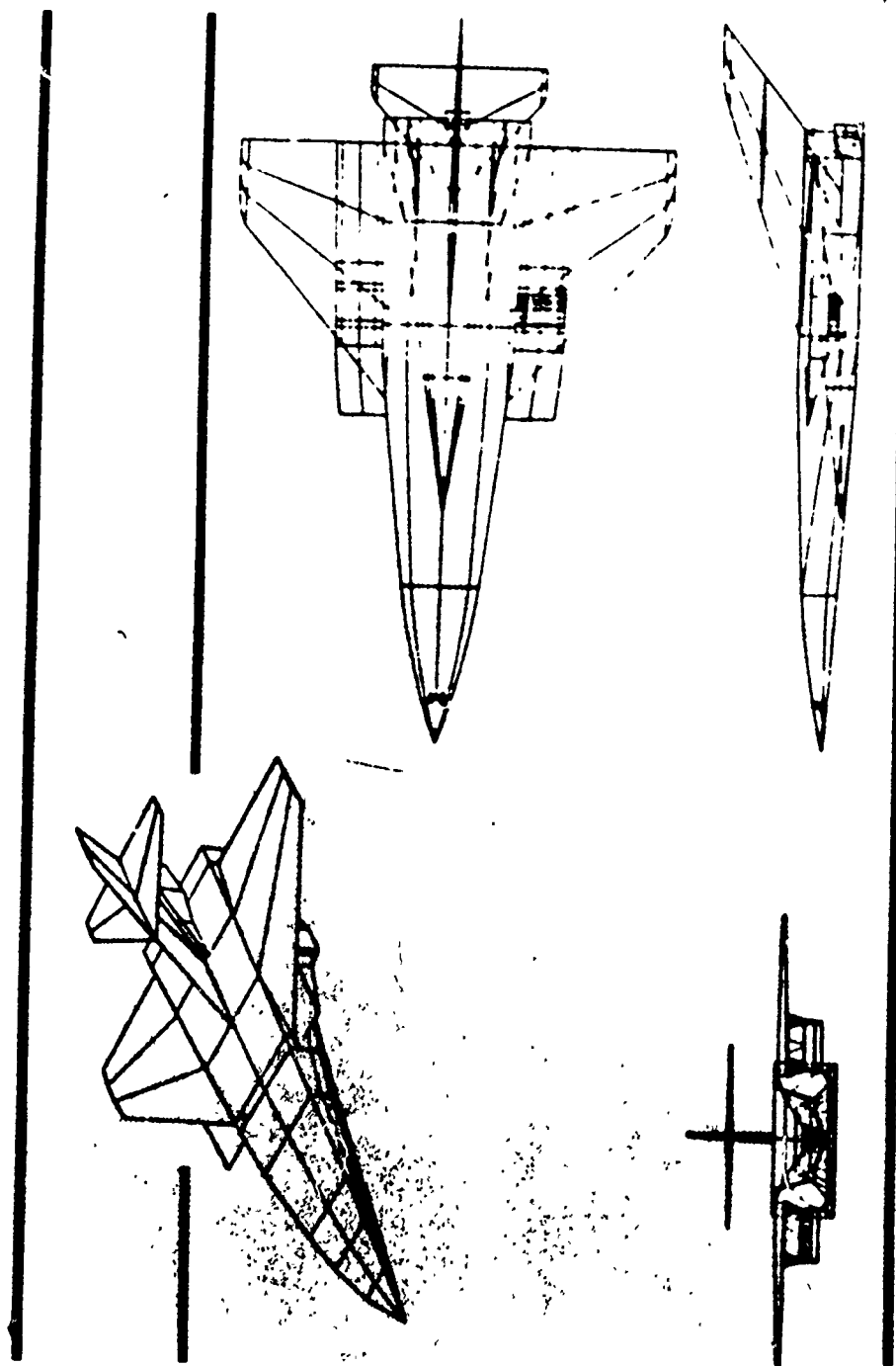


Figure 65. First Stage Booster Design

The final orbiter configuration powered by a single SSME, was based on a lifting body concept and featured a fully defined payload bay measuring 15x40 ft with a payload capability of 50,000 lb. The orbiter evolution from a wing-body to the highly efficient lifting body concept with an L/D 3.0 is shown in Figure 66. The clear lineage of the orbiter design to the FDL studies such as the X-24C lifting body concept is apparent. Extensive analysis and design efforts were conducted in refining the BETA configuration. A wind model was designed, fabricated and wind tunnel tested at Arnold Engineering and Development Center to assist in validating the prediction techniques. The model shown in Figure 67 was tested from Mach 0.5 to 8.0. The final gross takeoff weight for the BETA concept was approximately 1.9 million lb with an orbiter staging weight of around 600 thousand lb. At this weight the system is able to place a payload weight of 45,000 lb into a 100 nm polar orbit.

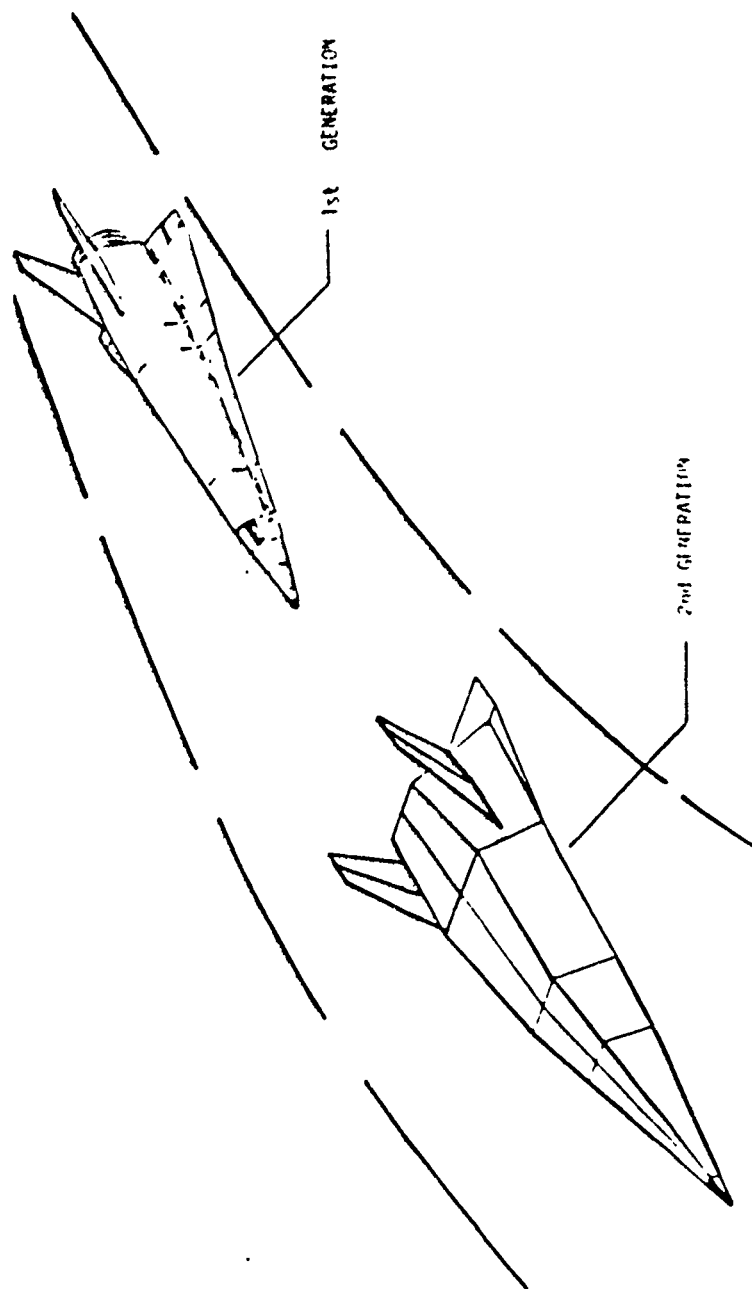


Figure 66. Orbiter Evolution

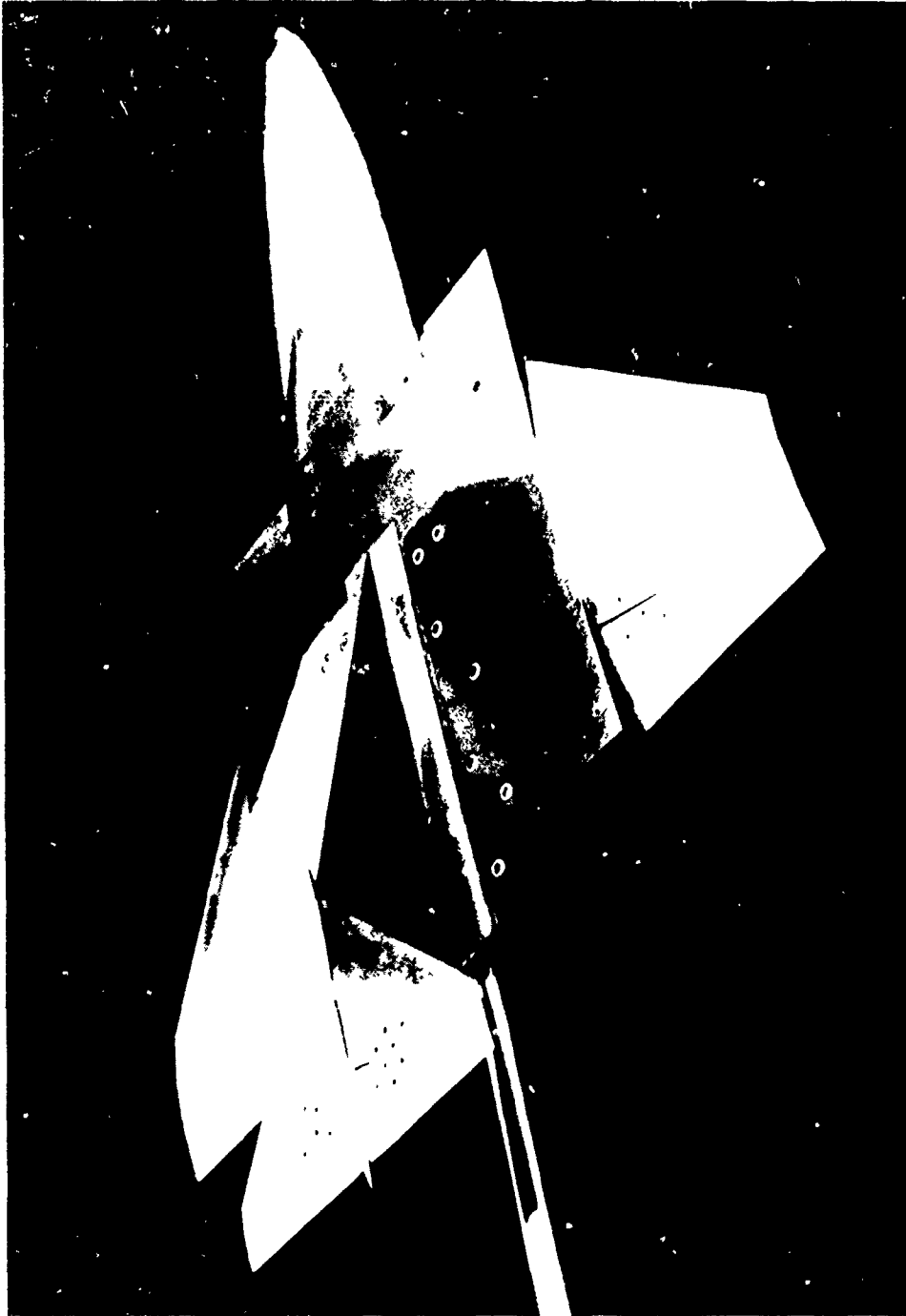


Figure 67. BETA Wind Tunnel Model

9. LESSONS LEARNED

As a result of the many research investigations conducted, there evolved certain guidelines that can be used in the formulation and definition of hypersonic configurations. These "lessons learned" are based on extensive analysis, wind tunnel tests and flight tests:

- (1) Flat bottom lower surface configurations produced the highest hypersonic L/D.
- (2) Higher performance and volumetric efficiency can be obtained with lifting body configurations.
- (3) The correlation parameter $\frac{M\sqrt{C^*}}{\sqrt{R_N}}$ can be used to correlate hypersonic wind tunnel data from several facilities.
- (4) A modified form of Newtonian theory can be accurately used to predict the force and pressure distributions on arbitrary configurations (S/HABP).
- (5) Skin friction drag is a major deterrent to producing favorable interference effects on hypersonic reentry vehicles.
- (6) Viscous interaction and rarefied flow can be major drivers on the aerodynamics characteristics at the design condition for high L/D lifting body configurations.
- (7) The drag and aerodynamic heating on the upper surface can be reduced when it is placed in the shadow of the free stream velocity vector.
- (8) Compact lifting body shapes can be developed with longitudinal, lateral and directional stability.
- (9) Highly swept delta planforms are most efficient for lifting bodies.

- (10) Inboard twin vertical tails can provide directional stability and rudder effectiveness across the Mach Number range.
- (11) Shock wave boundary layer interaction should be avoided at hypersonic speeds because of intense aerodynamic heating. Wings need to be highly swept back to avoid bow shock interaction.
- (12) Synergistic cruise turn with high L/D vehicles is most effective for large orbital plane changes.
- (13) Hypersonic air-breathing configurations are totally integrated including inlet, combustor and nozzle.
- (14) Aircraft and spacecraft configurations converge into a single class of vehicles for transatmospheric flight.
- (15) Re-radiative heat shields can survive the reentry environment (ASSET).
- (16) Ablative heat shields can be used successfully on medium L/D reentry vehicles (PRIME).
- (17) Excellent low speed characteristics can be obtained on a hypersonic high L/D lifting body configuration (X-24B).

REFERENCES

1. Malvestuto, Frank S., Jr, "Study To Determine Aerodynamic Characteristics On Hypersonic Re-Entry Configurations," WADD-TR-61-56, March 1962.
2. "Proceedings of 1962 X-20A (Dyna Soar) Symposium," ASD-TR-63-148, March 1963.
3. Sieron, T. R., Marcy, W. L., Onspaugh, C. M. and Clifford, J. B., "Study Performance Efficiency In Entry Design," AFFDL TR-65-44, Volumes I & II, October 1965.
4. Draper, A. C., Benson, B. R., Sieron, T. R., & Neumann, R. D., "Aerodynamic and Performance Analysis of a Super-Orbital Re-Entry Vehicle," John Wiley & Sons, Dynamics of Manned Lifting Planetary Entry, 1963.
5. Draper, Alfred C., Buck, Melvin L., Davis H. Max, and Nicholson, James F., "A Superorbital Design Concept for a Lifting Entry Vehicle," Proceedings of the AIAA Vehicle Design Symposium, November 1963.
6. Cosenza, C. J., Alexander, G. L., and Gazzerro, W. J., "A Program for Hypersonic Flight Testing in the Areas of Structures, Aerothermodynamics, and Structural Dynamics (ASSET)," FDL-TR-64-75, July 1964.
7. Landes, P. E., Marks, C. D., et al, "ASSET" Volumes 1-4, AFFDL-TR-65-31, April 1966.
8. "SV-5D Prime, Final Flight Test Summary," Martin-Marietta, ER 14465, September 1967.
9. "Prime Lifting Body Spacecraft, A Collection of Papers, USAF," SAMSO-TR-68-11, May 1968

10. Johnson, D. T., Bursey C., Nash R., "Performance Methods For Lifting Entry Vehicle Range Analysis," AFWAL-TR-82-3036, 1982.
11. Peterson, L. D., "Trajectory Optimizatn By Method of Steepest Descent," AFFDL-TR-67-108, 1967.
12. Brown, R. C., Vorwald, R. F., et al, "Six Degrees of Freedom Flight Path Generalized COmputer Program," Vol I, Part I & II, AFFDL-TR-64-1, 1964.
13. Hayne, D. S., "Maneuvering Reentry and Orbital Performance Optimization System," Vol I, II, & III, AFWAL-TR-82-3005, 1982.
14. Benson, B., and Nash R., "Constanct L/D Reentry Study," AFFDL-FDM-TM-63-11, 1963.
15. Johnson, David T., "Performance Estimation of Unpowered High Lifting Reentry Vehicles," AFFDL/FIMG-TM-65-16, 1965.
16. Bell, Roland V. 1 Lt and Hankey, Wilbur L., "Applications of Aerodynamic Lift in Accomplishing Orbital Plane Change," ASD-TDR-63-693, September 1965.
17. Hankey, W. L., and Schroder, L J., "Optimization of Lifting Re-entry Bodies," Proceedings of 12th Annual Air Force Science & Engineering Symposium, Vol I, 1965.
18. Dahlem, V., and Buck, M. L., "Analysis and Experimental Results of High Lift-to-Drag Configurations," AFFDL-TR-67-138, 1967.
19. Draper, A. C. and Buck, M. L., "Lifting Bodies - An Attractive Aerodynamic Configuration Choice For Hypervelocity Vehicles," AGARD Conference Proceedings No. 428, Aerodynamics of Hypersonic Lifting Vehicles, June 1986.

20. Lloyd, John T., and Sieron, Thomas R., "Development of High L/D Configurations," Proceedings of ASSET Symposium, AFFDL-TR-66-22, 1966.
21. Draper, Alfred C., and Buck, Melvin L., "Assessment of the Factors Affecting Advanced Lifting Entry Vehicles," AFFDL-TR-67-137, 1967.
22. Dahlem, Valentine, III, "Summary of Aerodynamic Characteristics of the FDL-6 High L/D Configuration," AFFDL-TR-72-48, 1972.
23. Lloyd, John. T., et al, "Preliminary Design of Hypersonic High L/D Test Vehicles," AFFDL-TR-66-12, May 1966.
24. DeCamp, Ronald W., and Sieron, Thomas R., "Summary of the FDL-5 High L/D Lifting Body Configuration," AFFDL-TM-73-20, March 1973.
25. Lloyd, J. T., et al, "Preliminary Design and Experimental Investigation of the FDL-5A Unmanned High L/D Spacecraft," AFFDL-TR-68-24, March 1968.
26. Johnson, David T., et al, "Technology Feasibility Study for High L/D Test Vehicles," FDM-TM-67-4, November 1967.
27. Buck, M. L. and McLaughlin, "A Technique For Predicting Pressure Distributions and Aerodynamic Force Coefficients For Hypersonic Winged Re-Entry Vehicles, ASD-TR-63-522, August 1963.
28. Gentry, A. D., Smyth, D. N., and Oliver, W. R., "The Mark IV Supersonic-Hypersonic Arbitrary Body Program, AFFDL TR-73-159, 1973.
29. Sieron, T. R. and Martinez, C., Jr. "Effects and Analysis of Mach Number and Reynolds Number On Laminar Skin Friction At Hypersonic Speeds, AFFDL-TR-65-5, April 1965.

30. Sieron, T.R., "Methods For Predicing Skin Friction Drag From Subsonic to Hypervelocity Speeds on a Flat Plate and Delta Wing," AFFDL-TM-62-45, August 1962.
31. Knowles, Leon, Sieron, Thomas R., & Tsucalis, John C., "Aerodynamics and Stability Characteristics of Hypervelocity Lifting Configuration, AFFDL-65-7, December 1965.
32. Neumann, R., McElderry, E., Gord, P., and Buck, M., "High L/D Vehicle Design," AFFDL-TR-69-82, February 1970.
33. Antonatos, Philip P., Draper, Alfred C., and Neumann, Richard D., "Aerothermodynamic and Cnfiguration Development," AIAA 7th Annual Meeting and Technical Display, Houston, Texas, October 19-22, 1970.
34. Draper, Alfred C., and Cosenza, Charles, J., "Technolgical Prospects for High Performance Spacecraft," Proceedings of SAI Space Technology Conference, Washington DC, May 8-10, 1968.
35. Goetsch, G. F., et al, "Lifting Reentry Test Vehicle Preliminary Designs For FDL-7MA and FDL-5MA Configurations," AFFDL-TR-68-97, January 1969.
36. Dahlem, V., Shereda, D., and Gord R., "Experimental Investigation at Hypersonic Speeds On Increasing Usable Volume of Lifting Bodies," AFFDL-TR-70-86, 1976.
37. Flaherty, J., and Smith, R. T., "Hypersonic Pressure Test of the FDL-6 High L/D Configuration at $M = 9.3$," AFFDL/FIMG TM-70-86, 1970.
38. Gentry, A. E., and Oliver, W. R., "Hypersonic Aerodynamic Analysis of High L/D Reentry Vehicles, AFFDL-TR-68-40, 1968.
39. Bradley, R.E., "An Analytical and Experimental Study of Slender Sharp Edged Hypersonic COnfigurations," AFFDL-TR-68-121, 1968.

40. Flaherty, J. I., and Shereda, D. E., "Analytical and Experimental Investigations of the FDL-6 Configuration at Mach 1.89, 2.3 and 3.0," AFFDL-TR-69-105, 1969.
41. Polcheff, G. L., "Preliminary Design Evaluation of the FDL-7 Incremental Growth Vehicle," AFFDL-TR-74-65, 1965.
42. Burke, G. L., "Heat Transfer and Pressure Distribution About Sharp and Blunt Elliptic Cones at Angles of Attack and High Mach Numbers," AFFDL-TDR-64-172, 1972.
43. Neumann, R. D., and Burke, G. L., "The Influence of Shock Wave-Boundary Layer Effects On the Design of Hypersonic Aircraft," AFFDL-TR-68-152, 1968.
44. Sliski, N. J., "An Analytical and Experimental Investigation of Hypersonic Viscous Interaction Effects," AFFDL-TR-73-58, 1973.
45. Sliski, N. J., Patterson, J. L., and Neumann, R. D., "Aerodynamic Heating to the Hypersonic Research Aircraft X-24C, AIAA Paper 78-37.
46. Patterson, J. L., "Determination of Interference Heating Effect on the HASR Missile Using the Thermographic Phosphor Technique," AFFDL-TR-73-75.
47. Stetson, K. F., "Hypersonic Boundary Layer Transition," AFWAL-TR-86-3089.
48. Spalding, D. B. and Chi, S. W., "The Drag of a Compressible Turbulent Boundary Layer on a Smooth Flat Plate With and Without Heat Transfer," J. Fluid Mechanics, Vol I, Part 1, Jan 1964, pp 117-143.
49. Savage, R. T., Jaeck, C. L., and Mitchell, J. R., "Investigation of Turbulent Heat Transfer at Hypersonic Speeds. Volume III. The Laminar-Turbulent PrMr Momentum Integral and Turbulent Nonsimilar Boundary Layer Computer Programs," AFFDL-TR-67-144, December 1967.

50. Hankey, W. L., Neumann, R. D. and Flinn, E. H., "Design Procedures for Computing Aerodynamic Heating at Hypersonic Speeds," WADC-TR-59-610.

51. Thomas, A. C. et al, "Advanced Re-entry Systems Heat Transfer Manual for Hypersonic Flight," AFFDL-TR-195-144, 1967.

52. Neumann, R. D., "Defining the Aerothermodynamic Methodology II," University of Texas Short Course on Hypersonics, November 1986.

53. Armstrong, J. G., "Flight Planning and Conduct of the X-24A Lifting Body Flight Research Program," AFFRC-TR-71-10, August 1972.

54. Selegan, David R., "Parametric Study of Nine Delta Wings on a Modified FDL-8 Vehicle $M = 0.4 - 1.2$," AFFDL-TM-71-26-FXS.

55. Armstrong, J. G., "Flight Planning and Conduct of the X-24B Research Aircraft Flight Test Program," AFFTC-TR-76-11.

56. Draper, Alfred C., Buck, Melvin, L., and Selegan, David R., "Aerospace Technology Demonstrators/Research and Operational Optics," AIAA Aircraft Prototype and Technology Demonstrator Symposium, Dayton OH, March 23-24, 1983.

57. Quest, R., "The Tip Tank Concept; An Economic Orbital Transportation System," S & E Space Technology Conference, May 1967.

58. Alexander, G. L., et al, "Design and Experimental Investigation of Reusable Launch Vehicle Configurations," AFFDL-TR-71-13, May 1971.

59. Draper, Alfred C., Buck, Melvin L., and Goesch, William H., "A Delta Shuttle Orbiter," Aeronautics and Astronautics, Volume 9, No. 1, January 1971.

60. Hayes, J. R., and Neumann, R. D., "Trends in the Space Shuttle Aerothermodynamic Data Base," AIAA 19th Aerospace Sciences Meeting, St Louis MO, January 12-15, 1981.

61. Draper, Alfred C., Lane, Paul, and Zima, William P., "A Flight Research Vehicle to Bridge Shuttle and Hypersonic Aircraft Technology," AIAA Atmospheric Flight Mechanics Conference, Hollywood, Florida, August 8-10, 1977.

62. Hogue, H. J. and Rudiger, "Concept Evaluation of a Maneuverable Reentry Research Vehicle and Related Experiments," AFWAL-TR-81-3125, November 1981.

63. Heald, D. A., et al, "Advanced Military Spaceflight Capability Technology Identification," AFWAL-TR-83-3076, July 1983.

64. Miller, R. M., "Advanced Military Spaceflight Capability," AFWAL-TR-85-3044, September 1985.

65. Gailey, J. W. and Paris, S. W., "Evaluation of AMSC Concepts," AFWAL-TR-86-3083, December 1986.

66. Butler, G. S., et al, "Geometric Optimums For Transatmospheric Military Vehicle," AFWAL-TR-85-3106, January 1986.

67. Andrews, D. G., et al, "Technology Identification For Aeroconfigured Orbital Transfer Vehicles," AFWAL-TR-83-3090, October 1983.

68. Lane, Paul, Jr., "Flight Research Concepts for Aerodynamic Maneuvering Space Vehicles," Air Power Symposium, Maxwell AFB AL, February 23-25, 1981.

69. Brackeen, R. E. and Marcy, W. L., "X-24B Growth Version Feasibility Study," AFFDL-TR-73-116, October 1973.

70. Plank, P. P., et al, "Experiments Impact On X-24C," AFFDL-TR-75-37, May 1975.
71. Kirlin, R. L., "Evolution of Bond-On Insulation TPS Material for X-24C," AFFDL-TR-76-25, 1976.
72. Shang, J. S., and Hankey, W. L., "Computation of Flow Past a Hypersonic Cruiser," Proceedings of the 2nd Symposium on the Numerical & Physical Aspects of Aerodynamic Flows, California State University, Long Beach CA, January 16-20, 1983.
73. Shang, J. S., and Schear, S., "Navier Stokes Solution for a Complete Re-entry Configuration," AIAA Journal of Aircraft, April 1986.
74. Ilgenfritz, D. W. and Paris, S. W., "High Leverage Hypervelocity Technology - Air-Breathing Research Vehicle," AFWAL-TR-88-3105, March 1989.
75. Norris, R. B., Paris, S. W. and White, E. T., "The Flying Wind Tunnel," AIAA Atmospheric Flight Mechanics Conference, Paper 89-3378, August 1989.
76. Paris, S.W., et al, "Research Vehicle Configurations For Hypervelocity Vehicle Technology," WRDC-TR-90-3003, Vol I, April 1990.
77. Draper, A. C. and Buck, M. L., "An Interim Technology Concept For An Innovative Fully Reusable Launch Vehicle," International Conference On Hypersonic Aerodynamics, Royal Aeronautical Society, September 1989.
78. Gord, P.R.; Langan, K.T.; and Stringer, M.E., "Advanced Launch Vehicle Configurations and Performance Trades," AGARD-CP-489, Space Vehicle Flight Mechanics Symposium, Paper No. 5, 13-16 November 1989.
79. Dahlem, V.; Gord, P.R.; and Langan, K.T., "Advanced Launch Vehicle Configuration and Performance Trades," 1990 JANNAF Propulsion Meeting, 3-5 Oct 1990, Anaheim, California, Paper VII-50.

80. Dahlem, V.; Gord, P.R.; and Langan, K.T., "Two Stage Fully Reuseable Space Launch Vehicle Configuration and Performance Trades," 1991 SAE Aerospace Atlantic, April 22-26 1991, Dayton, Ohio.

81. Wetzel, E.D., et al, "Research Vehicle Configurations For Hypervelocity Vehicle Technology," WRDC-TR-90-3003, Volume II, April 1990.